Journal of Alloys and Metallurgical Systems 9 (2025) 100170

Contents lists available at ScienceDirect

Journal of Alloys and Metallurgical Systems

journal homepage: www.journals.elsevier.com/journal-of-alloys-and-metallurgical-systems

High entropy alloys synthesized by mechanical alloying: A review

Yogesh Kumar Yadav [a], Mohammad Abu Shaz [a], Nilay Krishna Mukhopadhyay [b], Thakur Prasad Yadav [a,c,*]

[a] Department of Physics, Institute of Science, Banaras Hindu University, Varanasi 221005, India
[b] Department of Metallurgical Engineering, Indian Institute of Technology (Banaras Hindu University), Varanasi 221005, India
[c] Department of Physics, Faculty of Science, University of Allahabad, Prayagraj 211002, India

ARTICLE INFO

Keywords:
High entropy alloys (HEAs)
Conventional alloys
Mechanical alloying/milling
Nanostructured materials
Intermetallics

ABSTRACT

High entropy alloys (HEAs) have attracted an intense interest from scientists, researchers, academics and industrialists in the recent times because of their exceptional physical, functional and chemical properties, which are superior to those of conventional alloys. The vast number of scientific publications has eclipsed many synthesis and production techniques being adopted for HEAs. Although the production processes for traditional alloys are well-established, a closer look must be given to the various synthesis methods used for multicomponent alloys for industrial applications. This review paper will fill this vacuum by providing a thorough and comprehensive investigation into the production of quinary, senary and higher order alloy systems in HEAs via mechanical alloying/milling. The mechanical alloying is a non-equilibrium synthesis technique that combines elemental powders through high-energy ball milling and eventually nanostructured materials can be produced. The intrinsic mechanical alloying processes of plastic deformation, cold-welding and fracture causes the changes in the size, configuration, and dispersion of the particles. As a result, a uniformly sized, finely divided powder develops; giving rise to the materials the special qualities compared to traditionally alloyed materials. Mechanical alloying is established widely for the synthesis of HEAs and other advanced materials. Through the approaches of mechanical alloying, this review paper seeks to analyze and throw light on the synthesis of HEAs especially, providing insightful information on this process and its significance for developing complex HEAs.

1. Introduction

Metallic materials are essential to the advancement of society and human development [1]. Their distinct physical characteristics, which represent human ingenuity and inventiveness, have profoundly influenced our past [2–5]. The invention of metallic tools, which replaced stone ones, was a turning point that led to improvements in agriculture, building and crafting [6]. The need for stronger and more adaptable alloys increased as societies developed propelling technological advancement [7]. Strong tools and structures were made possible by metallurgy, which directly connected material growth to human civilization. Important historical eras such as the Bronze and Iron Ages demonstrate how metal working skills impacted military, cultural and economic development (Fig. 1) [8,9]. Metallic elements continue to influence our aspirations and civilization as we explore new boundaries, serving as the foundation for contemporary industry and technological breakthroughs [10].

The history of metallic alloys development has had an unparalleled surge in the last century, characterized by outstanding discoveries, breakthroughs, and an unwavering quest for knowledge (Fig. 1). The combined efforts of the scientific community and researchers have expanded the uses of metallic materials, making them essential parts of many different sectors. An essential component of this development is the field of metallic alloys, intended to improve particular qualities. Traditionally, alloys were made up of one or two main constituents [11,12]. But as soon as scientists started adding trace amounts of other elements to these alloys, the whole picture was altered. The incorporation of trace elements into alloys has demonstrated to be a revolutionary tactic, providing a sophisticated means of modifying the chemical and physical characteristics of metals.

The addition of carbon to iron to produce steel is a well-known illustration of this phenomenon [13–15]. Steel is far more durable than iron because of the addition of carbon, which gives the alloy a greater strength. This shows how a small change in composition can

* Corresponding author at: Department of Physics, Faculty of Science, University of Allahabad, Prayagraj 211002, India.
E-mail address: tpyadav@allduniv.ac.in (T.P. Yadav).

https://doi.org/10.1016/j.jalmes.2025.100170
Received 25 September 2024; Received in revised form 15 February 2025; Accepted 19 February 2025
Available online 28 February 2025

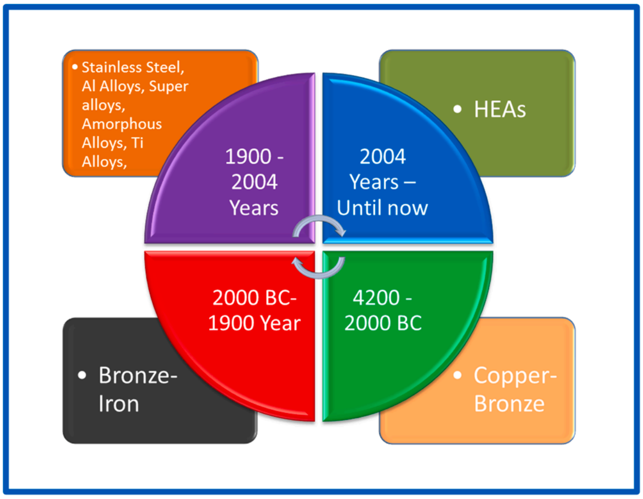

Fig. 1. From the first metallic alloys, such as copper bronze to the sophisticated compositions of contemporary high entropy alloys, a historical chart demonstrates the history of high entropy alloys (HEAs).

result in significant improvements to the material's qualities. Additionally, the work using ferromagnetic alloys demonstrate another aspect of this complex process. Researchers have managed to manipulate the magnetic characteristics of these alloys by adding trace amounts of particular impurities [16]. This skill has broad ramifications and impact on the advancement of technology that depends on magnetic phenomena. The complex interplay among elements in metallic compounds has therefore opened up new avenues for the customization of materials to satisfy the demands of contemporary industries, in addition to broadening the use of metals. Given this, a deeper examination of these alloying processes is necessary to recognize the breadth of scientific creativity that has driven the advancement of metals over the past century.

As is widely acknowledged, J.W. Yeh and coworkers in 2004 advocated the new concept of alloy development known as high entropy alloys (HEA) [17,18]. It is also interesting to note that Brian Cantor and his group independently came up with the similar idea as multi-principal multicomponent alloys (which is similar to HEAs) [19]. Yeh *et al.* (2004) suggested that this special class of alloys consist of five or more elements (equiatomic or nearly equiatomic) combined in concentrations between five to thirty-five atomic percent [18,20]. The historical diagram illustrating the development of HEAs is displayed in Fig. 1. The idea that solid solution phases with high mixing entropies typically exhibiting higher stability is the driving force for the development of HEAs [21]. These alloys have outstanding electrical and magnetic properties, remarkable strength and hardness, excellent wear resistance as well as thermal stability, and increased corrosion resistance (Fig. 2) [22–26]. In comparison with single-element equivalent alloy, HEAs combine a variety of elements inside a single lattice or in a nanoparticle structure and frequently exhibit better physical and chemical properties. Because of their complex nature and wide range of desirable properties as illustrate in Fig. 2, HEAs are seen attractive for technological applications [27].

These alloys have the potential to outperform conventional materials and expand the range of applications due to the complex interactions among their constituent parts. HEAs as seen in Fig. 3, show promise in a number of industries, including nuclear equipment, electronic devices, cryogenic conditions, and high-temperature applications. The increasing recognition and application of these special qualities underscore the important contribution of HEAs to the progress of materials science. HEAs are a unique family of materials that have been synthesized using a variety of techniques including powder metallurgical synthesis, deposition techniques, and melting and casting routes [28–31]. Although the bulk HEAs make up a sizable number of synthetic materials, nanocrystalline HEAs have consistently been explored and developed [32] by mechanical alloying technique. The attainment of nano crystallinity during the mechanical processing further gives added advantages in compositional space and a fascinating new dimension. The special features of nanocrystalline HEAs, which are typified by their finely grain-size structure at the nanoscale, have stimulated further research interest. These nanostructured alloys have excellent thermal

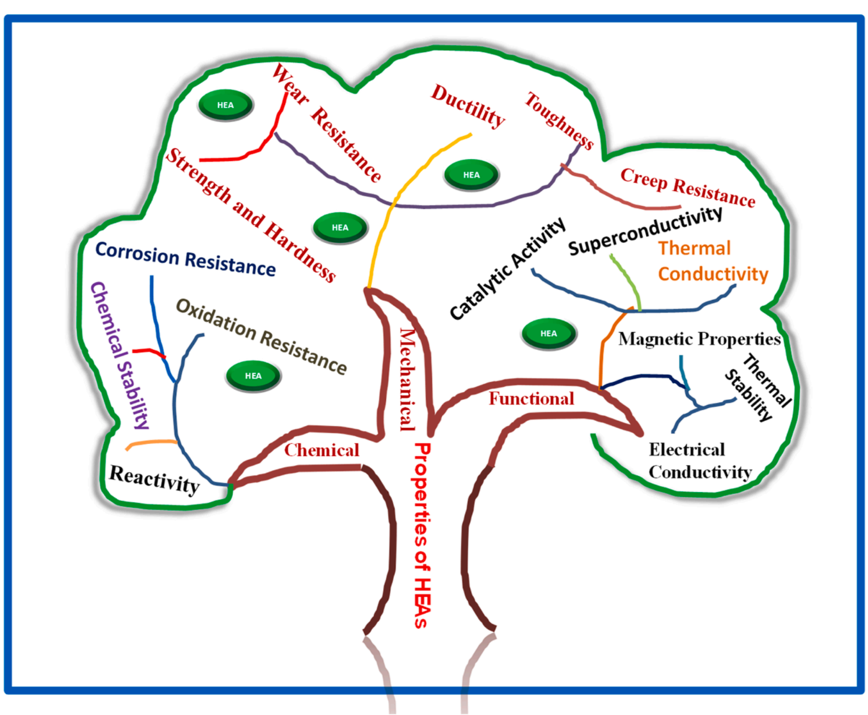

Fig. 2. This schematic figure, which is set up in a tree structure, shows the high entropy alloys' mechanical, functional, and chemical characteristics. It highlights the complex characteristics and functionalities of these alloys by visually classifying and detailing their qualities and interactions.

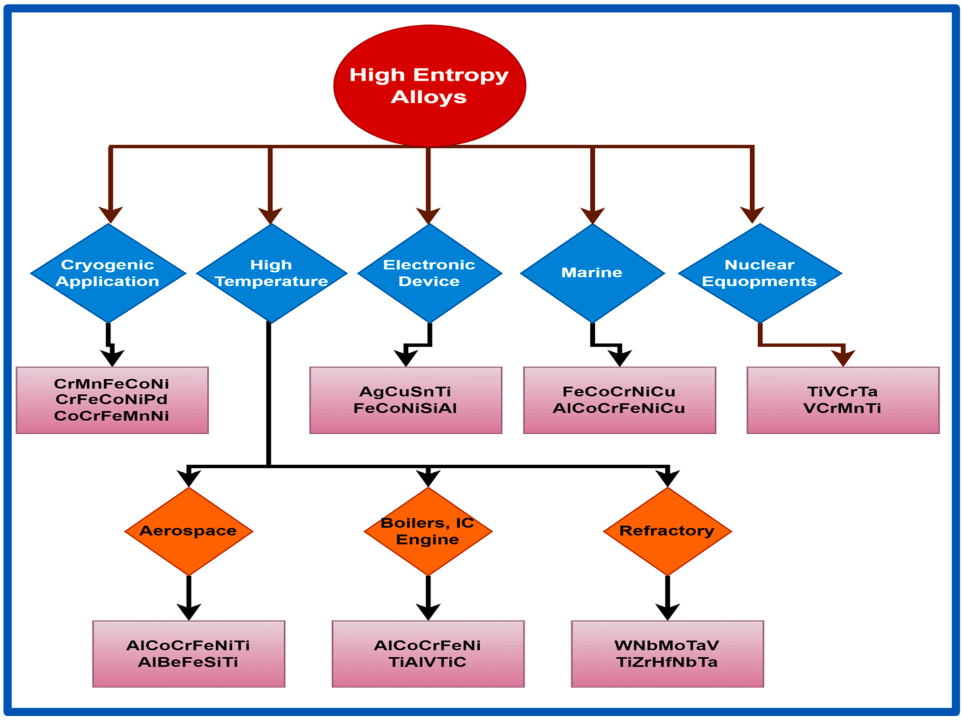

Fig. 3. Applications of various high entropy alloys (HEAs) across different sectors driven by their remarkable physical and chemical properties.

stability, remarkable magnetic behavior and improved mechanical properties [33,34]. Among all the techniques which are being used to synthesize nanocrystalline materials, mechanical alloying (MA) is a well-recognized solid-state nonequilibrium top-down technique [35–43].

In MA, elemental powders are ground in an effort to achieve atomic-scale alloying [44]. The repetitive welding and fracture of powder particles caught between milling medium is an intricate process that defines it [45]. The extent of these processes depends on the mechanical properties of the powder components, which makes it a flexible and regulated method of generating nanocrystalline HEAs. The first nanocrystalline Al-Cr-Cu-Fe-Ti-Zn HEA alloy was successfully synthesized via MA in 2008 by Varalakshmi *et al.* (2008) whose pioneering work is credited with the synthesis of nanocrystalline HEAs through MA [46, 47]. An equilibrium phase during thermal annealing follows the transition from elemental materials to amorphous phases during MA, as described in the structural evolution model of HEAs put forward by Chen *et al.* (2009) [48]. They examined four different alloys: $Cu_{0.5}NiAlCo$ (quaternary) to $Cu_{0.5}NiAlCoCrFeTi$ (septenary). Cu and Ni first formed a solid solution during MA, into which additional elements progressively dissolved. After extensive milling, this solid solution finally took the form of amorphous structures. Following thermal annealing, the recovery of the amorphous powders started at 100 °C and crystallization happened between 250 and 280 °C, and at higher temperatures, equilibrium phase precipitation and grain growth happened. Cu-Ni-Co-Zn-Al-Ti HEA synthesized by Varalakshmi *et al.* [28] was further examined for understanding the impact of nonequiatomic compositions on the formation of HEAs by adjusting the Cu content up to 50 at. % (Cu_x-Ni-Co-Zn-Al-Ti; x = 0, 8.33, 33.33, 49.98 at. %) [49].They also studied the phase development and stability of mechanically alloyed powder at a temperature of 1073 K (800 °C). Up to quinary compositions (Cu-Ni-Co-Zn-Al), the nanocrystalline equiatomic Cu-Ni-Co-Zn-Al-Ti alloys showed an FCC structure; in the hexanary alloy (Cu-Ni-Co-Zn-Al-Ti), however, the structure was BCC. With a focus on the Ni-Co-Al-Fe-Cu-Cr HEA, Esparza *et al.* (2011) employed MA and produced a number of binaries (Ni–Co) to senary alloys (Ni–Co–Al–Fe–Cu–Cr) based on Ni, Co, Al, Fe, Cu, and Cr [50]. A high-energy ball mill was used for the trials, and the milling times were set at 0, 10, 20, and 30 hours. They suggested that all of the systems under study produce a FCC solid solution, but the phase formation response varies depending on the system. After brief milling durations, a combination of BCC and FCC solid solutions occurs in the quaternary (Ni-Co-Al-Fe) to senary (Ni-Co-Al-Fe-Cu-Cr) systems. It seems that Fe and Cr dissolve into the FCC solid solution somewhat slowly. Fig. 4 provides a clear illustration of the dissolution sequence of the elements.

Furthermore, it was found that the presence of these components encourages the development of a BCC solid solution, which is stable at temperatures as high as 1273 K. Al-Co-Cr-Cu-Fe and Ni-Co-Cr-Cu-Fe are equiatomic high-entropy alloys that were synthesized by Praveen *et al.* (2012) utilizing MA and spark plasma sintering (SPS) [51]. While Cu-rich FCC and sigma (σ) phases, together with FCC and BCC phases

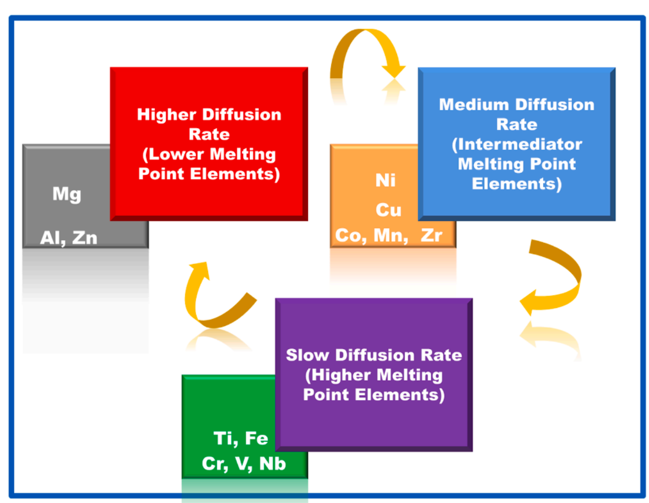

Fig. 4. Schematic diagram illustrating changes in material and illustrating the relationship between dissolution orders and milling time as well as how the order of dissolution changes with milling.

formed after SPS, simple FCC and BCC phases evolved after MA. Cu-rich FCC and σ phases were formed, as further studies of Ni-Co-Cu-Fe, Ni-Co-Cr-Fe, and Ni-Co-Fe equi-atomic alloys also showed similar behavior. For Al-Co-Cr-Cu-Fe, the measured hardness was 770 ± 10 HV, while for Ni-Co-Cr-Cu-Fe, it was 400 ± 10 HV. Vaidya *et al.* (2019) reported that by December 2018 there were 180 journal papers on mechanically alloyed HEAs, which represents a noteworthy milestone in materials research [47].

Building on these studies, we conducted a thorough literature review to learn more about the state of the art in the study of HEAs synthesized by mechanical alloying. We used specific keywords like "high entropy alloy," "mechanical milling (MM)," and "mechanical alloying" in our searches on the Scopus database to make sure we looked into the data thoroughly. Specifically, we have emphasized the growing interest in HEAs synthesized by MA and the lack of comprehensive reviews that critically analyze this topic. We highlighted that, despite the significant number of studies on HEAs produced by MA, very few offer detailed insights into the synthesis, properties, and applications of these materials. To bridge this gap, we conducted a thorough literature review using Scopus, summarizing findings from 293 Scopus-indexed papers published by December 2024. The inclusion of Table 1 in the introduction provides an overview of the key developments in this area, categorizing research by publication year, phase, and composition, while references ensure comprehensive coverage of the field.

Our aim is to provide a data-driven and critical analysis that advances the understanding of HEAs synthesized by MA, offering clarity on the state of the art and paving the way for further research in this rapidly evolving field. Additionally, Table 2, summarizing all abbreviations, enhances readability and accessibility for the readers.

2. An explanation of high entropy alloys

A great deal of information has been published on the synthesizing, processing, and characteristics of high-entropy materials by Zhang (2019), George (2019), Guo *et al.* (2011), and Chen *et al.* (2018) [345–348]. Two key characteristics of HEAs are proposed to classify the materials based on entropy and concentration criteria. Understanding these two criteria is helpful to understand the characteristics of HEAs compared to the conventional alloys.

2.1. Concentration-based definition

HEAs were originally defined by concentration, as presented by Yeh *et al.* (2004) and Cantor *et al.* (2004) [18,19]. Zhang *et al.* (2014) and Murty *et al.* (2019) elaborated this idea further, characterizing HEAs as complex alloys made up of five or more elements, usually present in roughly equiatomic concentrations ranging from five to thirty-five atomic percent for each component (Fig. 5) [20,21]. Because of their distinct composition, which adds a higher level of compositional complexity, HEAs differ from typical dilute alloys. The inclusion of various elements in almost equiatomic ratios is the fundamental idea of HEAs.By adding a wide range of constituent combinations to the alloys; this method gives HEAs their unique characteristics and importance in materials research.

2.2. Definition based on entropy

HEAs are defined as materials that, in their solid solution phase having high mixing entropy (~1.6 R) [349,350]. This idea is based on the concept that when several components with different atomic sizes and properties are combined into a single and cohesive structure, the degree of disorder and configurational entropy increases. In that sense, HEAs are unique and different from the traditional alloys as the high entropy is essential to the stabilization of solid solution phases. According to Carroll *et al.* (2015), HEAs can be divided into three different classes according to their mixing entropy definitions illustrate in Fig. 5 [351]. (i) Low entropy alloys, often referred to as standard alloys, which consist of one or two main elements in an arbitrary solution state. (ii) Medium entropy alloys usually contain two or four primary elements having moderate mixing entropy. (iii) High entropy alloys have a high degree of mixing entropy (1.6 R) and at least five primary constituents.

The physical properties of HEAs—atomic size difference (δ), valence electron concentration (VEC), mixing entropy (ΔS_{mix}), mixing enthalpy (ΔH_{mix}), and parameter Ω-form the theoretical foundation for HEA development. Many researchers including Guo *et al.* (2015), Zhang *et al.* (2018), Chang *et al.* (2020), and others [352–359], have written extensively about these essential characteristics. These characteristics can be help to understand the stability of HEAs.

As shown in the following formula, configurational entropy of mixing can be expressed as:

$$\Delta S_{mix} = -R \sum C_i \ln C_i \tag{1}$$

Where C_i is molarity and R is a gas constant. According to their mixing entropy value, the alloys are divided into three categories: high entropy alloys (ΔS_{mix}> 1.5 R), medium entropy alloys (1 R < ΔS_{mix}< 1.5 R), and low entropy alloys (ΔS_{mix}< 1 R) [348].

The mixing enthalpy,

$$\Delta H_{mix} = \sum_{i=1}^{n} {}_{i \neq j} \Omega_{ij} C_i C_j \tag{2}$$

$$\Omega ij = 4\Delta H_{mix}^{AB}$$

In this case, ΔH_{mix}^{AB} is the mixing enthalpy of binary liquid AB alloys related to the phase stability of HEAs [360,361]. The mixing enthalpy required by HEA to synthesized a solid solution typically ranges from −15 kJ/mol to 5 kJ/mol. The atomic size difference in the alloy is depicted as another potential evolution parameter of HEA solid solution generation:

$$\delta = 100\sqrt{\sum_{i=1}^{n} C_i\left(1 - \frac{r_i}{\bar{r}_i}\right)^2}, \bar{r} = \sum_{i=1}^{n} C_i r_i \tag{3}$$

Where, C_i and r_i are atomic percentage and atomic radius [362,363].

Hume-Rothery guidelines state that an atomic size difference between one and six is necessary for the production of HEAs [362]. Furthermore, the valence electron concentration (VEC), denoted as VEC $=\sum_{i=1}^{n} C_i (VEC)_i$, can be used to forecast the phase structure of HEAs. Here, $(VEC)_i$ stands for the valence electron concentration of the i-th component [364]. HEA forms BCC when VEC is less than 6.87, BCC-FCC when VEC is between 6.87 and 8, and FCC when VEC is more than 8. The ensuing phases are FCC and BCC. To predict the formation of solid solution HEAs, another important parameter, $\Omega = T_m \Delta S_{mix} / \Delta H_{mix}$, is presented, taking into account the components of ΔS_{mix}, ΔH_{mix}, and the melting temperature (T_m) [365]. The production of a rapid solid solution happens when Ω is greater than 1.1and δ is smaller than 6.6 % [366]. We are able to anticipate the synthesis of HEAs that form solid solutions with five or more components by theoretically computing this thermodynamic property. Fundamentally, the Ω parameter, valence electron concentration, and atomic size difference provide a complete approach to predict the phase structure and formation of solid solution HEAs, which is useful for developing materials synthesis strategies. We have created Table 3 to summarize all the thermodynamic properties of HEAs mentioned above, including their equations, limiting values, and relevance to the synthesis of HEAs. This table is designed to enhance clarity and facilitate easy understanding for the readers.

Numerous researches, including Tong *et al.* (2005), Gaskell *et al.* (2017), Joo *et al.* (2020), and others have shown that HEAs with multi-principal elemental combinations display a variety of distinctive effects shown in Fig. 6 [367–374] which are mentioned as follows. (i) High Entropy: The integration of numerous primary components leads to a high entropy that characterizes HEAs. Their unique qualities are partly due to their high entropy (Fig. 6); (ii) Lattice Distortion: HEAs that have

Table 1
An overview of the literature by year on the synthesis of high-entropy alloys (HEAs) through mechanical milling, with information on phase and composition.

Sr. No.	Years	Composition	Phase	References
1	2008	Al-Fe-Ti-Cr-Zn-Cu	BCC	Varalakshmi, *et al.* [52]
2	2009	Cu–Ni–Al–Co–Cr–Fe–Ti	Amorphous	Chen, *et al.* [53]
3	2009	Co-Cr-Fe-Ni-Cu-Al	BCC+FCC	Zhang, *et al.* [54]
4	2009	Co-Cr-Fe-Ni-Cu-Al	BCC	Zhang, *et al.* [55]
5	2010	Cu-Ni-Co-Zn-Al-Ti	BCC	Varalakshmi *et al.* [56]
6	2010	Cu-Ni-Co-Zn-Al-Ti	FCC+BCC	Varalakshmi, *et al.* [57]
7	2010	Al_{70} -Ni_{10}-Ti_{10}-Zr_5-Ta_5	Amorphous	Wei *et al.* [58]
8	2010	Al-Fe-Ti-Cr-Zn-Cu	BCC+FCC	Varalakshmi, *et al.* [59]
9	2010	Co-Cr-Fe-Ni-Ti-Al	BCC+FCC	Zhang, *et al.* [60]
10	2011	Al-Fe-Cr-Ni	BCC	Vura, *et al.* [61]
11	2011	Ni-Co-Al-Fe-Cu-Cr	BCC+FCC	Gómez-Esparza *et al.* [62]
12	2011	Ni-Co-Al-Fe-Cu-Cr-Ti	BCC+FCC	Gómez-Esparza, *et al.* [63]
13	2012	Al-Co-Cr-Cu-Fe	FCC+BCC	Praveen, *et al.* [64]
14	2012	Ni-Co-Al-Fe-Cr-Ti	BCC+ECC	Esparza, *et al.* [65]
15	2013	Al-Co-Cr-Cu-Fe-Ni	FCC+BCC+B2	Sriharitha, *et al.* [66]
16	2013	Al-Cr-Cu-Fe-Ni-Zn	BCC	Koundinya, *et al.* [67]
17	2013	Al-Co-Cr-Fe	BCC	Praveen, S. *et al.* [68]
18	2013	Cu-Zn-Ti-Fe-Cr	BCC+FCC	Mridha, *et al.* [69]
19	2013	Fe-Ni-Cr-$Co_{0.3}$-$Al_{0.7}$	BCC+FCC	Chen, *et al.* [70]
20	2013	Co-Ni-Fe-Cr-$Al_{0.6}$-$Ti_{0.4}$	BCC+FCC	Fu, *et al.* [71]
21	2013	$Al_{0.6}$-Co-Ni-Fe-$Ti_{0.4}$	BCC+FCC	Chen, *et al.* [72]
22	2013	Al-Co-Cr-Fe-Ni	FCC	Zhu, *et al.* [73]
23	2013	Co-Cr-Fe-Ni-Cu-Al-Ti-X-V-Mo	BCC	Fazakas *et al.* [74]
24	2014	Al-Co-Cr-Cu-Ni-Fe-Zn	BCC	Sivaprasad, *et al.* [75]
25	2014	Al_{20}-Co_{20}-Cu_{20}-Zn_{20}-Ni_{20}	FCC	Mohanty, *et al.* [76]
26	2014	Co-Cr-Fe-Ni-Mn-Al	BCC+FCC	Wang, *et al.* [77]
27	2014	$Al_{0.5}$-Cr-Fe-Ni-$Co_{0.3}$-$C_{0.2}$	FCC+BCC	Fang, *et al.* [78]
28	2014	Al-Co-Cr-Cu-Ni-Fe-Zn	BCC	Sivaprasad, *et al.* [79]
29	2014	Co-Cr-Fe-Ni-Al	BCC	Ji, *et al.* [80]
30	2014	Fe-Si-B-Al-Ni (Nb)	BCC+FCC	Wang, *et al.* [81]
31	2015	Co-Cr-Fe-Ni-Mn	BCC+FCC	Ji, *et al.* [82]
32	2015	$Al_{0.75}$-Fe-Ni-Cr-Co	BCC+FCC	Chen, *et al.* [83]
33	2015	Al-Co-Cr-Fe-Ni and Mn-Co-Cr-Fe-Ni.	BCC+FCC	Ang, *et al.* [84]
34	2015	Al-Co-Fe-Mo-Ni-Ti	BCC	Baldenebro-Lopez, *et al.* [85]
35	2015	Al-Co-Ni-Cr-Fe	BCC	Chen, *et al.* [86].
36	2016	Al-Co-Cr-Cu-Fe-Zn_x	BCC+FCC	Murali, *et al.* [87]
37	2016	Co-Cr-Fe-Cu-Ni	FCC+BCC (minority)	Yu, *et al.* [88]
38	2016	Co-Cr-Fe-Ni-$Mn_{0.5}$-$Ti_{0.5}$	BCC	Niu, *et al.* [89]
39	2016	Ni-Co-Al-Fe-(Cr, Cu, Mo, Ti)	FCC+BCC	Gómez-Esparza, *et al.* [90]
40	2016	Cu-Ni-Co-Zn-Al	FCC	Salemi, *et al.* [91]
41	2016	Al_2-Nb-Ti_3-V_2-Zr	BCC and Intermetallic α and β	Tan, *et al.* [92]
42	2016	Al-Cu-Cr-Fe-Mn-W	BCC+ FCC	Kumar, *et al.* [93]
43	2016	Fe-Si-B-Al-Ni (Co, Cu, Ag)	FCC and Amorphous	Xu, *et al.* [94]
44	2017	Co-Cr-Cu-Fe-Ni	FCC	Thangaraju, *et al.* [95]
45	2017	Al-Co-Cr-Fe-Ni	FCC+BCC	Mohanty, *et al.* [96]
46	2017	$Ni_{1,5}$-$Co_{1,5}$-Cr-Fe-$Ti_{0,5}$	FCC	Moravcik, *et al.* [97]
47	2017	Co-Cr-Fe-Mn-Ni	FCC	Joo, *et al.* [98]
48	2017	Co-Cr-Fe-Ni-W	FCC	Shang, *et al.* [99]
49	2017	Cu-Zr-Al-Ti-Ni	BCC+FCC	Ge, *et al.* [100]
50	2017	Al-Co-Cr-Cu-Fe-Ni	FCC	Ganji, *et al.* [101]
51	2017	Fe-Ni-Co-Cr-Al-Mn	FCC	Prasad, *et al.* [102]
52	2017	Al-Co-Cu-Cr-Fe-Ni-Si_x	BCC	Kumar, *et al.* [103]
53	2017	Al-Mg-Ni-Cr-Ti	BCC	Rameshbabu, *et al.* [104]
54	2017	Fe-Ni-Co-Cr-Al	BCC+FCC	Vaidya, *et al.* [105]
55	2017	Fe-Si-B-Al-Ni-Mo	Amorphousand Nanocrystalline	Bureš, *et al.* [106]
56	2017	Co-Cr-Fe-Ni-Mo	BCC+FCC	Sathiyamoorthi, *et al.* [107]
57	2018	Nb_{25}-Mo_{25}-Ta_{25}-W_{25} and Ti_8-Nb_{23}-Mo_{23}-Ta_{23}-W_{23}	BCC	Pan, *et al.* [108]
58	2018	Fe-Co-Ni-Cr-Mn-Al	FCC	Alcalá, *et al.* [109]
59	2018	Al-Co-Cr-Fe-Ni-Si	FCC+BCC	Tian, *et al.* [110]
60	2018	W-Mo-Nb-Zr-V	BCC	Oleszak, *et al.* [111]
61	2018	W-Mo-V-Cr-Ta	BCC	Das, *et al.* [112]
62	2018	Al-Co-Cr-Fe-Ni-Mn	BCC	Shivam, *et al.* [113]
63	2018	Nb-Mo-Ta-W-V-Ti	BCC+FCC	Long, *et al.* [114]
64	2018	Al-Co-Cr-Fe-Ni-Si_x	BCC+FCC	Kumar, *et al.* [115]
65	2018	Co-Cr-Fe-Ni-Mn	FCC	Xie, *et al.* [116]
66	2018	$Al_{0.3}$-Co-Cr-Fe-Mn-Ni	BCC+FCC	Pohan, *et al.* [117]
67	2018	Fe-Si-B-Al-Ni-Co_x	BCC	Wang, *et al.* [118]
68	2018	Al-Co-Cr-Fe-Ni	BCC	Shivam, *et al.* [119]
69	2018	Al-Co-Cr-Fe	BCC	Praveen, *et al.* [120]
70	2018	Co-Cr-Cu-Fe-Ni-Si_x	BCC+FCC	Kumar, *et al.* [121]
71	2018	Co-Cr-Cu-Fe-Ni-Mo_x	FCC	Yang, *et al.* [122]
72	2019	Fe-Ni-Co-Mn-V	BCC+FCC	Alijani, *et al.* [123]
73	2019	Mo-Nb-Ta-Ti-V	BCC	Wang, *et al.* [124]
74	2019	Fe-Co-Cr-Ni-Mn–Al_x	BCC	Cheng, *et al.* [125]

(*continued on next page*)

Table 1 (*continued*)

Sr. No.	Years	Composition	Phase	References
75	2019	Al-Co-Cr-Fe-Ni	BCC+FCC	Arab, *et al.* [126]
76	2019	Cr-Mn-Fe-Co-Ni	FCC	Tian, *et al.* [127]
77	2019	Fe-Co-Cr-Ni-Mn-$Ti_{0.1}$-$C_{0.1}$	FCC	Liu, *et al.* [128]
78	2019	Al-Co-Cr-Fe-Ni-Ti	BCC	Shivam, *et al.* [129]
79	2019	Al-Cu-Ni-Fe-Cr	BCC+FCC	Yurkova, *et al.* [130]
80	2019	Co-Ni-Fe-Mn-Cr	FCC	Chen, *et al.* [131]
81	2019	Co-Cr-Ni-Cu-Zn	BCC+FCC	Sun, *et al.* [132]
82	2019	Cr-Mo-Nb-Ti-W	BCC+ Laves	Raman, *et al.* [133]
83	2019	Al-Co-Cr-Fe-Ni–ZrO_2	BCC+FCC	Ghanbariha, *et al.* [134]
84	2019	Co-Cr-Cu-Fe-Ni-V-X	FCC	Shu, *et al.* [135]
85	2019	Mo-Nb-Ta-Ti-V	BCC+FCC	Liu, *et al.* [136]
86	2019	Nb-Mo-Ta-W-V-Cr	BCC	Long, *et al.* [137]
87	2019	Cr-Mn-Fe-Co-Ni	FCC	Ni, *et al.* [138]
88	2019	Ti-Al-Ni-Co-Fe	BCC	Sekhar, *et al.* [139]
89	2019	Al-Cr-Fe-Mn-Ni-Ti	BCC+FCC	Mishra, *et al.* [140]
90	2019	Co-Cr-Fe-Ni and Co-Cr-Fe-Mn-Ni	FCC	Vaidya, *et al.* [141]
91	2020	Zr_x-Fe-Ni-$Si_{0.4}$-$B_{0.6}$	Amorphous	Sang, *et al.* [142]
92	2020	Al-Cu-Ni-Fe-Cr	BCC	Chen, *et al.* [143]
93	2020	Al-Co-Cr-Fe-Ni	BCC	Shivam, *et al.* [144]
94	2020	Al-Cr-Cu-Fe-Zn	BCC	Cardoso, *et al.* [145]
95	2020	Al-Co-Cr-Fe-$Ni_{2.1}$	FCC + B2 Phases	John, *et al.* [146]
96	2020	Fe-Co-Ni-$B_{0.5}$-$Si_{0.5}$	FCC	Zaara, *et al.* [147]
97	2020	Fe-Co-Ni-Cu-Zn	FCC	Yingzhe, *et al.* [148]
98	2020	Al_{35}-Cr_{14} -Mg_6-Ti_{35}-V_{10}	BCC	Chauhan, *et al.* [149]
99	2020	Co-Cr-Cu-Fe-Ni	BCC+FCC	Pandey, *et al.* [150]
100	2020	Mg-Al-Si-Cr-Fe	BCC	Singh, *et al.* [151]
101	2020	Al-Co-Fe-Ni-Mo-Ti	BCC	Avila-Rubio, *et al.* [152]
102	2020	Co-Cr-Fe-Ni-Al	FCC+BCC	Rogachev, *et al.* [153]
103	2020	Mg-V-Ti-Cr-Fe	BCC	de Marco, *et al.* [154]
104	2020	Fe-Co-Cr-Ni-Cu	FCC+BCC	Singh, *et al.* [155]
105	2020	Al-Cr-Fe-Mn-Ni-W	BCC+FCC	Dewangan, *et al.* [156]
106	2020	Al-Cr-Fe-Co-Ni-Zn	BCC	Shivam, *et al.* [157]
107	2020	Co-Cr-Fe-Ni-Nb	FCC+HCP (Laves)	Průša, *et al.* [158]
108	2020	Ti-Zr-Nb-Mo-Ta	FCC+BCC	Zhu, *et al.* [159]
109	2020	Ti-Nb-Ta-Mo-Zr	BCC	Normand, *et al.* [160]
110	2020	Hf-Ta-Ti-Nb-Zr	BCC	Shkodich, *et al.* [161]
111	2020	$Cr_{0.26}$-$Fe_{0.24}$ -$Al_{0.5}$ and $Cr_{0.15}$ -$Fe_{0.14}$-$Al_{0.30}$-$Cu_{0.13}$-$Si_{0.28}$	BCC+FCC	Alshataif, *et al.* [162]
112	2020	Cu-Mo-Ta-W-V	BCC	Alvi, *et al.* [163]
113	2020	Cu-Cr-Fe-Ti-Ni	BCC	Shkodich, *et al.* [164]
114	2020	Co-Cr-Fe-Mn-Ni-V	FCC	Vaidya, *et al.* [165]
115	2020	Al-Co-Cr-Fe-Ni	BCC+FCC	Fourmont, *et al.* [166]
116	2020	Fe-Co-$Ni_{1.5}$-Cu-$B_{0.5}$-$Y_{0.2}$	FCC	Wang, *et al.* [167]
117	2020	Co-Cr-Cu-Fe-Ni	FCC+BCC	Ziaei, *et al.* [168]
118	2020	Bi-Sb-$Te_{1.5}$-$Se_{1.5}$	Rhombohedral Crystal structure	Raphel, *et al.* [169]
119	2020	Co-Cr-Cu-Fe-Ni	FCC	Rao, *et al.* [170]
120	2020	Al_{20}-Fe_{20}-Mg_{20}-Ni_{20}-Ti_{20}	FCC+BCC	Mishra, *et al.* [171]
121	2020	(Hf-Ta-Ti-Nb-Zr) C and (Hf-Ta-Ti-Nb-Mo) C	FCC	Moskovskikh, *et al.* [172]
122	2020	Al-Cu-Si-Zn-Fe	BCC+FCC	Sharma, *et al.* [173]
123	2020	Fe-Cr-Ni-Al-Ti	BCC	Yang, *et al.* [174]
124	2020	Fe-Co-Ni-Al-Cr_x	FCC+BCC	Duan, *et al.* [175]
125	2020	$Al_{0.1}$-Co-Cr-Fe-Ni	FCC+BCC	Sokkalingam, *et al.* [176]
126	2020	Nb-Mo-Ta-W	FCC	Roh, *et al.* [177]
127	2020	Al-Co-Cr-Ni	BCC	Vallimanalan, *et al.* [178]
128	2021	Ti-Zr-Hf-Ta-Nb	BCC	Kovalev, *et al.* [179]
129	2021	Co-Fe-Ni-Cr-Mn	FCC	Chen, *et al.* [180]
130	2021	Co_x-Cr-Cu-Fe-Mn-Ni	FCC+BCC	Zhang, *et al.* [181]
131	2021	Al_x-Co-Cr-Fe-Mn-Ni	FCC+BCC	Ruiz-Esparza-Rodríguez, *et al.* [182]
132	2021	$Al_{0.3}$-Cr-Fe-Ni-$Co_{0.3}$-$Si_{0.4}$	BCC+FCC	Ammar, *et al.* [183]
133	2021	Al-Co-Cr-Fe-Ni	FCC+BCC	Rogachev, *et al.* [184]
134	2021	Ni-Fe-Co-Cr	FCC	Chen, *et al.* [185]
135	2021	Al-Cr-Fe-Mn-Ni-W_x ($x = 0, 0.05, 0.1, 0.5$)	Ordered B2 + BCC+FCC	Dewangan, *et al.* [186]
136	2021	Mg-Al-Mn-Fe-Cu	C15 Laves Phase and B2	Pandey, *et al.* [187]
137	2021	Mg-Al-Ti-Fe-Ni	BCC	Cardoso, *et al.* [188]
138	2021	Al-Cr-Fe-Ni-Ti	BCC	Bololoi, *et al.* [189]
139	2021	Al-Ni-Co-Fe-Cr-Ti	B2 and σ Phase	Yurkova, *et al.* [190]
140	2021	Nb-Mo-Ta-W	BCC	Nam, *et al.* [191]
141	2021	Al-Co-Cr-Fe-Ni	BCC+FCC	Parakh, *et al.* [192]
142	2021	Al-Co-Cr-Fe-Ni	BCC+FCC	Fourmont, *et al.* [193]
143	2021	Co-Cr-Fe-Mn-Ni-$Ti_{0.1}$	FCC	Akhlaghi, *et al.* [194]
144	2021	Al-Cu-Fe-Mn-$Ti_{-0.75}$-Si	BCC	Kim, *et al.* [195]
145	2021	Nb-Ta-Ti-Zr	BCC	Xiang, *et al.* [196]
146	2021	$(Ni_{40}$-Fe_{30}-Co_{20}-$Al_{10})_{90}Ti_{10}$	FCC	Wang, *et al.* [197]
147	2021	Al-Cu-Fe-Mn-Ti-X (X = Mg, Si)	BCC	Chae, *et al.* [198]

(*continued on next page*)

Table 1 (*continued*)

Sr. No.	Years	Composition	Phase	References
148	2021	Co-Cr-Fe-Ni/Al	BCC +FCC	Liu, *et al.* [199]
149	2021	Fe-X-Co-Cr-Ni	BCC+FCC	Moazzen, *et al.* [200]
150	2021	Mg-Al-Si-Cr-Fe-Ni	BCC+FCC	Singh, *et al.* [201]
151	2021	Al_2-Cr-Fe-Mn-Ti	BCC, Laves C14, and L21 Phases.	Jahangiri, *et al.* [202]
152	2021	Co-Cr-Fe-Ni-Y_2-O_3	FCC	Tekin, *et al.* [203]
153	2021	Al_2-Nb-Ti_3-V_2-Zr_x	BCC + Intermetallic	Zhi, *et al.* [204]
154	2021	Co-Cr-Fe-Ni-Mn	FCC	Liao, *et al.* [205]
155	2021	Al-Cr-Fe-Ni-X (X = Cu, Si, Co)	FCC+BCC + Intermetallic	Erdogan, *et al.* [206]
156	2021	Mg-Al-Si-Cr-Fe	BCC	Singh, *et al.* [207]
157	2021	Al-Co-Cr-Cu-Fe-Ni-Si_x (x = 0 and 0.9)	BCC+FCC	Chandrakar, *et al.* [208]
158	2021	Al-Co-Cr-Ni-Ti–C	B2 Phase	Sekhar, *et al.* [209]
159	2021	Al_x-Cr-Nb-V-Mo	BCC	Kang, *et al.* [210]
160	2021	Al-Co-Cr-Fe-Ni–Zr-O_2	FCC+BCC	Ghanbariha, *et al.* [211]
161	2021	Fe_{35}-Mn_{10}-Cr_{20}-Ni_{35}	FCC	Zhou, *et al.* [212]
162	2021	Cu-Cr-Fe-Ni-Ti-Al_x	FCC+BCC	Ruiz-Jasso, *et al.* [213]
163	2021	Cu-Cr-Fe-Ti-V	BCC+FCC	Antão, *et al.* [214]
164	2021	$Cr_{0.21}$-$Fe_{0.20}$-$Al_{0.41}$-$Cu_{0.18}$and $Cr_{0.14}$-$Fe_{0.13}$-$Al_{0.26}$-$Cu_{0.11}$-$Si_{0.25}$-$Zn_{0.11}$	BCC+FCC	Alshataif, *et al.* [215]
165	2021	Fe-Co-Ni-Cr-Al and Fe-Co-Ni-Cr-Mn	FCC+BCC	Xue, *et al.* [216]
166	2021	Al-Cu-Fe-Mn-Mg-Ti	BCC	Chae, *et al.* [217]
167	2021	Fe-Cr-Cu-Mn-Ti	FCC+BCC, and HCP	Sivasankaran, *et al.* [218]
168	2021	Co_{35}-Cr_5-Fe_{20-x}-Ni_{20+x}-Ti_{20}	FCC + Intermetallic	Mishra, *et al.* [219]
169	2021	Cr-Cu-Fe-Ni-Zn	FCC+BCC	Rao, *et al.* [220]
170	2021	Cu-Ni-Co-Zn-Al	FCC	Salemi, *et al.* [221]
171	2021	Al-Co-Fe-Ni-Zn and Al-Co-Fe-Ni-Mo-Ti-Zn.	BCC+FCC	Avila-Rubio, *et al.* [222]
172	2021	Al-Co-Cr-Fe-Ni-X (X = Cu, Mn, Ti)	FCC+BCC	Oh, *et al.* [223]
173	2021	Fe-Ni-Co-Cr and Fe-Ni-Co-Cr-Mn	FCC	Chu, *et al.* [224]
174	2021	Al_x-Co-Cr-Cu-Fe-Ni	BCC+FCC	Ziaei, *et al.* [225]
175	2022	Fe-Cr-Co-Ni-Cu	FCC+BCC	Toroghinejad, *et al.* [226]
176	2022	$Al_{0.8}$-$Co_{0.5}$-$Cr_{1.5}$-Cu-Fe-Ni	FCC+BCC	Huang, *et al.* [227]
177	2022	Co-Cr-Fe-Ni-Cu	FCC	Shkodich, *et al.* [228]
178	2022	Co-Cr-Ni-Ti-Mo_x	BCC	Addepalli, *et al.* [229]
179	2022	Co-Cr-Fe-Ni-$Al_{0.3}$	FCC+BCC	Zhang, *et al.* [230]
180	2022	Ni-Co-Cr-Al-Si	FCC	Shahbazkhan, *et al.* [231]
181	2022	Al-Fe-Cu-Zn-Ti	BCC	Daryoush, *et al.* [232]
182	2022	Ti-Al-$V_{0.5}$-Cr-Mo	BCC	Gao, *et al.* [233]
183	2022	Al-Co-Cr-Mn-Mo	BCC	Avila-Rubio, *et al.* [234]
184	2022	Al-Cr-Cu-Mn-Ni	FCC+ BCC	Toroghinejad, *et al.* [235]
185	2022	Al-Co-Cr-Fe-Ni-Ti-Zn	FCC +BCC	Kalantari, *et al.* [236]
186	2022	Ni-Mn-Fe-Cu	FCC	Kumar, *et al.* [237]
187	2022	W-Ta-Mo-Nb-V	BCC	Hu, *et al.* [238]
188	2022	Al-Cu-Fe-Mn-Ti-V	BCC+HCP	Zhang, *et al.* [239]
189	2022	Al-Co-Fe-Cr-V-Ni and Al-Co-Fe-Cr-V-Ti	BCC+FCC	Yurkova, *et al.* [240]
190	2022	Fe-Co-Ni-Cu_x- Mn	BCC+FCC	Zhou, *et al.* [241]
191	2022	Fe-Co-Ni-Cr-Nb	FCC+ Amorphous	Yakın, *et al.* [242]
192	2022	Al_x Co-Cr-Fe-Ni (x = 0, 0.3, 0.6, 1 mol)	BCC+FCC	Bhattacharya, *et al.* [243]
193	2022	Mg_{35}-Al_{15}-Ti_{25}-V_{10}-Zn_{15}	BCC+FCC	de Brito Ferraz, *et al.* [244]
194	2022	Al-Co-Cr-Fe-Mn-Ni	BCC	Abdi, *et al.* [245]
195	2022	Co-Cr-Fe-Mn-Ni	FCC	Nagarjuna, *et al.* [246]
196	2022	Mo-Nb-Si-Ti-W	BCC	Prakash, *et al.* [247]
197	2022	Cr-Nb-Mo-W-V	BCC	Tagir, *et al.* [248]
198	2022	$(Co\text{-}Cr\text{-}Fe\text{-}Ni\text{-}Mn)_{90}M_{10}$ (M = Al, Hf)	Amorphous	Wang, *et al.* [249]
199	2022	(Hf-Mo-Ti-W-Zr) C	FCC	Kavak, *et al.* [250]
200	2022	W_{10}-Mo_{27}-Cr_{21}-Ti_{22}-Al_{20}	BCC	Naser-Zoshki, *et al.* [251]
201	2022	Al-Co-Cr-Fe-Ni	BCC+FCC	Rao, *et al.* [252]
202	2022	Fe–Cr–Ni–Mo–W	FCC+BCC	Ivannikov, *et al.* [253]
203	2022	Co-Cr-Fe-Ni	FCC	Sure, *et al.* [254]
204	2022	Co-Cr-Fe-Ni-X, where X = Al, Cu, Mn, or Ti	FCC	Rogachev, *et al.* [255]
205	2022	Al-Cr-Fe-Mn-Mo	BCC	Stasiak, *et al.* [256]
206	2022	Al-Fe-Ni-Cr-Co-$Ti_{0.5}$	FCC +BCC	Huan, *et al.* [257]
207	2022	Ni_2-Cu-Cr-Fe-Al_x	BCC	Kush, *et al.* [258]
208	2022	$Al_{0.8}$-Cr-Fe-$Ni_{2.2}$	FCC+BCC	Vo, *et al.* [259]
209	2023	Al-Cr-Fe-Ni-Ti-Zn	FCC+BCC	Kalantari, *et al.* [260]
210	2023	Ni_{46}-Al_{12}-Co_{18}-Cr_8-Fe_{12}-Mo_4	FCC	Maharana, *et al.* [261]
211	2023	Fe-Co-Cr-Ni-Al	BCC+FCC	Cheng, *et al.* [262]
212	2023	Co-Cr-Cu-Fe-Mn-Ni_x	FCC	Zhang, *et al.* [263]
213	2023	Li-Mg-Al-Ti and Li-Mg-Al-Ti-V	HCP and BCC	Hashimoto, *et al.* [264]
214	2023	Co-Cr-Fe-Ni-Ti	FCC	Rogachev, *et al.* [265]
215	2023	Al-Co-Cr-Fe-Ni	FCC+BCC	Kambarov, *et al.* [266]
216	2023	Al-Co-Ti-Zn	HCP+BCC	Yebaji, *et al.* [267]
217	2023	Al-Co-Cr-Fe-$Ni_{2.1}$	BCC+FCC	Li, *et al.* [268]
218	2023	Cr-Mn-Fe-Co-Mo	BCC	Pradhan, *et al.* [269]
219	2023	Co-Cr-Cu-Fe-Ni	FCC	Liu, *et al.* [270]
220	2023	Hf-Mo-Nb-Ta-Ti	BCC	Zhan, *et al.* [271]
221	2023	Al-Fe-Ni-Ti-Zn	FCC+BCC	Kalantari, *et al.* [272]
222	2023	Cu-Cr-Fe-Ti-Ni	FCC+BCC	Zeraati, *et al.* [273]
223	2023	Fe_{30}-Co_{20}-Ni_{20}-Mn_{20}-Al_{10}	FCC	Ammar, *et al.* [274]

(*continued on next page*)

Table 1 (*continued*)

Sr. No.	Years	Composition	Phase	References
224	2023	(Fe-Co-Ni)$_{75}$Cu$_{25-x}$Si$_x$	FCC	Javdan, *et al.* [275]
225	2023	Fe$_{30}$-Co$_{20}$-Ni$_{20}$-Mn$_{20}$-Al$_{10}$	FCC	Ammar, *et al.* [276]
226	2023	Al$_{0.1-0.5}$(Mn)-Co-Cr-Fe-Ni	BCC+FCC	Özbilen, *et al.* [277]
227	2023	Ti-Al-V$_{0.5}$-Cr-Mo	BCC	Gao, *et al.* [278]
228	2023	Fe$_{40}$-Mn$_{19}$-Ni$_{15}$ -Al$_{15}$-Si$_{10}$-C$_1$	BCC	Jain, *et al.* [279]
229	2023	Al-Co-Fe-Mn-Ni	FCC+BCC	Pourmohammadi, *et al.* [280]
230	2023	Ni-Mn-Fe-Cr-Cu	FCC+BCC	Kumar, *et al.* [281]
231	2023	Co-Cr-Fe-Ni-Si	FCC	Yaykaşlı, *et al.* [282]
232	2023	Co-Cr-Fe-Mn-Ni–Al$_2$-O$_{3p}$	FCC	Dai, *et al.* [283]
233	2023	Ti-Nb-Mo-Ta-W	BCC	Sarkar, *et al.* [284]
234	2023	Fe-Cr-Co-Ni-Mn	FCC+BCC	Alleg, *et al.* [285]
235	2023	Al-Cr-Fe-Ni-Cu and Al-Cr-Fe-Nb-Mo	BCC+FCC	Chen, *et al.* [286]
236	2023	Co$_x$-Cr-Fe-Ni-Ti	BCC+FCC	Manea, *et al.* [287]
237	2023	Al-Co-Ni-Fe and Al-Co-Ni-Fe-Cr	BCC	Nazaretyan, *et al.* [288]
238	2023	Al-Co-Cu-Fe-Ni	FCC	Mansouri, *et al.* [289]
239	2023	Al-Co-Fe-Ni-Ti-Zn	FCC+BCC	Kalantari, *et al.* [290]
240	2023	Fe-Co-Ni-Mn-Al	FCC+BCC	Luo, *et al.* [291]
241	2023	Cr-Mn-Fe-Co-Ni	FCC	Xing, *et al.* [292]
242	2023	Fe-Co-Ni-Al	BCC+FCC	Lee, *et al.* [293]
243	2023	Cr-Cu-Fe-Ni-Ti-Alx	FCC+BCC	del Ángel-González, *et al.* [294]
244	2023	Al-Si-Cr-Mn-Fe-Ni-Cu	B2-type	Shadangi, *et al.* [295]
245	2023	W-V-Ta-Ti-Cr	BCC	Chen, *et al.* [296]
246	2023	W-Nb-Mo-V-Ta	BCC	Boztemur, *et al.* [297]
247	2023	Fe-Ni-Mn-Cu	FCC+BCC	Jahani, *et al.* [298]
248	2023	Alx-Co-Cr-Fe-Ni-Nb-$_{1\text{-}x}$-Si$_{0.\ 1}$	BCC	Nozari Nezhad, *et al.* [299]
249	2023	Fe-Co-Ni-Mn-V$_x$	FCC+BCC	Zhou, *et al.* [300]
250	2024	Al-Co-Mo-Fe-Ni	BCC+FCC	Verma, *et al.* [301]
251	2024	Al–Ti–Fe–Mn–Ni	BCC + Intermetallic	Sharma, *et al.* [302]
252	2024	Co-Cr-Fe-Mn-Ni	FCC	Bulut, *et al.* [303]
253	2024	Ni$_{25}$-Co$_{20}$-Cu$_{10}$-Fe$_{25}$-Mn$_{20}$	FCC	Mamnooni, *et al.* [304]
254	2024	Co-Cr-Fe-Ni	FCC	Olejarz, *et al.* [305]
255	2024	Al-Co-Cr-Fe and Al-Co-Cr-Fe-Ni	BCC+FCC	Custodio, *et al.* [306]
256	2024	Al-Co-Cu-Ni-Ti	BCC+FCC	Okumuş, *et al.* [307]
257	2024	Al-Co-Cr-Fe-Ni	FCC+BCC	Rao, *et al.* [308]
258	2024	Co-Cr-Fe-Ni-Ta	FCC + Laves Phases	Tang, *et al.* [309]
259	204724	Ni-Al-Fe-Co-Cr	FCC+BCC	Sushma, *et al.* [310]
260	2024	Fe-Mn-Ni-Cr-Al	FCC+BCC	Abbas, *et al.* [311]
261	2024	Co$_{20}$-Cr$_{20}$-Fe$_{20}$-Mn$_{20}$-Ti$_{20}$ and Co$_{20}$-Cr$_{20}$-Fe$_{20}$-Mn$_{20}$-Ti$_{20}$-Ni$_{20}$	BCC+FCC	Datta, *et al.* [312]
262	2024	Al-Co-Cr-Fe-Ni	B2 +FCC	Kratochvíl, *et al.* [313]
263	2024	Nb-Mo-Ta-W-V-C	BCC	Han, *et al.* [314]
264	2024	Al-Co-Cu-Mn-Ni and Al$_{0.25}$-Co-Cu-Mn-Ni	FCC	Mohammadi, *et al.* [315]
265	2024	Co-Cr-Fe-Mn-Ti-Ni	BCC+FCC	Datta, T., *et al.* [316]
266	2024	Fe-Co-Ni-Cr	FCC	Basem, *et al.* [317]
267	2024	Al-Co-Cr-Fe-Ni–ZrO$_2$	FCC+BCC	Hajilou, *et al.* [318]
268	2024	Cu-diamond/Cu-diamond-Cu$_2$NiAlAgZn	FCC	Sun, *et al.* [319]
269	2024	Cr-W-Ti-Mo-Nb	BCC	Simsek, *et al.* [320]
270	2024	Ta-Mo-Nb-Cr-Tix	BCC + Laves Phase	Gao, *et al.* [321]
271	2024	Cu$_{40}$-Fe$_{30}$-Mn$_{20}$-Cr$_5$-Ti$_5$	FCC	Sharma, *et al.* [322]
272	2024	Zr-Nb-Ta-Mo-W	BCC	Sakar, *et al.* [323]
273	2024	Co$_{35}$-Fe$_{10}$-Ni$_{30}$-Ti$_{20}$-M$_5$(M= Mn, Cu, and Al)	FCC+BCC	Mohapatra, *et al.* [324]
274	2024	Mo-Nb-Zr-Ti-V	BCC+HCP	Tolentino, *et al.* [325]
275	2024	(Fe-Co-Ni)$_{75}$Cu$_{25\text{-}x}$Si$_x$	FCC+BCC+ Intermetallic	Javdan, *et al.* [326]
276	2024	W-Ta-V-Cr	BCC	Yoo, *et al.* [327]
277	2024	Co$_{0.22}$-Cr$_{0.23}$-Fe$_{0.29}$-Ni$_{0.20}$-Ti$_{0.06}$	FCC	Kovalev, *et al.* [328]
278	2024	Fe-Co-Ni-Mn-Cr	FCC	Mane, *et al.* [329]
279	2024	Ti$_{62}$-Nb$_{12}$-Mo$_{12}$-Ta$_{12}$-W$_2$	BCC+FCC	Chen, *et al.* [330]
280	2024	Fe-Co-Cr-Ni-Mn	FCC	Wang, *et al.* [331]
281	2024	WC/Al-Co-Cr-Fe-Ni-Ti$_{0.5}$	BCC+FCC	Wang, *et al.* [332]
282	2024	Fe-Ni-Mn-Cu-X (X: Co, Cr, Mo, Ti, W)	FCC+BCC	Jahani, *et al.* [333]
283	2024	Nb-Ta-Zr-Mo-W	BCC	Zakir, *et al.* [334]
284	2024	Ti-V-Fe-Ni, (Ti-V-Fe-Ni) $_{95}$- Zr$_5$ and (Ti-V-Fe-Ni)$_{90}$ Zr$_{10}$	BCC+FCC	Singh, *et al.* [335]
285	2024	Cu$_{40}$-Zn$_{24}$-Ni$_{24}$-Ag$_8$-Hg$_4$	FCC	Sharma, *et al.* [336]
286	2024	Fe$_{40}$-Mn$_{20}$-Cr$_{20}$-Ti$_{10}$-Al$_{10}$	BCC+FCC	Jain, *et al.* [337]
287	2024	(Nb-Mo-Ta-W-V) C	BCC+BCT	Han, *et al.* [338]
288	2024	Fe-Ni-Co-Cu-Mo.	FCC	Jimenez-Arevalo, *et al.* [339]
289	2024	Co-Cr-Fe-Ni-Y$_2$O$_3$	FCC+BCC	Zhao, *et al.* [340]
290	2024	Cr-Cu-Fe-Ni-Zn	BCC+FCC	Rao, *et al.* [341]
291	2024	Fe-Ni-Mn-Cu	BCC+FCC	Jahani, *et al.* [342]
292	2024	Al$_{10}$-Cr$_{25}$-Co$_{20}$-Ni$_{25}$-Fe$_{20}$	BCC+FCC	Jeyasimman, *et al.* [343]
293	2024	Co-Cr-Ni-Fe-Ta$_x$	FCC+BCC	Chen, *et al.* [344]

Table 2
List of abbreviations used in the study.

S. No.	Name	Abbreviated name
1	High entropy alloy	HEA
2	Mechanical alloying	MA
3	Additive manufacturing	AM
4	Spark plasma sintering	SPS
5	Severe plastic deformation	SPD
6	High-energy ball milling	HEBM
7	Mechanical milling	MM
8	High entropy oxides	HEOs

a lot of components deviate from typical crystal forms due to lattice distortion. Improved mechanical and functional qualities may result from this; (iii) Sluggish Diffusion: Compared to other alloys, the complicated atomic organization in HEAs causes slower atomic diffusion. The processing and performance of the alloy may be impacted by this slow diffusion; (iv) Cocktail Effects: Cocktail effects are the synergistic interactions that occur when numerous ingredients are present in HEAs at the same time. When these interactions occur, materials with simple solid solution may be synthesized.

3. Methods used to process HEAs

By overcoming the constraints of conventional materials, Zhang *et al.* have presented a breakthrough design idea for HEAs in their work [375]. As more is learned about this emerging field of study, HEAs demonstrate increased adaptability and a wider range of compositional designs. Many new HEA variants have been developed, such as nano-HEAs, amorphous HEAs, two-phase or even multi-phase HEAs, in addition to the traditional structures that can produce ordered or disordered solid solutions. In order to expedite the development and implementation of high-entropy alloys, it is necessary to implement high-throughput technology to simplify the processes of HEAs preparation and characterization. HEAs can be obtained using a range of processing techniques, as described by Alshataif *et al.* (2020) and Moghaddam *et al.* (2021), each of which has advantages and disadvantages [376,377]. Among all techniques, MA stands out for its effectiveness for several reasons, as illustrated by the mechanical alloying process shown in Fig. 7. This is a detailed examination of several approaches, with an emphasis on the reasons that MA is regarded as the most effective. (i) Casting and Melting: Using this conventional process, the constituent parts of HEAs are melted and then cast into the appropriate shape. Large-scale HEA production is appropriate with it [378–380]. (ii) Powder metallurgy: Using this technique, powdered ingredients are blended, compacted, and sintered resulting in HEAs. It is appropriate for both bulk and nanocrystalline HEAs because it permits control over microstructure and content [29,381,382]. (iii) Additive manufacturing (AM): Often referred to as 3D printing, AM builds HEAs layer by layer using a CAD model. It increases the application possibilities of HEAs by permitting complex geometries and variable design [383–385]. (iv) Spark plasma sintering (SPS): It is a fast-sintering method that solidifies powdered HEA precursors by using pressure and pulsed direct current. It is well known to produce HEA materials that are thick and finely grained [386–388]. Fig. 8 provides a detailed overview of the general process for ball milling and spark plasma sintering [389]. (v) Casting and rapid solidification: This process prevents the production of coarse grains by quickly cooling molten HEAs to generate amorphous or nanocrystalline structures [386]. (vi) Electrodeposition: To alter surface characteristics and prevent corrosion, HEA coatings are electrochemically applied to substrates [390,391]. (vii) Mechanical Alloying: An atomically homogenous mixture of elemental

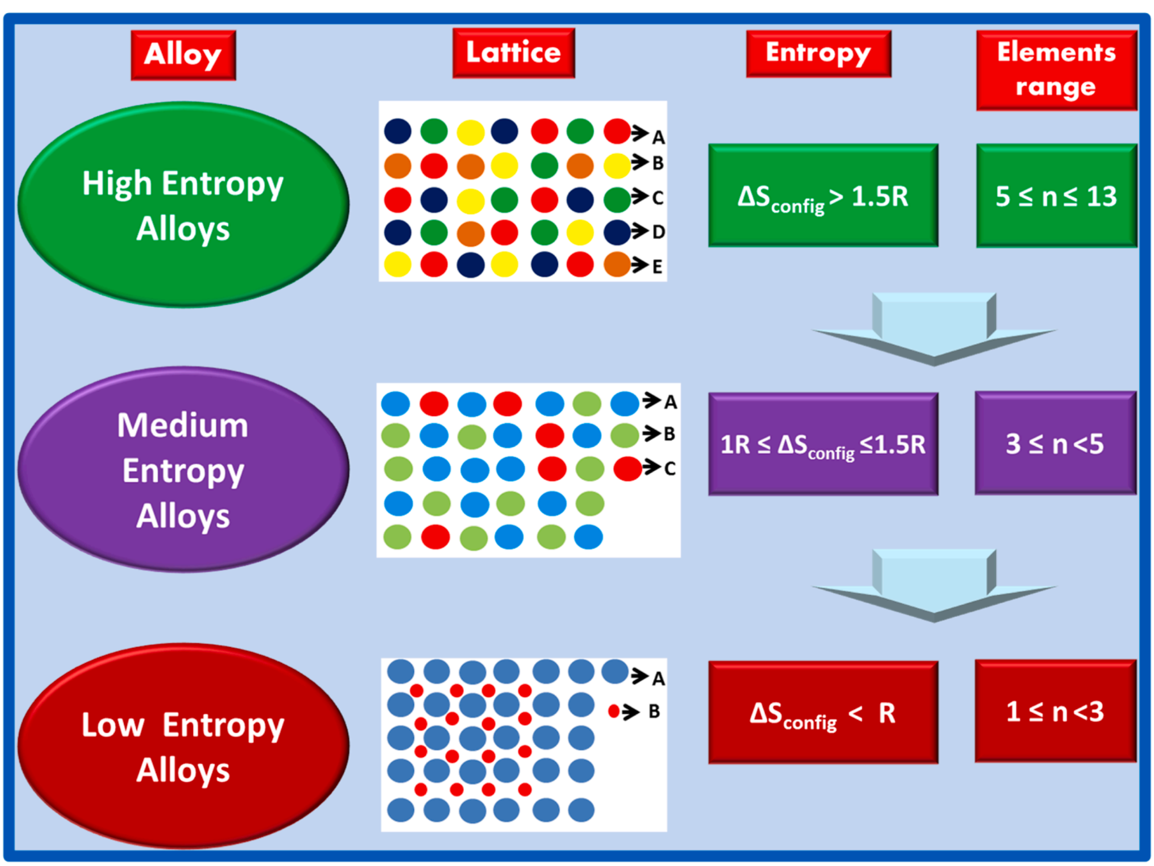

Fig. 5. An illustration of how HEAs are categorized according to the ranges of elemental composition and corresponding configurational entropy. Plotting HEAs' major elements and the associated configurational entropy against a lattice representation of how the HEAs are categorized.

Table 3
Summary of the thermodynamic properties of HEAs, including their equations, limiting values, and their relevance to the synthesis of HEAs.

Sr. No	Thermodynamic Properties	Formula	Limiting Values and Criteria for Phase
1	Mixing Entropy (ΔS_{mix})	$\Delta S_{mix} = -R \sum C_i \ln C_i$	High Entropy Alloys ($\Delta S_{mix} >$ 1.5 R), Medium Entropy Alloys (1 R < $\Delta S_{mix} <$ 1.5 R), and Low Entropy Alloys ($\Delta S_{mix} <$ 1 R)
2	Mixing Enthalpy (ΔH_{mix})	$\Delta H_{mix} = \sum_{i=1\ i\neq j}^{n} \Omega_{ij} C_i C_j \quad \Omega_{ij} = 4\Delta H_{mix}^{AB}$	Solid Solution Typically Ranges from −15 kJ/mol to 5 kJ/mol
3	Valence Electron Concentration (VEC)	$VEC = \sum_{i=1}^{n} C_i (VEC)_i,$	HEA forms BCC When VEC is Less than 6.87, BCC-FCC When VEC is between 6.87 and 8, and FCC More than 8.
4	Atomic Size Difference (δ)	$\delta = 100\sqrt{\sum_{i=1}^{n} C_i \left(1 - \frac{r_i}{\bar{r}_i}\right)^2}, \bar{r} = \sum_{i=1}^{n} C_i r_i,$	Solid Solution Happens When δ is Smaller than 6.6 %
5	Parameter (Ω)	$\Omega = T_m \Delta S_{mix} / \Delta H_{mix},$	Solid Solution Happens When Ω is Greater than 1.1

powders can be produced by employing high-energy ball milling (HEBM) in a solid-state process [44,47]. The distinct benefits that each of these techniques provides for handling HEAs add to their adaptability and usefulness in a range of commercial and academic settings. The process for fabricating HEAs via solid-state processing (SSP) techniques is illustrated in Fig. 8 and Fig. 9 [392]. This approach includes mixing of multiple alloying elements at room temperature and subsequently consolidating them at higher temperatures. Among these, MA is especially well established due to its capacity to accomplish uniform element mixing, exact control over alloy composition, and effective scalability.

This process produces nanocrystalline HEAs with remarkable efficiency and yields material quality. An in-depth analysis of MA will be covered in the section that follows.

4. Mechanical alloying/milling (MA/MM)

The MA is one of the greatest solutions for addressing the synthesis of HEAs since it is scalable for industrial applications, produces nanocrystalline structures with superior mechanical properties, and allows for fine control over alloy composition. When synthesizing complex HEA materials, MA is the method of choice due to its adaptability and effectiveness over melting and casting techniques. Vaidya *et al.* (2019) presented the MA approach for making HEAs, which combines many procedures utilizing MA to achieve a homogeneous blend of constituent powders at the nanoscale [47]. To achieve a homogeneous mixture at the atomic or nanoscale, powder particles undergo repeated deformation, fracturing, and fusion in a process known as MA, as illustrated in Fig. 7 [36]. This method is frequently employed to generate alloys and composite materials. The following steps are usually involved in the process (Fig. 7).

4.1. Powder blending

The final properties of the resulting alloy are dictated by the selection and proportioning of constituents, which are fine powders of elemental or compound materials or in combination. In order to effectively achieve a uniform combination of constituent powders, powder blending is a critical and important step [36,393]. To prepare alloy formation, this process is crucial for determining the initial composition and uniform distribution.

4.1.1. Significance and method of powder blending for HEA synthesis

The importance of powder blending in establishing microscale uniformity and composition control has been highlighted in literature [380,394,395]. For mechanical alloying to be effective, achieving microscale homogeneity requires blending the powders until all elements are uniformly distributed. In the end, a well-mixed, uniformly dispersed alloy is formed by this homogenous blending, which produces a constant reaction environment that is necessary for starting and maintaining reactions during milling. It is important to achieve a homogeneous distribution of the powders by using strong mixing procedures, such as shaking or mechanical stirring. Process the powder in an inert environment (such as nitrogen or argon) to avoid undesired reactions or oxidation, depending on how reactive the elemental powders are. The combined powders are put in a milling container that is appropriate for the task. These containers are usually constructed of materials that are compatible with the mechanical alloying process such as tungsten carbide or hardened steel. Sealing the container reduces the chance of contamination by maintaining a regulated environment. A homogenous HEA is formed by the subsequent milling process, which is facilitated by successful powder blending and involves the use of HEBM or other MA processes to further purify the mixture.

4.2. High-energy ball milling (HEBM)

High-energy ball mill is a mechanical device used to give the particles high kinetic energy to the powder mixture [44,396–399]. These powder particles are subjected to impact with the balls made of steel or ceramic during the milling process. The collision causes the particles to fracture, deform plastically, and cold weld as shown in Fig. 10[400]. HEBM is necessary for producing an atomic or nanoscale homogeneous mixture of elemental powders [401–403]. This exact level of mixing is required for the development of HEAs, which are composed of multiple primary elements. HEBM enhances reactivity leading to the formation of new surfaces and interfaces that can improve the diffusion among the elements during the milling process. This technique is capable to produce a nanocrystalline structure with a finely-grained microstructure. The cold welding and controlled deformation can customize the HEA's microstructure (Fig. 10) [404]. Comparing HEBM to conventional procedures, it turns out to be an incredibly quick and effective way to synthesize HEAs. Strong mechanical forces used during milling speed up the alloying process and cut down on the amount of time needed for synthesis.

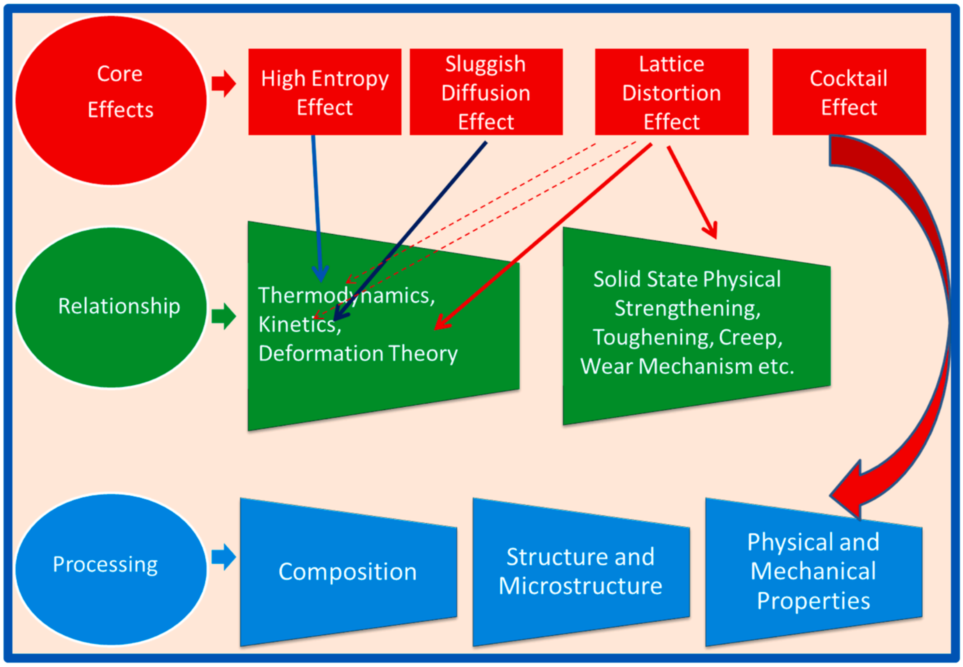

Fig. 6. The four basic effects of HEAs and their impact on microstructure and properties are explored. It also demonstrates how these effects interact to form the unique microstructural features and performance characteristics of HEAs, underscoring their potential benefits in a range of advanced applications.

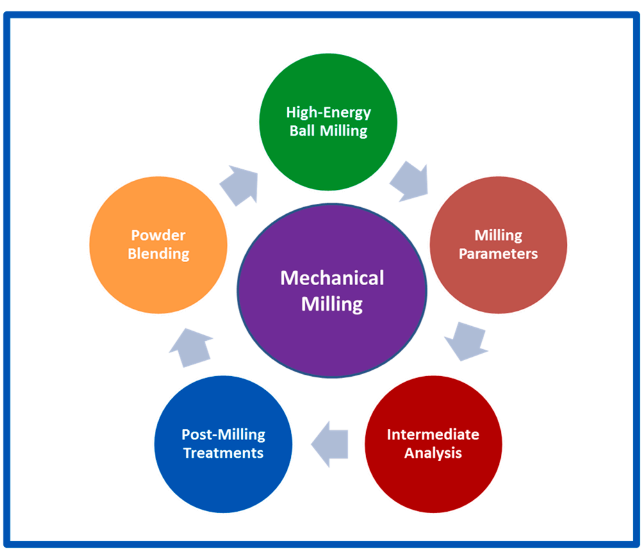

Fig. 7. The mechanical milling process and its workflow are described in detail in the schematic picture, which also highlights the important processes and how they contribute to the creation of HEAs for different purposes.

4.2.1. Method of HEBM for HEA synthesis

To keep the environment under control and to avoid contamination and oxidation, the grinding container should be sealed properly. The ball-to-powder ratio, milling time, and milling speed should be optimized depending on the desired HEA qualities as the particle size, microstructure, and alloying degree are all influenced by these factors. The powder particles repeatedly fracture, distort, and undergo cold welding (Fig. 10). The milling operation can be stopped occasionally to avoid excessive heating, and to assess the powder mixture at intermediate states. The post-milling treatments, such as annealing or sintering are conducted to further refine the microstructure and improve the characteristics of the synthesized HEA, depending on the specific requirements.

4.2.2. Milling parameters and optimization strategy

A crucial part of the HEBM process for the synthesis of HEAs is controlling milling parameters such as milling time, speed, ball-to-powder ratio, and process control agents (PCAs) [405–407]. Helia *et al.* (2023) reports a high-entropy Al-Fe-Ni-Ti-Zn alloy with crystallites that are around 35 nm in size and both FCC and BCC crystallization phases was synthesized [272]. Using a high-energy planetary ball mill in an argon atmosphere, the alloy was synthesized with the following specifications: a ball-to-powder mass ratio of 1:20 and a milling time of 120 hours at 350 rpm. Ethanol (99.7 %, approximately 5 ml) has been used as a process control agent (PCA) to stop cold welding during the procedure. Shkodich *et al.* (2022) reported the synthesis of an FCC-structured Co-Cr-Fe-Ni-Cu HEA with a grain size of 8 nm [228]. The alloy was prepared using HEBM for 120 minutes at 694/1388 rpm. Stainless steel cylindrical jars and 7 mm diameter balls were employed, with a ball-to-powder weight ratio of 20:1. The vial was filled with argon gas at a pressure of 4 bar to maintain an inert atmosphere during the process.

According to Daryoush *et al.* (2022), every parameter plays a critical role in defining the final microstructure and properties of the alloy [408]. The alloy is significantly impacted by the milling period, or the length of the HEBM operation. Extended milling periods lead to higher energy input into the powder mixture, resulting in more deformation, fracture, and cold welding. This can enhance homogeneity and produce finer particle sizes. However, excessively long milling times may introduce adverse effects like increased contamination or grain coarsening. Milling speed, the rate at which the milling container rotates, determines the velocity of the milling balls. Higher milling speeds cause more intense collisions between the balls and powder particles. This accelerates the milling process, resulting in finer particles and more uniform mixing. However, very high speeds can raise the temperature inside the milling chamber, leading to unwanted thermal effects. The ball-to-powder ratio, the mass of the milling balls relative to the powder mixture, also plays a critical role. Higher ratios result in more ball impacts per unit of powder, promoting a more vigorous milling process. This typically enhances homogeneity, reactivity, and produces finer particle sizes. However, extremely high ratios can lead to excessive wear on the milling container and balls, necessitating frequent replacements.

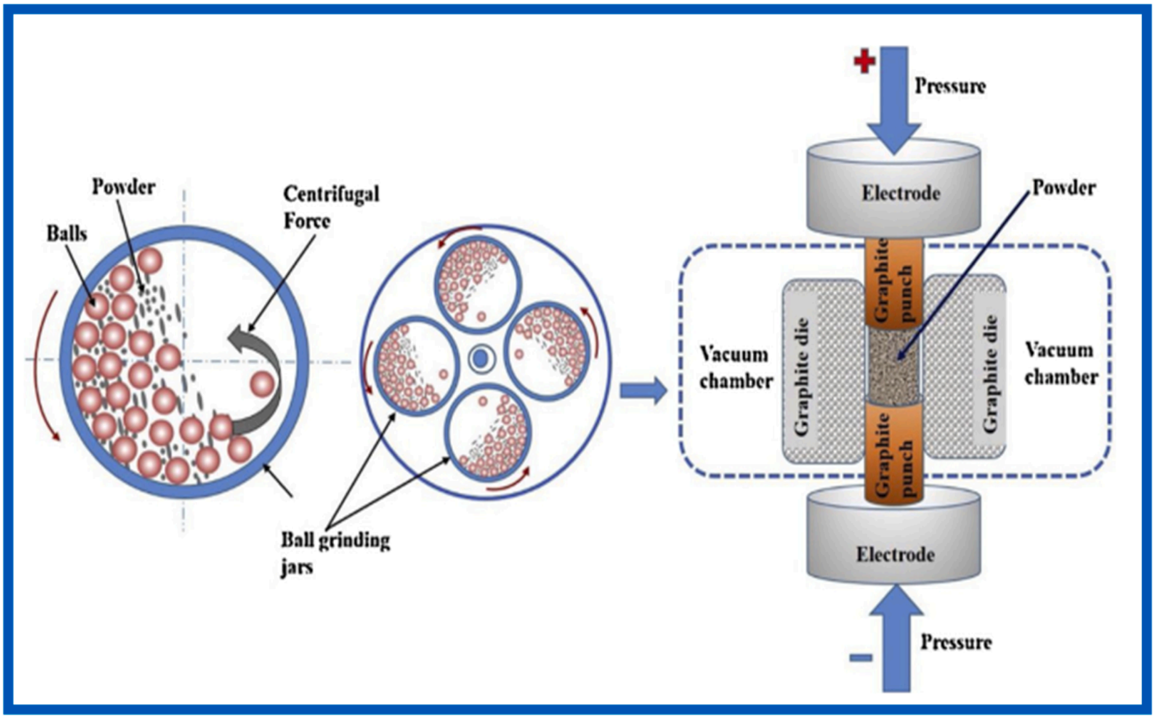

Fig. 8. Overview of high-energy ball milling and sintering processes for high entropy alloys (HEAs) [392]. Copyright 2019, Elsevier.

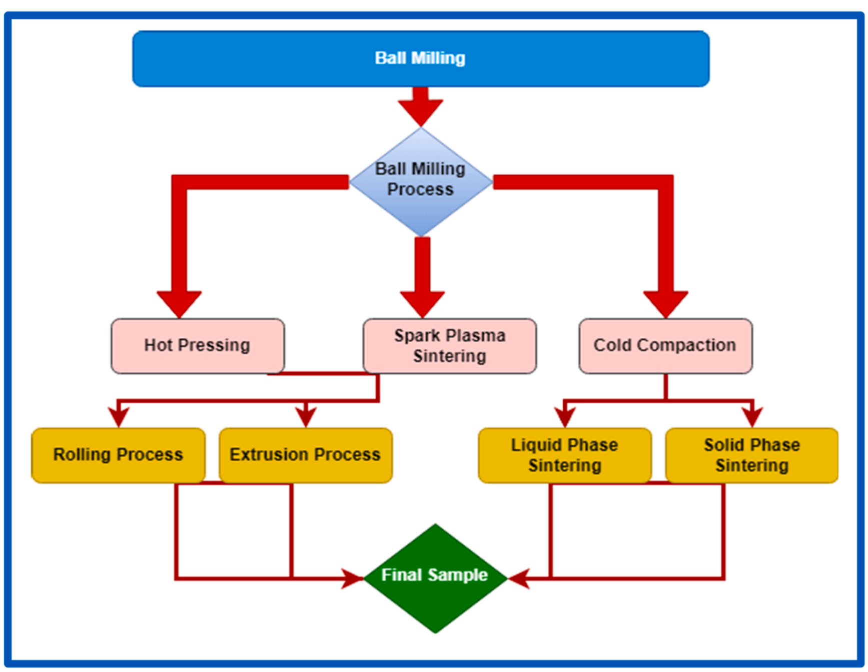

Fig. 9. A detailed overview of the various solid-state processing techniques used to fabricate high entropy alloys (HEAs). It outlines the key steps and methodologies involved in the production of HEAs, including processes such as spark plasma sintering, and hot isostatic pressing.

Process control agents (PCAs) are additives used to regulate and optimize various milling parameters. PCAs alter the milling environment, improve powder flowability, prevent agglomeration, and reduce the tendency of powders to stick to the vial or milling balls. The presence of PCAs significantly impacts the alloying behavior, milling kinetics, and the final characteristics of the synthesized materials. They are essential for producing materials with specific microstructures and properties for a wide range of applications, making them crucial for optimizing the MA process in the synthesis of HEAs and other advanced materials.

The particular needs of the intended HEAs determine the best combination of milling time, speed, ball-to-powder ratio and process control agents. In order to achieve the desired microstructure and qualities, optimized parameters are often found through systematic correlation and experimentation. To weigh the advantages of improved mixing and responsiveness against potential disadvantages like higher temperatures or wear, it is imperative to make iterative modifications and closely monitor the grinding process. Researchers and engineers can fine-tune the synthesis process and customize the microstructure and properties

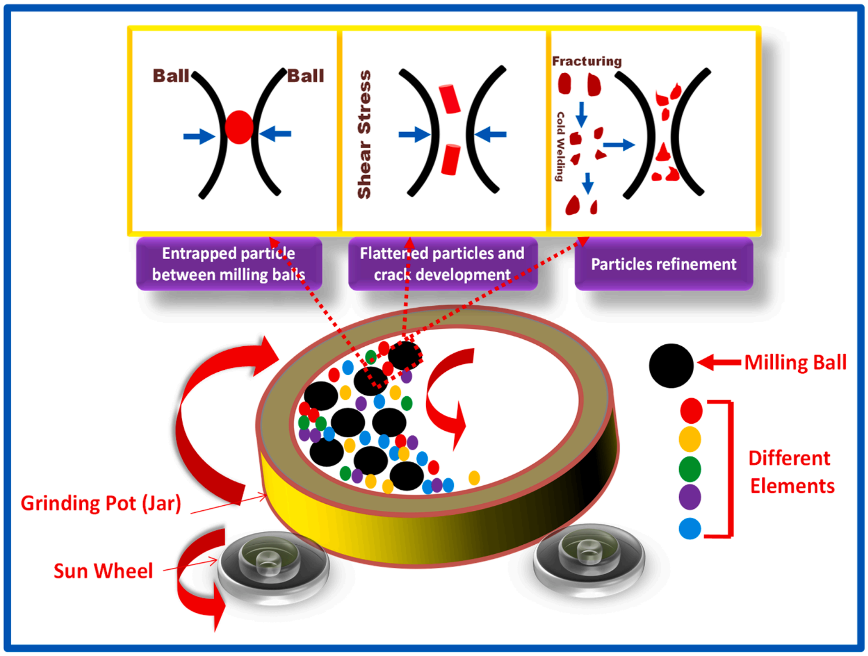

Fig. 10. The order and functions of the system component parts providing a thorough understanding of each step in the planetary ball milling process.

of the HEAs (Fig. 2) to match the required standards for a variety of materials science and engineering applications by carefully manipulating these milling parameters.

4.3. Intermediate analysis and post-milling treatments

The intermediate analysis step of the MA process comprises characterizing and evaluating the powder mixture at various milling stages [36]. El-Eskandarany and coworker (2015) demonstrated that altering the milling settings can result in the desired microstructure and characteristics. Their research offers insightful information on how the alloying process is progressing [409]. Common techniques for intermediate analysis when mechanically grinding HEAs, include: X-ray diffraction (XRD) techniques keep track of changes in phase composition during milling. In order to better understand alloying kinetics for optimizing milling parameters, XRD is important in determining the degree of alloying and the development of desired phases. Detailed information about particle morphology, size, distribution, and microstructural change at the nanoscale is provided by transmission electron microscopy (TEM). TEM aids in milling parameter optimization and in understanding of mechanical alloying processes. Scanning electron microscopy (SEM) provides insights into the evolution of microstructure by visualizing changes in particle form, size, and distribution. When combined with TEM and SEM, energy-dispersive X-ray spectroscopy (EDS) can provide information on elemental composition; verify homogeneity, and spot elemental contamination or segregation.

Using these techniques, scientists can modify the synthesized HEAs microstructure and characteristics of materials. After the MA process, post-milling treatments are extra processing procedures used to improve the properties of the alloy by optimizing the microstructure [410,411]. For ball-milled synthesized HEAs, Wang *et al.* (2022), Wu *et al.* (2019), and Zhuang *et al.* (2018) described standard post-milling processes [412–414]. One such process is annealing, a high-temperature heat treatment meant to stabilize the microstructure of the alloy, encourage diffusion, and lessen internal tensions. The mechanical qualities of synthesized HEAs, such as their toughness and ductility, can be enhanced by annealing. Research on Hot Isostatic Pressing (HIP) has been presented by Bernal *et al.* (2004), Tang *et al.* (2015), Joseph *et al.* (2018), and Varalakshmi *et al.* (2010) [415–418]. By exposing a powdered combination to high temperatures and pressures in an inert gas atmosphere, HIP turns it into a completely dense alloy with improved mechanical characteristics. The technique of SPS has also been covered in the literature. Using high pressure and current on the ground powder mixture, SPS is a fast consolidation technique that speeds up the sintering and densification of the material [419–421]. The mechanical and electrical characteristics of synthesized HEAs can be enhanced by this technique. The microstructure and characteristics of synthesized HEAs can also be tailored for particular purposes by using heat treatment procedures including as solution treatment, ageing, and quenching [422–426]. Researchers can further improve the properties and performance of mechanically milled HEAs by using suitable post-milling treatments, which will make them suited for a variety of industrial applications, including structural materials, automotive, and aerospace.

5. Types of ball mills for synthesis

A variety of ball mill types are frequently employed in the ball mill-based synthesis of HEAs. High-energy interactions between the powder mixture and the milling balls are provided by the design of these mills, which aid in mechanical alloying and the synthesis of homogenous alloy compositions. The following are a few varieties of ball mills that are used to synthesize HEAs.

5.1. Planetary ball mill: operation and working principle

For the synthesis of materials with regulated properties, planetary ball mills are sophisticated milling machines that find several industrial and research uses (Fig. 10 and Fig. 11) [44,427–429]. They provide a high-energy milling environment that is appropriate for mechanically combining, homogenizing, and alloying powders. The parts and functioning of a planetary ball mill are explained in depth [430,431]. The sun wheel, sometimes referred to as the sun gear, is an essential component of this system. It usually revolves in a fixed direction around its own axis while being powered by a motor. Planetary ball mills are equipped with one or more grinding jars, which are installed eccentrically on the sun wheel. These jars are also known as planetary bowls or milling cups (Fig. 11). Because of the eccentric configuration, the

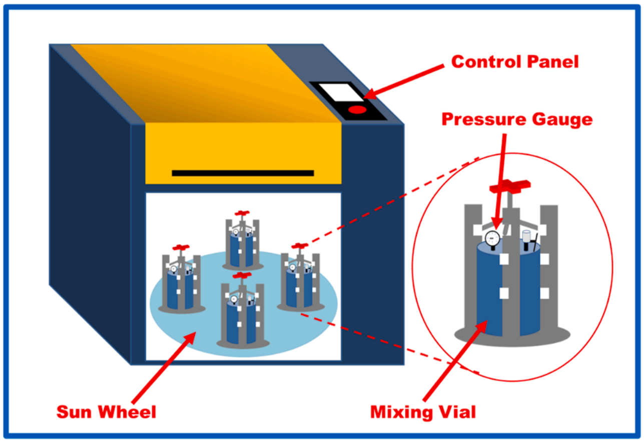

Fig. 11. This schematic shows the sun wheel, control panel, mixing vial, and pressure gauge as parts of a planetary ball milling system. Also draws attention to the crucial components and their functions in efficient material processing.

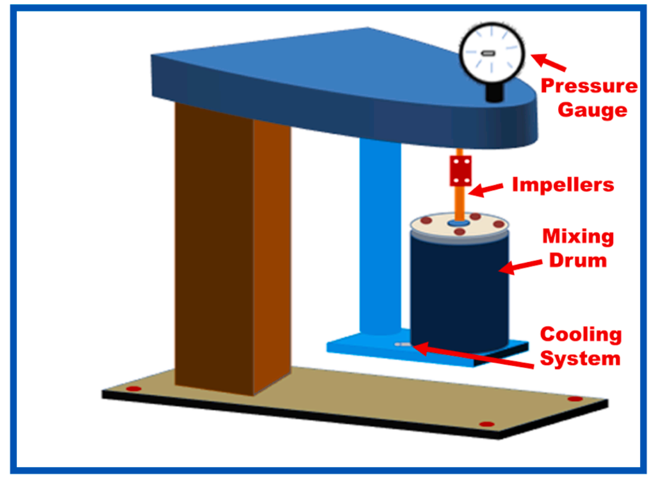

Fig. 12. An overview of the main parts of the system and their functions during the milling process is given by this schematic design, which shows a high-energy attritor ball milling system with mixing drum, pressure gauge, and impellers.

grinding jars revolve around their own axes and also circle around the sun wheel's center axis. The powder combination is placed to each grinding jar together with milling balls composed of sturdy materials like zirconia, tungsten carbide, or stainless steel. By repeatedly colliding with the powder mixture and one another while rotating, the milling balls engage in the high-energy impacts and mechanical alloying process [44].

The sun wheel, which is powered by a motor, rotates to start the planetary ball mill. The sun wheel revolves in a fixed direction, usually in a clockwise or counterclockwise orientation, around its own axis [432,433]. The sun wheel grinding jars begin to revolve around their own axes simultaneously (Fig. 10). The sun wheel rotation and the grinding jars revolution are in harmony. The grinding jars also revolve around the sun wheel center axis as a result of the eccentric design, producing a planetary motion. High-energy impacts are produced between the milling balls and the powder mixture inside the grinding jars by the planetary motion and rotation of the jars. The powder combination is mechanically alloyed by these high-energy collisions, which also cause the components to become more homogeneous and reduce in particle size. A consistent alloy composition is formed as a result of the complete blending and homogenization of the components achieved by the milling balls and powder mixture repeated impacts. Because planetary ball mills can synthesize fine powders and facilitate effective mixing and alloying, they are a popular choice for high-energy milling for the synthesis of HEAs.

5.2. *Attritor ball mill: functionality and principles of operation*

Another mill known as attritor mill is stirred ball mill shown in Fig. 12 [434]. These high-energy milling machines are used in many different industries, but they are most commonly used in the synthesis of materials and the manufacture of nanoparticles. These mills use a stationary vertical axis to which rotating arms or impellers are mounted, providing a novel approach to the operation [435]. The Attritor mill's design facilitates effective material dispersion, grinding, and mixing. The main components of attritor mills are explained in depth by Zhao *et al.* (2017) [436]. The vertical shaft, which is a key part of an attritor mill, is usually composed of sturdy materials like stainless steel and stays in place while the machine is in use. Impellers or stirrers, which are fixed to the vertical shaft, are in charge of agitating the powder mixture and the milling medium, which are often balls [409,437]. The exact model and application requirements will determine the number and design of impellers. Balls or other small grinding media are frequently added to the milling chamber. The high-energy impacts that occur throughout the milling process are facilitated by these balls. The milling media and the powder combination are kept in this chamber. It is made to be resistant to the mechanical forces produced during the milling process. In order to regulate the temperature produced during high-energy milling, particularly in procedures that are prone to heat generation; some attritor mills may be equipped with a cooling system.

The powder combination is put into the milling chamber; it could contain different ingredients for the synthesis of materials. Balls, or milling medium, are also inserted. The milling media inside the chamber moves as a result of the vertical shaft with impellers beginning to rotate. The powder mixture and the balls receive kinetic energy from the impellers. High-energy interactions between the powder particles and the milling media are produced by the combination of the impellers design and rotating movement. Particle size reduction, mechanical alloying, and vigorous mixing result from this. Attritor mills are especially useful for synthesizing HEAs because of their high mixing levels, which are essential for attaining homogeneity in the powder combination and encouraging interactions between various components [36,47]. The final particle size and distribution can be controlled by varying the milling time, speed, and size and composition of the milling media.

5.3. *Vibratory ball mill: mechanism and operating principles*

High-frequency vibrations are used by vibratory ball mills, a kind of milling apparatus, to help mix and grind materials inside a milling vessel [438]. According to Kumar *et al.* (2018) and Kavak *et al.* (2022), there are a number of benefits associated with this milling approach, including as effective mixing, shortened processing times, and the capacity to generate powders that are finely ground [439,440]. The synthesis of HEAs is one of the many uses for these powders. The following are the principal elements: The powder and milling media are placed inside a vessel, which is often constructed of ceramic or stainless steel. There is a room for milling in this vessel. Electromagnetic drives and eccentric motors are the two driving systems that produce vibrations in a ball mill. The vessel and its contents are subjected to high-frequency vibrations produced by these drives. The jar is filled with small grinding rods or balls to help in the grinding operation. Particle size is decreased and the powder is mixed by the interaction between the grinding media and the powder.

High-frequency vibrations are produced by vibratory ball mills using either an electromagnetic drive or an eccentric motor [441,442]. The milling vessel contents move and come into conflict as a result of these vibrations. The powder mixture and milling media undergo vigorous mixing and grinding as the milling vessel vibrates. Particle-to-particle and particle-to-media collisions are facilitated by the high-frequency vibrations, which effectively combine and ground the powders. Particle size reduction is achieved through mechanical alloying and grinding caused by the frequent impacts between the powders and the milling media. Powders with a regulated particle size distribution and fine grinding are produced by this technique.

5.4. High-energy ball mill and its working principle

According to Baláž (2008) and Lizer and M. (Eds.) (2010), high-energy ball mills are a specific kind of milling machinery made for uses like producing nanoparticles and synthesizing materials. [443, 444]. These mills—shaker mills and planetary mills with high-speed rotationare designed to run at high rotating speeds, which causes the powder combination and the milling media (balls) to collide violently. High-energy ball mills are ideal for synthesizing HEAs and other advanced materials because of their distinctive design, which allows for quick alloying and the production of finely grained microstructures. High-energy ball mills have a milling vessel that holds the powder combination and the milling media. This vessel is usually constructed of ceramic or stainless steel. The milling vessel rotation is driven at high speeds by a high-speed rotation mechanism installed in these machines, such as a planetary gearing system or shaker mechanism. To help in the grinding and mixing of the powder mixture, the milling vessel is filled with milling media, which are often composed of ceramic or hardened steel.

According to Francioli *et al.* (2015), high-energy ball mills rotate at substantially faster rates than conventional ball mills. The tremendous kinetic energy produced by the high-speed rotation efficiently grinds and mixes the powder blend [445,446]. The powder mixture is collided with by the milling media, which are balls, inside the milling vessel while it rotates rapidly. Strong collisions between the powder particles and the balls lead to efficient alloying, mixing, and decrease of particle size. High-energy ball mills work especially well for quick alloying because of their powerful impacts and quick rotational speeds, which encourage quick atom diffusion between powder particles and quick alloy production (Fig. 4). These mills use a high-energy milling method that produces materials with fine-grained microstructures. This is helpful for the synthesis of HEAs because fine-grained microstructures lead to better performance and improved mechanical characteristics.

5.5. Horizontal ball mill and its working principle

According to Liao *et al.* (2011), Partyka *et al.* (2007), and Boschetto *et al.* (2006), the horizontal ball mill is a common piece of milling equipment used in many different industries for material grinding, mixing, and blending [447–449]. They are composed of a horizontally spinning cylinder that is filled with grinding media, which are usually metal balls. These mills horizontal orientation makes it possible to precisely manage the milling parameters and process huge volumes of material with efficiency, which makes them ideal for synthesis of HEAs. A cylindrical drum or container that revolves around its horizontal axis serves as the main part of horizontal ball mills. The grinding medium and the powder combination that needs to be processed are kept inside this revolving cylinder. Balls-shaped grinding media are placed inside the cylinder. Usually constructed from strong components like steel or ceramic, these balls come in different sizes to provide the appropriate milling impact. A motor attached to a gearbox or belt drive system connects to the rotating cylinder to power horizontal ball mills. The cylinder receives rotating motion from the motor, which causes the grinding media and powder mixture to tumble and cascade.

According to Marczuk *et al.* (2019), when the horizontal cylinder rotates, centrifugal forces are produced inside the mill [450]. These forces produce a tumbling and cascading motion as the grinding media, or balls, travel within the cylinder along a circular route. There are high-energy interactions between the balls and the powder mixture as a result of the movement of the grinding media. These impacts lead to the breaking and size reduction of the powder particles and help in the component mixing and blending. Because the grinding media tumbles in horizontal ball mills, materials are mixed efficiently. This guarantees that the ingredients in the powder combination are distributed uniformly, resulting in homogeneity in the finished product.

5.6. Cryo ball milling and its working principle

Cryomilling is a mechanical attrition process where particles are milled in a slurry with milling balls and a cryogenic liquid, usually liquid nitrogen, as described by Witkin *et al.* (2006) [451]. By cooling the materials to −196°C (-321°F), this process preserves their brittleness and enables the development of smaller particle sizes and better qualities. It is important to distinguish various cryogenic deformation techniques from cryomilling, which involves the contact of powders with the cryogenic liquid. Similar to friction stir processing and equal channel angular pressing, cryomilling can create nanostructures inside of powders. A revolving chamber full of milling balls in a ball mill creates impacts that break the material without producing heat, which could change its properties. Low temperatures are maintained through continuous nitrogen ventilation, which avoids stickiness and agglomeration. A fine powder that is ready for usage is the end result. HEAs can be effectively made via cryoball milling, which permits fine grinding and uniform mixing of component elements without permitting heat degradation. The synthesis of the Co-Cr-Fe-Mn-Ni HEA was demonstrated by Laurent-Brocq *et al.* (2019) using cryo-milling, and it was noted that nanoindentation studies indicated a notable increase in hardness in comparison to traditional techniques like melting and casting [452]. According to Kumar *et al.* (2018), cryo-milling produces nanocrystalline HEA powders with a tight size distribution and comparatively few impurities [453]. Their research showed that after cryo-milling at 123 K, large-scale nanocrystalline HEA powders may be created in a matter of hours. They proposed that this process can produce HEA nanoparticles smaller than 10 nm, which would allow for effective large-scale manufacturing. Furthermore, they observed that during the cryo-milling procedure, the crystal structures of both bulk HEAs and HEA nanoparticles are preserved. This demonstrates how cryoball milling may be used to synthesize HEAs while preserving their structural integrity.

6. Varieties of high entropy alloys synthesized through high energy ball milling

A solid-state powder manufacturing method called mechanical alloying is utilized to make HEAs and a variety of other materials. The following are a few varieties of HEAs produced via mechanical alloying:

6.1. Single-phase HEAs

A unique class of materials called single-phase HEAs is described by King *et al.* (2016) [454]. The phase distribution mapping of HEAs with differing element counts is shown in Fig. 13 [455]. Fig. 14 presents a pie chart illustrating the distribution of single-phase and multi-phase HEAs produced via ball milling, as compiled from a comprehensive literature review. The chart provides a visual representation of the prevalence of different phases in HEAs synthesized using this technique. HEAs are distinguished by a homogeneous microstructure made up of a single solid solution phase. This phase is characterized by the almost equiatomic proportions of multiple major elements, usually three or more, distributed homogeneously. These components are evenly distributed throughout the microstructure, preventing any one element from predominating and giving these materials their distinct qualities that differentiate them from conventional alloys. Shkodich *et al.* (2022) have made a noteworthy contribution to the synthesis of HEA through their study [228]. They succeeded to synthesize an equiatomic

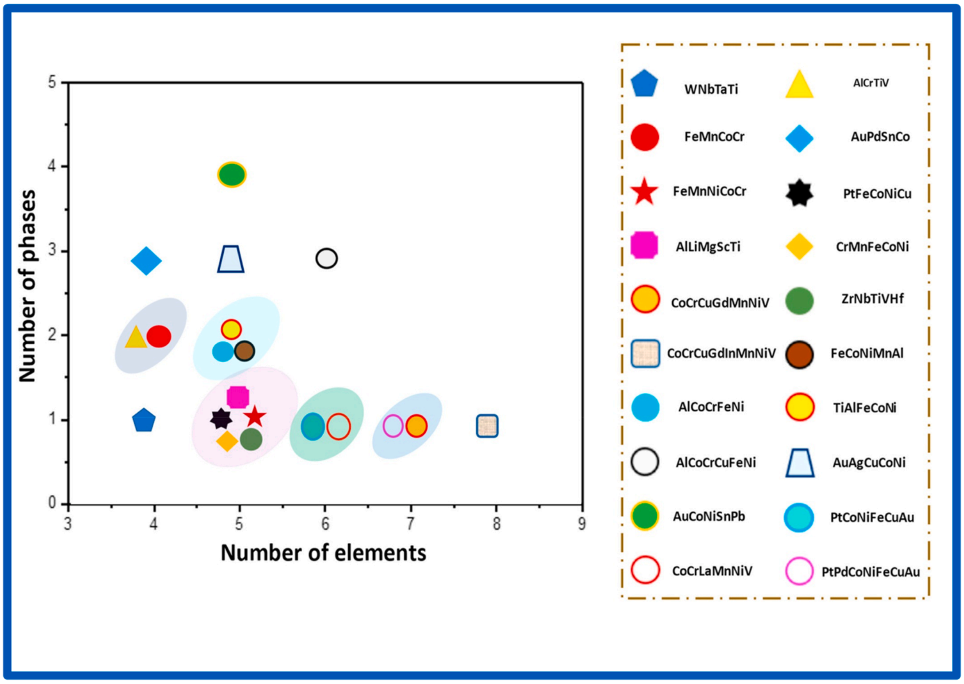

Fig. 13. Phase distribution map of high entropy alloys (HEAs) as a function of element composition [455]. Copyright 2022, Elsevier.

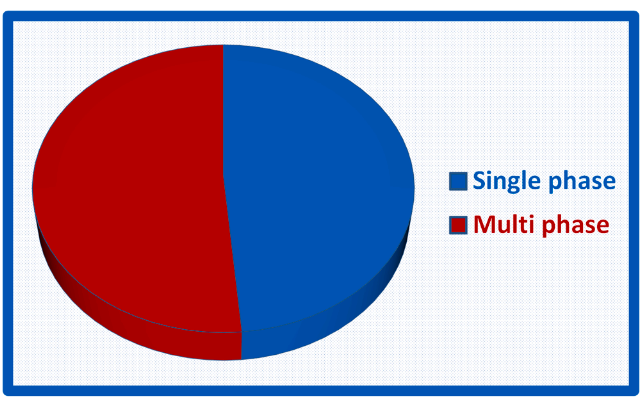

Fig. 14. The distribution of different phases formed in high entropy alloys (HEAs) that have been synthesized using mechanical alloying, as compiled from a comprehensive literature survey.

nanocrystalline Co-Cr-Fe-Ni-Cu HEA powder, which has a lattice parameter (a) of 3.597 ± 0.005 Å and a single FCC structure. This was achieved by using a quick (120 min) method called HEBM. Their research also demonstrates the effectiveness of utilizing a synergistic strategy that combines the SPS and HEBM processes. Superior structural and elemental homogeneity in equiatomic Co-Cr-Fe-Ni-Cu HEA powders and bulk materials can be easily achieved by this ideal integration.

Shivam *et al.* (2020) have made a significant contribution to the field of HEAs with their study [144]. After 30 hours of milling, they saw the production of a single-phase solid solution in equiatomic Al-Co-Cr-Fe-Ni HEA with a BCC structure. For this BCC structure, the lattice parameter (a) was found to be 2.88 ± 0.01 Å. This alloy demonstrated remarkable mechanical characteristics, including a high hardness of approximately 919 HV and excellent yield strength of 2700 MPa. With an effective Curie temperature of 617°C (890 K) and a saturation magnetization (Ms) of 70.05 emu/g, the alloy additionally showed excellent magnetic characteristics. The synthesis of a single-phase FCC Co-Cr-Cu-Fe-Ni HEA by MA at two distinct milling speeds (200 and 350 rpm) is reported by Thangaraju (2017) [95]. Annealing was done on the mechanically alloyed powders at different temperatures (300, 500, 700, and 800°C). According to the study, after 5 hours at 350 rpm and 50 hours at 200 rpm of milling, a stable FCC solid solution formed. Up to 800°C, this single FCC phase maintains its thermal stability before splitting into two FCC phases. Vaidya *et al.* (2019) reported the synthesis of single-phase FCC-structured Co-Cr-Fe-Ni and Co-Cr-Fe-Mn-Ni HEAs prepared through mechanical alloying (MA). The study examined the phase stability of these HEAs within the temperature range of 1073–1373 K for up to 96 hours. Heat treatment of the MA powders revealed the formation of Cr_7C_3, accompanied by Cr depletion in the FCC matrix [456].

Single-phase HEAs are special because of their atomic-level mixing, which is accomplished by MA, a solid-state powder processing method. In a HEBM method, powder particles are repeatedly fractured, welded, and then re-welded in the MA process. The powder reactants and the milling media are subjected to high temperatures and mechanical forces during this MA process. Under these circumstances, the constituent elements can mix more closely at the nanoscale, resulting in the production of a homogenous powdered alloy. For the alloy to have the appropriate qualities, a homogenous distribution is essential because it reduces the possibility of unwanted secondary phases forming and impairing the alloy's functionality.

6.2. Dual-phase HEAs

One flexible method for synthesizing dual-phase HEAs as well as single-phase HEAs is MA, a solid-state powder processing technique [289,404]. Dual-phase HEAs have two different phases coexisting in the alloy matrix, each of which gives the material a different set of characteristics. Through meticulous manipulation of the alloy's elemental composition and milling parameters, such as ball-to-powder ratio, time, and speed, researchers can attain a precisely regulated distribution of the two phases with customized characteristics. Through their innovative work, Song *et al.* (2018) have made a substantial advancement in the production of bulk Cr-Mn-Fe-V-Ti HEA [457]. This material has a dual-phase microstructure with an average grain size of about 97 nm, consisting of both FCC and BCC phases. Mechanical testing also revealed excellent mechanical characteristics, with the bulk HEA showing a remarkable Vickers hardness of 835 HV and compressive strength of

2279.53 MPa. The remarkable hardness and strength of the bulk Cr-Mn-Fe-V-Ti HEA are mainly ascribed to the cooperative action of dislocation and grain boundary strengthening processes. The study emphasizes how crucial it is to carefully regulate the MA process's parameters in order to produce milled powder with an optimal microstructure and make it easier to produce bulk HEAs with exceptional qualities. These results highlight the importance of parameter adjustment in obtaining superior material properties and further our understanding of HEA synthesis and processing.

The fabrication of a dual-phase Al-Co-Cr-Fe-Ni-$Si_{0.5}$ high-entropy alloy by MA was reported by Yang *et al.* (2024), who also examined the impact of ball-milling duration [458]. They found that the hardness and modulus of the powder increased to 12.33 ± 1.26 GPa and 79.9 ± 6.21 GPa, respectively, upon the addition of Si. With annealing, the alloy created solid solutions of BCC and FCC, with the FCC phase being tunable. Grain size rose, lattice distortion and dislocation density reduced, and the BCC phase content increased to 79 % from 46 % after two hours of solid-solution treatment at 1110 °C. This improved dislocation, fine-crystal strengthening, and solid-solution, leading to a more homogeneous element distribution. The first step is to choose the alloy's constituent composition while keeping phase stability and desirable attributes in mind.

Jahani *et al.* (2023) investigated the synthesis of Fe-Ni-Mn-Cu-X (X: Co, Cr, Mo, Ti, W) HEAs fabricated through mechanical alloying. Their findings revealed that after 15 hours of milling, the Fe-Ni-Mn-Cu and Fe-Ni-Mn-Cu-Co alloys exhibited a single FCC structure, while the remaining alloys showed an FCC + BCC mixed structure. Elemental analysis indicated a homogeneous distribution of Fe and Ni in all alloys, although Cu exhibited segregation. Interestingly, Fe-Ni-Mn-Cu-Ti and Fe-Ni-Mn-Cu-W alloys also displayed a homogeneous distribution of Mn, whereas other compositions revealed Mn-rich regions. Magnetic property analysis demonstrated that, except for the Fe-Ni-Mn-Cu-Ti alloy, all the alloys exhibited soft magnetic behavior. Furthermore, the addition of Co to the base Fe-Ni-Mn-Cu alloy enhanced its saturation magnetization, while the inclusion of Cr, Mo, Ti, and W reduced it [459].

Sriharitha *et al.* (2013) investigated Al_x-Co-Cr-Cu-Fe-Ni (x = 0.45, 1, 2.5, 5 mol) HEA synthesized through mechanical alloying. Their study revealed that alloys with lower Al content ($Al_{0.45}$-Co-Cr-Cu-Fe-Ni and Al-Co-Cr-Cu-Fe-Ni) exhibited FCC phases along with a BCC phase, whereas higher Al content alloys ($Al_{2.5}$Co-Cr-Cu-Fe-Ni and Al_5-Co-Cr-Cu-Fe-Ni) displayed a single B2 phase. DSC analysis indicated that the BCC phase observed in the alloys could correspond to an Fe–Cr type solid solution. Interestingly, the BCC phase disappeared at elevated temperatures for $Al_{0.45}$-Co-Cr-Cu-Fe-Ni and Al-Co-Cr-Cu-Fe-Ni, while the Al_5-Co-Cr-Cu-Fe-Ni alloy retained its B2 structure even after heating in the DSC. Furthermore, the phases in these alloys remained nanocrystalline despite exposure to high temperatures. These findings challenge the applicability of existing solid solution formation criteria for high entropy alloys in explaining the phase evolution observed in this study [460].

Zhang *et al.* (2010) reported the synthesis of Co-Cr-Fe-Ni-Ti-Al HEA via MA. Supersaturated BCC and FCC solid solutions were observed after 18 hours of ball milling, with the 30-hour milled powder achieving excellent chemical homogeneity, refined morphology, and a mean particle size of less than 5 µm. Upon annealing at 600 °C for 1 hour, the 30-hour milled powder transformed into two BCC solid solutions, and the simple solid solution structure was maintained even after annealing at 1000 °C. The mechanically alloyed powder was consolidated by spark plasma sintering (SPS) at 800 °C for 10 minutes, resulting in a dense sample with 98 % relative density and a Vickers hardness of 432 HV [461].

Praveen *et al.* (2012) studied equiatomic Al-Co-Cr-Cu-Fe and Ni-Co-Cr-Cu-Fe HEAs synthesized by MA and SPS. After MA, FCC and BCC phases were observed, while SPS led to the formation of Cu-rich FCC and sigma (σ) phases alongside FCC and BCC. Additional investigations on Ni-Co-Cu-Fe, Ni-Co-Cr-Fe, and Ni-Co-Fe alloys confirmed the formation of Cu-rich FCC and σ phases. Hardness values were reported as 770 ± 10 HV for Al-Co-Cr-Cu-Fe and 400 ± 10 HV for Ni-Co-Cr-Cu-Fe. The study highlighted that configurational entropy alone cannot suppress the formation of Cu-rich FCC and σ phases, with the enthalpy of mixing playing a key role in phase evolution during sintering [462].

Usually, two main elements and extra alloying elements are included in dual-phase HEAs to facilitate the development of the intended phases. The ball-to-powder ratio, milling time, and milling speed are important factors that affect the microstructure and phase distribution of the final alloy. Researchers can regulate the level of mixing and fine-tuning of the powder particles during MA by adjusting these parameters. The powder components are put into a high-energy ball mill coupled with milling medium during MA, and the milling procedure is done under carefully regulated circumstances. The alloy experiences solid-state reactions and phase changes during MA, which eventually results in the establishment of a dual-phase microstructure. The uniform mixing of the constituent powders at the atomic level results in the fine dispersion of the two phases inside the alloy matrix. Researchers can modify the elemental composition and milling settings of dual-phase HEAs to customize their properties to satisfy certain application needs. For instance, depending on the requirements of the application, combining phases with different mechanical properties can result in improved wear resistance, enhanced corrosion resistance, or optimal mechanical strength.

6.3. Nanocrystalline HEAs

Mechanical alloying, a solid-state powder processing method, is used to synthesize an intriguing family of materials known as nanocrystalline HEAs [386,409]. This process involves subjecting powder particles that contain the appropriate elemental ingredients to HEBM. This results in the formation of nanocrystalline grains with diameters on the order of nanometers, as well as microstructure refinement [407].

In a high-energy ball mill, powder particles are repeatedly fractured, fused, and re-welded during the MA process. Intense mechanical and thermal energy are applied to the powder particles during milling as a result of the milling media and powder reactants colliding. According to Vaidya *et al.* (2019) research, MA and SPS can be used to produce nanocrystalline Co-Cr-Fe-Ni and Co-Cr-Fe-Mn- Ni alloys that have an FCC structure that is extremely stable [141]. Among the ingredients, cobalt and manganese notably have the slowest dissolving kinetics during the MA process because of their limited solid solubility and unique crystal structure. Furthermore, the vast FCC phase field shown in quaternary and quinary phase diagrams is reflected by the almost constant lattice parameter of the FCC phase at high temperatures, guaranteeing the structural stability of the FCC phase even in the presence of compositional variations. These results confirm that, in nanocrystalline Co-Cr-Fe-Ni and Co-Cr-Fe-Mn-Ni HEAs produced by MA and SPS techniques, a stable FCC phase forms. The exceptional durability of the FCC phase in these entropy-maximized multicomponent alloys is largely due to the high solid solubility of binary constituents combined with the non-equilibrium processing characteristic in MA. A homogenous alloy powder with a refined microstructure is formed through the facilitation of atomic diffusion under these conditions. When compared to traditional coarse-grained alloys, the mechanical characteristics are greatly improved upon nanoscale microstructure refinement. High hardness, enhanced strength, and greater wear resistance are common characteristics of nanocrystalline HEAs, which makes them appealing for structural applications needing exceptional mechanical performance. The high hardness of nanocrystalline HEAs is a result of the existence of nanoscale grains, which is advantageous for applications requiring resistance to wear and deformation. Hardness can be further enhanced by the increasing number of grain boundaries in nanocrystalline materials, which can obstruct dislocation movement [463].

A high entropy Cu-Ni-Co-Zn-Al-Ti nanostructured alloy was presented by Varalakshmi *et al.* (2010) in their research paper [56]. This alloy was successfully synthesized by MA and then vacuum hot pressing

(VHP) at 800 °C and 30 MPa of pressure. Two small FCC phases were seen upon VHP analysis of the as-milled equiatomic Cu-Ni-Co-Zn-Al-Ti alloy, but a BCC phase predominated. The alloy demonstrated remarkable properties, including a compressive strength of 2.36 GPa and an extraordinarily high hardness of 7.55 GPa, indicating its significant potential for use in future applications. Grain boundary strengthening and dislocation interactions are two phenomena that result in increased strength in nanocrystalline HEAs due to their tiny grain size. Because of their enhanced strength, nanocrystalline HEAs can be used in situations where load-bearing capacity and structural integrity are crucial. Because of their finely tuned microstructure, nanocrystalline HEAs are more resistant to wear than their coarse-grained equivalents. Improved wear resistance and an extended service life in abrasive settings are the result of the high density of grain boundaries and nanoscale grains that prevent the spread of wear particles and cracks. Recent studies have shown that certain nanocrystalline HEAs may have increased ductility, even though nanocrystalline materials are usually associated with great strength and hardness [464]. Strength and ductility can be balanced by adjusting the composition and manufacturing conditions, which increases the materials' potential range of uses. Ultimately, there are many promising prospects for synthesizing sophisticated materials with better mechanical qualities thanks to the synthesis of nanocrystalline HEAs via MA. The goal of ongoing research in this area is to fully realize the promise of nanocrystalline HEAs for a range of technical applications, including as those in the aerospace, automotive, and biomedical industries, by refining their composition and manufacturing methods.

6.4. Amorphous HEAs

Mechanical alloying is combined with quick solidification techniques like melt spinning or spray deposition to synthesizing amorphous HEAs [464–466]. This new technology has gained recognition in the world of material research because to its ability to manufacture alloys with long-range atomic order, which confers specific properties that make them highly wanted for applications in both structural and functional materials. In a high-energy ball mill, elemental powders are subjected to substantial mechanical forces during the initial step of the process, known as MA. The repeated cold welding, fracturing, and rewelding of the powder particles produced by this method, results in a homogenized and finely dispersed combination of alloying elements. This amorphous precursor serves as the foundation for all further steps in the process of synthesis of amorphous HEAs.

The synthesis of a new class of amorphous HEA $Zr_xFeNiSi_{0.4}B_{0.6}$ has been suggested by Liming Sang *et al.* via the MA technique [142]. $Zr_xFeNiSi_{0.4}B_{0.6}$ (x = 1, 1.5) HEA powders have a stable FCC solid solution structure but also display some amorphous features. Furthermore, after 180 hours of milling, the $Zr_{2.5}$-Fe-Ni-$Si_{0.4}$-$B_{0.6}$pseudo-HEAs powders completely amorphized. Particularly, these amorphous pseudo-HEAs powders, $Zr_{2.5}$-Fe-Ni-$Si_{0.4}$-$B_{0.6}$, exhibit exceptional thermal stability, with a crystallization temperature (T_x) of roughly 689°C. Importantly, components with large negative ΔH_{mix} and strong δ values are needed to facilitate the transition of MA into the amorphous phase. In $Zr_xFeNiSi_{0.4}B_{0.6}$ HEAs, the amorphous phase is known to develop when $\Delta H_{mix} \leq$ -57.85 kJ/mol and $\delta \geq 0.191$. Following MA, rapid solidification techniques are employed to freeze the amorphous precursor into a solid state and prevent it from establishing a crystalline structure. Spray deposition and melt spinning are the two techniques that are most commonly employed for this [375]. Melt spinning is a process that entails melting the amorphous precursor and rapidly quenching it by ejecting it onto a rotating copper wheel [467]. Because of the fast-cooling rates achieved with this approach, a crystalline lattice cannot form, preserving the amorphous structure [468]. During the spray deposition process, melted alloy is atomized into tiny droplets, which travel through a cooling chamber and rapidly cool down. The alloy's amorphous condition is preserved because of the quick solidification, which stops the atoms from developing a regular crystalline structure.

There are several unique features of amorphous HEAs in comparison to their crystalline counterparts. Because amorphous HEAs are harder due to their lack of crystalline structure, they are suitable for applications where wear resistance is crucial [21,468]. Because amorphous HEAs lack grain boundaries, which reduce their susceptibility to corrosion, they are exceptionally corrosion-resistant in hostile environments. Utilizing the advantages of amorphous alloys, Xiao *et al.* (2022) have presented a unique crystal-amorphous Fe-Mn-Co-Cr-Ni HEA [469]. This novel alloy features an amorphous shell and a nanocrystalline HEA phase. Due to the substantial Cr concentration within the amorphous shell, the wide amorphous shell acts as a transmission tunnel, permitting increased diffusion rates of Cr atoms (Fig. 4). As a result, a strong passive layer forming capacity is demonstrated by the crystal-amorphous Fe-Mn-Co-Cr-Ni HEA, which enhances its anticorrosion performance. The remarkable anticorrosion properties of the crystal-amorphous Fe-Mn-Co-Cr-Ni HEA are demonstrated by its corrosion current density, which is roughly 0.147 $nAcm^{-2}$. This effectively prevents pitting corrosion. This new alloy offers a fresh perspective on creating cutting-edge materials with exceptional anticorrosion capabilities. Because amorphous HEAs can display significant soft magnetic properties, they are valuable in applications such as transformers and magnetic sensors.

6.5. Composite HEAs

Composite HEAs combine the benefits of high entropy phases and reinforcing phases to provide enhanced mechanical, thermal, or electrical properties [470]. MA can be combined with other consolidation techniques, such as hot pressing or SPS, to synthesize composite HEAs with specific properties in a versatile manner. The thermal stability of a Co-Cr-Fe-Ni HEA composite produced by MA and SPS was studied by Sathiyamoorthi *et al.* (2017) [107]. For 600 hours, the sintered Co-Cr-Fe-Ni pellet showed exceptional thermal stability at 700°C, or 0.57 times the melting point. Grain growth kinetics analysis showed that the ultrafine-grained alloy was more resistant to grain growth than its microcrystalline counterpart. Building on these discoveries, the research suggests an alloy design with a two-phase aggregate with oxide dispersion and a thermally stable composite microstructure. Initially, the constituent elements of the high entropy phase and the reinforcing phases (such as carbides, nitrides, or oxides) are mechanically alloyed together using HEBM. This process ensures a homogenous dispersion of the components at the nanoscale and makes it easier to mix the phases closely. During consolidation, the powder is subjected to high temperatures and pressures, which forces the particles to mix and form a thick, solid substance. Following consolidation; a composite structure develops in which the matrix is distributed with reinforcing phases and a high entropy phase.

The distribution and geometry of the reinforcing phases can be changed to get the required properties. Reinforcing phases, such as carbides, nitrides, or oxides, can significantly enhance the mechanical properties of composite HEAs. These phases act as strengthening agents, increasing hardness, strength, and wear resistance in contrast to monolithic HEAs. Composite HEAs may have superior thermal stability because of the reinforcing phases, which can stop phase shifts and grain growth at high temperatures [107]. This capability comes in particularly handy in applications where structural integrity demands high temperatures. By adding specific reinforcing phases, composite HEAs can exhibit tailored electrical or thermal conductivity characteristics. To enhance thermal insulation, for example, adding ceramic phases makes composite HEAs suitable for application as thermal barrier coatings in airplanes. To meet specific application requirements, the distribution and composition of reinforcing components in composite HEAs can be adjusted. Its versatility allows for the optimization of properties including hardness, strength, conductivity, and corrosion resistance for a broad range of engineering applications. Composite HEAs exhibit multifunctional capabilities by combining the benefits of multiple phases into a single material. This enables the synthesis of contemporary materials with enhanced performance and utility for a range of applications.

6.6. Gradient HEAs

The fabrication of gradient HEAs has shown promise in the controlled milling of elemental compositions using MA [471]. Scientists may produce gradient structures inside the alloy matrix by varying the elemental concentrations and milling conditions. An FCC-structured HEA with a gradient layer ($Fe_{40}Mn_{40}Co_{10}Cr_{10}$) $C_{3.3}$was presented by Chen *et al.* (2020) [472]. The HEA's strength is greatly increased by this design while yet having enough ductility. While the good ductility is associated with back stress strain hardening, the ultra-high strength is mostly attributed to a synergistic strengthening mechanism.

The design of the gradient structure presents a new method in producing high-performance HEAs. These gradient HEAs remarkable property combinations increased strength, toughness, and thermal stability offer exciting prospects for cutting-edge engineering applications. During the MA process, elemental powders are repeatedly cold welded, cracked, and rewelded in a high-energy ball mill (Fig. 10). The ball-to-powder ratio, milling time, and milling speed can all be accurately controlled by designers to get the right final alloy compositional homogeneity, phase distribution, and grain size. Furthermore, elemental compositions with varying concentrations can be added successively or concurrently to the alloy matrix during milling to produce gradient structures. These gradient structures can take two different forms: compositional gradients, where the concentration of alloying components varies spatially across the alloy, or microstructural gradients, where the grain size or phase distribution progressively fluctuates. Compositional gradients offer the advantage of focused optimization for specific application requirements by enabling the change of material properties like as hardness, corrosion resistance, and thermal conductivity along the length or depth of the alloy. Furthermore, microstructural gradients provide a means of enhancing mechanical properties such as fatigue resistance, ductility, and strength by creating tailored interfaces or phase boundaries inside the alloy. This gradient architecture improves the material's overall mechanical performance while promoting dislocation interactions, lowering stress concentrations, and preventing crack propagation.

All things considered, MA is a versatile process that may be utilized to build several HEAs with particular microstructures and properties. This creates new opportunities for the synthesis of advanced materials with a variety of industrial applications.

6.7. High entropy oxides

High entropy oxides (HEOs) are a subclass of high entropy materials that, like HEAs, have a distinctive multi-principal elemental (cationic) arrangement. One flexible and affordable way to synthesize HEOs is through mechanical alloying [473]. Due to its superior qualities, which include increased mechanical strength, thermal stability, and prospective uses in electrochemistry, catalysis, and energy storage, HEOs have attracted a lot of attention [474]. Through a series of fractures, cold welding, and mechanical alloying, a homogenous solid solution is formed by high-energy ball milling of a mixture of oxide precursors. Tekin *et al.*, for instance, suggested using mechanical alloying to synthesize nanocrystalline Co-Cr-Fe-Ni-Y_2O_3 HEA [475]. After that, these alloys were annealed at different temperatures reaching 1100°C, which produced a solid solution of FCC that was stable. Depending on the oxides utilized, the high-energy impacts during mechanical alloying cause repeated deformation, fracture, and cold welding of the particles, which ultimately result in the creation of a single-phase solid solution with a cubic or spinel structure. (Co, Cu, Mg, Ni, Zn) O high-entropy oxide was synthesized in a work by Balcerzak *et al.* (2019), demonstrating the promise of HEOs for high-temperature applications with an electrical conductivity measurement of 8.03×10^2 S cm^{-1} at 1148 K [476]. Oxide precursors are combined with milling media, like tungsten carbide or stainless-steel balls, during the milling process. Depending on how sensitive the material is, the milling can be done in a controlled environment or in ambient settings. With the flexibility this technology provides, researchers can customize the composition and properties of the material for particular uses in HEO synthesis.

We have compiled the aforementioned HEAs, including their phases, milling parameters, compositions, and lattice parameters, in Table 4 for clarity and ease of reference.

7. Properties of these mechanical alloying HEAs

The properties of HEAs synthesized through mechanical alloying vary depending on their composition, processing parameters, and other treatments [477]. Many of these alloys achieve ultrafine-grained or nanocrystalline structures, and their exceptional mechanical strength is attributed to solid solution strengthening and grain refining. Additionally, this microstructure increases their hardness, which fits them for applications requiring resistance to wear [478]. Some HEAs exhibits respectable ductility and toughness in spite of their high strength, which can be further enhanced by post-milling procedures like annealing [479]. The consistent elemental distribution and the capacity of particular elements, like Cr, Al, or Ti, to result in stable passivation layers are frequently cited as the reasons for the remarkable corrosion resistance of HEAs [480]. Because of their phase stability and slow diffusion, these alloys also exhibit remarkable thermal stability, maintaining their mechanical characteristics at high temperatures. They are therefore appropriate for high-temperature applications where resistance to creep is crucial.

After MA, HEAs is quite functionally versatile. Some compositions, such those with Ti, Zr, or V, have good kinetics for both hydrogen absorption and desorption, which makes them promising for storing hydrogen [481–484]. Other alloys have adjustable magnetic characteristics that are beneficial for energy and electronic applications, especially those based on Fe-Co-Ni. Furthermore, many MA HEAs have catalytic qualities that allow them to function effectively in chemical reactions like CO_2 reduction or hydrogen storage [485,486]. Properties can be tailored to match particular application requirements due to the exact control of composition and microstructure during the mechanical alloying process. In order to prevent phase segregation and promote the development of solid solution phases or amorphous structures, homogeneity is ensured by uniform mixing at the atomic level. Their endurance is further demonstrated by their improved fatigue resistance and capacity to function under cyclic loading situations. These characteristics demonstrate the versatility and technological potential of mechanically alloyed HEAs by making them ideal for a broad range of applications, from energy storage and conversion systems to structural components.

8. Opportunities as well as challenges

For material scientists and engineers, MA offers a potential way to investigate the world of HEAs. Based on Table 1, the pie chart in Fig. 15 provides a clear visualization of the year-wise percentage increase in the synthesis of HEAs, highlighting the growing interest and advancements in this area over time. Efforts should be made to explore the intriguing possibilities and challenges associated with MA for HEA synthesis: A flexible method to synthesize HEAs, which allows for the controlled mixing and alloying of several constituent powders. By manipulating the kinds and amounts of elemental powders, MA enables the synthesis of a broad variety of alloy compositions and provides accurate control over the composition of HEAs. Achieving desirable qualities in HEAs requires uniform distribution of elements throughout the alloy, which is ensured by MA, which also promotes homogeneous mixing of constituent

Table 4
Summary of HEAs with their milling parameters, phases, compositions, and lattice parameters.

Sr. No.	Composition	Phase	Ball to Powder Ratio and Milling Time	Process Control Agent (PCA)	Lattice Parameter	References
1	Co-Cr-Fe-Ni-Cu	FCC	20: 1 and 30 min	Argon gas	3.589 ± 0.005 Å	[228]
2	Al-Co-Cr-Fe-Ni	BCC	10:1 and 30 h	Toluene	2.88 ± 0.01 Å	[144]
3	Co-Cr-Cu-Fe-Ni	FCC	10:1 and 5 h	Stearic Acid	3.602 Å	[95]
4	Co-Cr-Fe-Ni and Co-Cr-Fe-Mn-Ni	FCC	10:1 and 15 h	Toluene	…	[456]
5	Cr-Mn-Fe-V-Ti	BCC and FCC	10:1and 60 h	Ethanol	BCC = 2.8741 Å FCC = 4.1842 Å	[457]
6	Al-Co-Cr-Fe-Ni-$Si_{0.5}$	BCC and FCC	40 h	Argon Gas	BCC = 2.8745 and FCC = 2.8806 nm	[458]
7	Fe-Ni-Mn-Cu-X (X: Cr, Mo, Ti, W)	BCC and FCC	10:1 and 15 h	Stearic Acid	…	[459]
8	Al_x-Co-Cr-Cu-Fe-Ni ($x = 0.45$)	BCC and FCC	10:1 and 20 h	Toluene	BCC = 0.288 nm and FCC = 0.353 nm	[460]
9	Co-Cr-Fe-Ni-Ti-Al	BCC and FCC	15:1 and 18 h	N-Heptane	…	[461]
10	Al-Co-Cr-Cu-Fe and Ni-Co-Cr-Cu-Fe	FCC and BCC	10:1 and 15 h	…	FCC=3.62 Å	[462]
11	Co-Cr-Fe-Mn-Ni	FCC	10:1 and 15 h	Toluene	0.352 nm	[141]
12	Cu-Ni-Co-Zn-Al-Ti	BCC	10:1 and 10 h	Toluene	0.290 nm	[56]
13	Zr_x-Fe-Ni-$Si_{0.4}$-$B_{0.6}$	Amorphous	15:1 and 180 h	Argon Gas	…	[142]
14	Co-Cr-Fe-Ni	FCC, BCC, CrC and CrO	15 h	Oxygen	…	[107]

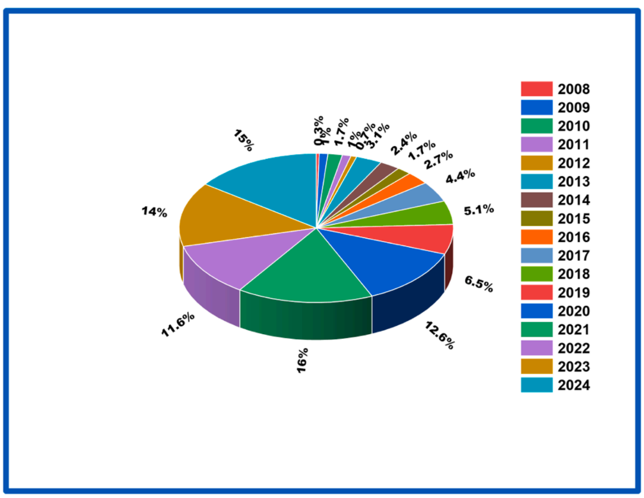

Fig. 15. The pie chart illustrates the year-wise percentage increase in the synthesis of HEAs through mechanical alloying (MA), providing a clear visualization of the trend over time.

powders. MA allows for the specific development of nanocrystalline or ultrafine-grained structures in HEAs by carefully regulating milling parameters as speed, duration, and ball-to-powder ratio. For large-scale HEA production, MA is a simple process to scale up, which makes it appropriate for both industrial and laboratory-scale research.

A proactive approach to these issues can provide to opportunities for innovation, optimization, leading to the progress of materials research. Although the reactivity of some elemental powders poses challenges in HEA synthesis, it remains a viable option. For reactive elements or materials that are sensitive to oxygen, MA is frequently carried out in ambient settings, which can cause oxidation and contamination of powders. In order to accomplish the appropriate alloying and microstructural refinement, MA is an energy-intensive process that requires high-powered ball mills and extended milling times, which raises energy consumption and operating costs. Due to the abrasive nature, milling equipment may wear down and degrade in course of operation, requiring regular maintenance and the replacement of liners and milling media, which raises maintenance costs. The synthesis process is made more complex by the need for rigorous optimization and knowledge of numerous parameters, including milling speed, time, ball-to-powder ratio, and milling environment, in order to achieve the ideal milling parameters to synthesize HEAs. Despite these difficulties, MA presents a number of advantages for the synthesis of HEAs, such as its adaptability, scalability, and capacity to customize microstructures, making it a viable technique for advancing HEA research and development. By addressing the challenges with meticulous process optimization and equipment maintenance, MA for HEA synthesis can be made even more effective and efficient.

9. Conclusion

In summary, MA can be considered as a unique process that can yield HEAs with a broad variety of features and attributes. Attempts have been made to review the synthesis criteria, MA methods, types of ball mills and many HEAs that can be produced using this method, which delves into many facets of the synthesis of HEAs by MA. Future research should focus on other important aspects of the MA process, such as milling speed, ball-to-powder ratio, process control agent, and milling time, even if the main focus to be on obtaining a homogeneous solid solution of components by adjusting milling parameters. These variables affect the heat produced during milling as well as the dispersion of the main ingredients during the solid solution process. Furthermore, when fine HEA particles are evenly distributed throughout the solid solution, MA significantly improves the mechanical qualities of HEAs, such as hardness, high-temperature strength, thermal stability, corrosion resistance, oxidation resistance, and wear resistance. The need to customize the synthesis process to attain desired mechanical properties in a variety of settings is highlighted by the observation that variations in milling duration result in variances in controlling the properties and crystal structures. It is also important to note that in case HEAs, MA generates phases of solid solutions with many phases and complicated structures, highlighting the complexity of these new mateials. In general, the knowledge gathered from this discussion highlights the role of MA in synthesizing HEAs with exceptional mechanical qualities, opening new avenues for research and developments in materials science and engineering.

CRediT authorship contribution statement

YADAV THAKUR PRASAD: Writing – review & editing, Visualization, Validation, Supervision, Resources, Project administration, Methodology, Investigation, Funding acquisition, Formal analysis, Conceptualization. **Mukhopadhyay Nilay Krishna:** Writing – review & editing, Resources, Formal analysis. **Abu Shaz Mohammad:** Writing – review & editing, Resources. **Yadav Yogesh Kumar:** Writing – original draft, Formal analysis, Data curation.

Declaration of Competing Interest

The authors declare that they have no known competing financial interests or personal relationships that could have appeared to influence the work reported in this paper.

Acknowledgement

The author would like to extend sincere gratitude to late Professor O. N. Srivastava for his important and long-lasting support in establishing and sustaining a highly productive laboratory in the prestigious Physics Department at Banaras Hindu University, Varanasi-221005. The department's research culture and quality climate have been greatly influenced by Prof. Srivastava's commitment, knowledge, and mentoring, which has laid the groundwork for many scientific projects and breakthroughs. Furthermore, the authors would like to express their gratitude for the financial support provided by the Institute of Eminence (IoE), Banaras Hindu University. Additionally, the author (YKY) would like to thank the University Grants Commission (UGC) for granting the fellowship. TPY thanks the Council of Science and Technology Uttar Pradesh (Ref. no.CST/D-833; Project ID: 4057) for the financial support.

References

[1] S.S. Mishra, U. Kumar, B.B. Raj, H. Ko, T.P. Yadav, Multifaceted investigation into the impact of Ga substitution for Al in V2MnAl inverse Heusler alloys, Phys. B: Condens. Matter (2024) 416345, https://doi.org/10.1016/j.physb.2024.416345.

[2] N. Mandal, A.B. Santos, A. Chakraborty, S. Sarkar, R. Rao, N.R. Glavin, A.K. Roy, V. Kochat, T.P. Yadav, N.K. Mukhopadhyay, D.S. Galvão, C.F. Woellner, C. S. Tiwary, Plasmonically Active Atomically Thin Titanium-Based Quasicrystals for Dopamine Sensing, ACS Appl. Nano Mater. 7 (13) (2024) 15395–15405.

[3] Karen Harvey, History and material culture: A student's guide to approaching alternative sources, Routledge, 2013.

[4] A. Verma, J.D. Tanwar, J.S. Tawale, P. Kushwaha, B. Borgohain, P.K. Siwach, T. P. Yadav, H.K. Singh, Elucidation of annealing effects on austenite–martensite and magnetic phase transitions in Mn2Ni1.6Sn0.4 ribbons synthesized from bulk alloys prepared by RF induction melting, J. Magn. Magn. Mater. 603 (2024) 172270.

[5] N. Mandal, P. Kumbhakar, A. Dey, P. Kumbhakar, U. Chatterjee, Christiano J. S. de Matos, TP Yadav, NK Mukhopadhyay, K. Biswas, V. Kochat, CS Tiwary, Optical Resonator-Enhanced Random Lasing using Atomically Thin Aluminium-based Multicomponent Quasicrystals, Opt. Laser Technol. 175 (2024) 110746.

[6] K. Jha, P. Jaishwal, T.P. Yadav, S.P. Singh, Self-assembling of coiled-coil peptides into virus-like particles: Basic principles, properties, design, and applications with special focus on vaccine design and delivery, Biophys. Chem. 318 (2025) 107375.

[7] A. Parveen, S. Sonkar, T.P. Yadav, P.K. Sarangi, A.K. Singh, S.P. Singh, R. Gupta, Asparagus racemosus Leaf Extract Mediated Bioconversion of Nickel Sulfate into Nickel/ Nickel Hydroxide Nanoparticles: in-vitro Catalytic, Antibacterial, and Antioxidant Activities, Biomass Conversion and Biorefinery 14 (5).

[8] {C}Pigott, Vincent C.{C}., ed. The archaeometallurgy of the Asian old world. Vol. 16. UPenn Museum of Archaeology, 1999.

[9] Nissim Amzallag, "From metallurgy to Bronze Age civilizations: the synthetic theory, Am. J. Archaeol. 113 (4) (2009) 497–519.

[10] TP Yadav, NK Mukhopadhyay, RS Tiwari, ON Srivastava, Characterization of Mechanically milled $Al_{65}Cu_{20}Fe_{15}$ icosahedral quasicrystalline alloy, Trans. Indian Inst. Met. 56 (6) (2003) 577–581.

[11] N.K. Mukhopadhyay, T.P. Yadav, O.N. Srivastava, An investigation on the transformation of the icosahedral phase in Al-Fe-Cu system during mechanical milling and subsequent annealing, Philos. *Mag. A* 82 (16) (2002) 2979–2993.

[12] T.P. Yadav, M.A. Shaz, R.S. Tiwari, O.N. Srivastava, Investigation of Transition from Decagonal to Vacancy ordered phase on replacement of Co by Cu in $Al_{70}Co_{15-x}Cu_xNi_{15}$, *Zeitschrift fur Krystallographic* 218 (1) (2003) 12–16.

[13] Takehide Senuma, "Physical metallurgy of modern high strength steel sheets, ISIJ Int. 41 (6) (2001) 520–532.

[14] Qiang Yue, et al., "Analysis of iron and steel production paths on the energy demand and carbon emission in China's iron and steel industry, Environ., Dev. Sustain. 25 (5) (2023) 4065–4085.

[15] Zhiyuan Fan, S.Julio Friedmann, "Low-carbon production of iron and steel: Technology options, economic assessment, and policy, Joule 5 (4) (2021) 829–862.

[16] Diandra L. Leslie-Pelecky, Reuben D. Rieke, "Magnetic properties of nanostructured materials, Chem. Mater. 8 (8) (1996) 1770–1783.

[17] Srivatsan T.S., Gupta M., (2020). High Entropy Alloys: Innovations, Advances, and Applications.

[18] J.-W. Yeh, et al., "Nanostructured high-entropy alloys with multiple principal elements: novel alloy design concepts and outcomes, Adv. Eng. Mater. 6 (5) (2004) 299–303.

[19] Cantor, Brain, et al., "Microstructural development in equiatomic multicomponent alloys, *Mater. Sci. Eng.: A* 375 (2004) 213–218.

[20] Murty, B.S., Yeh Jien-Wei, Ranganathan S., Bhattacharjee P.P. High-entropy alloys. Elsevier, 2019, ISBN: 9780128160688.

[21] Yong Zhang, et al., "Microstructures and properties of high-entropy alloys, Prog. Mater. Sci. 61 (2014) 1–93.

[22] Y. Zhang, X. Yang, P.K. Liaw, "Alloy design and properties optimization of high-entropy alloys, Jom 64 (2012) 830–838.

[23] Y.J. Zhou, et al., "Solid solution alloys of AlCoCrFeNiTix with excellent room-temperature mechanical properties, Appl. Phys. Lett. 90 (18) (2007).

[24] Yong Zhang, et al., "Minor alloying behavior in bulk metallic glasses and high-entropy alloys, Sci. China Ser. G: Phys., Mech. Astron. 51 (2008) 427–437.

[25] Caiyun Shang, et al., "High-entropy alloy coatings with excellent mechanical, corrosion resistance and magnetic properties prepared by mechanical alloying and hot-pressing sintering, Surf. Interfaces 9 (2017) 36–43.

[26] Jiacheng Duan, et al., "A novel high-entropy alloy with an exceptional combination of soft magnetic properties and corrosion resistance, Sci. China Mater. 66 (2) (2023) 772–779.

[27] A.K. Maddheshiya, S.P. Singh, D. Singh, P.S. Yadav, R.R. Yadav, T.P. Yadav, Theoretical investigation on the elastic and mechanical properties of high-entropy alloys with partial replacement of Sc in Hf0.25Ti0.25Zr0.25Sc0.25−xAlx (x≤ 15%), Z. F. üR. Naturforsch. A 78 (11) (2023) 1051–1059.

[28] Zhiming Li, et al., "Combinatorial metallurgical synthesis and processing of high-entropy alloys, J. Mater. Res. 33 (19) (2018) 3156–3169.

[29] José Manuel Torralba, Paula Alvaredo, Andrea García-Junceda, "High-entropy alloys fabricated via powder metallurgy. A critical review, Powder Metall. 62 (2) (2019) 84–114.

[30] E. Colombini, et al., "High entropy alloys obtained by field assisted powder metallurgy route: SPS and microwave heating, Mater. Chem. Phys. 210 (2018) 78–86.

[31] Xin Wang, Wei Guo, Yongzhu Fu, "High-entropy alloys: emerging materials for advanced functional applications, J. Mater. Chem. A 9 (2) (2021) 663–701.

[32] S.S. Mishra, S. Mukhopadhyay, T.P. Yadav, N.K. Mukhopadhyay, O.N. Srivastav, Synthesis and characterization of hexanary Ti–Zr–V–Cr–Ni–Fe high-entropy Laves phase, J. Mater. Res. 34 (5) (2019) 807–818.

[33] Tushar Borkar, et al., A combinatorial assessment of AlxCrCuFeNi2 (0< x< 1.5) complex concentrated alloys: Microstructure, microhardness, and magnetic properties. Acta Mater. 116 (2016) 63–76.

[34] B. Niu, et al., "Alloying and thermal behaviour of CoCrFeNiMn0. 5Ti0. 5 high-entropy alloy synthesized by mechanical alloying, Mater. Sci. Technol. 32 (1) (2016) 94–98.

[35] Naresh Kaushik, Anoj Meena, Harlal Singh Mali High, entropy alloy synthesis, characterisation, manufacturing & potential applications: a review, Mater. Manuf. Process. 37 (10) (2022) 1085–1109.

[36] C. Suryanarayana, "Mechanical alloying and milling, Prog. Mater. Sci. 46 (1-2) (2001) 1–184.

[37] B.S. Murty, S.J.M.R. Ranganathan, "Novel materials synthesis by mechanical alloying/milling, Int. Mater. Rev. 43 (3) (1998) 101–141.

[38] T.P. Yadav, O.N. Srivastava, "Synthesis of nanocrystalline cerium oxide by high energy ball milling, Ceram. Int. 38 (7) (2012) 5783–5789.

[39] T.P. Yadav, et al., "Studies on the formation and stability of nano-crystalline Al50Cu28Fe22 alloy synthesized through high-energy ball milling, Mater. Sci. Eng.: A 393 (1-2) (2005) 366–373.

[40] T.P. Yadav, et al., "On the evolution of a nanocrystalline phase from the Al-Cu-Fe quasicrystalline alloy during high energy ball milling, Trans. Indian Inst. Met. 58 (6) (2005) 1169–1176.

[41] N.K. Mukhopadhyay, Thakur Prasad Yadav, "Some aspects of stability and nanophase formation in quasicrystals during mechanical milling, Isr. J. Chem. 51 (11-12) (2011) 1185–1196.

[42] T.P. Yadav, et al., "Phase transformations in Al70Ni24Fe6 decagonal system during high energy ball milling, Philos. Mag. 86 (3-5) (2006) 397–404.

[43] T.P. Yadav, et al., "Formation of Al3Ni2-type nanocrystalline τ 3 phases in the Al–Cu–Ni system by mechanical alloying, Philos. Mag. Lett. 87 (10) (2007) 781–789.

[44] Thakur Yadav, Prasad, R.M. Yadav, D.P. Singh, "Mechanical milling: a top-down approach for the synthesis of nanomaterials and nanocomposites, Nanosci. Nanotechnol. 2 (3) (2012) 22–48.

[45] J.S. Benjamin, "Fundamentals of mechanical alloying, in: Materials Science Forum, 88, Trans Tech Publications Ltd, 1992.

[46] S. Varalakshmi, M. Kamaraj, B.S. Murty, "Synthesis and characterization of nanocrystalline AlFeTiCrZnCu high entropy solid solution by mechanical alloying, J. Alloy. Compd. 460 (1-2) (2008) 253–257.

[47] Mayur Vaidya, Garlapati Mohan Muralikrishna, Budaraju Srinivasa Murty, "High-entropy alloys by mechanical alloying: A review, J. Mater. Res. 34 (5) (2019) 664–686.

[48] Yu-Liang Chen, et al., "Structural evolution during mechanical milling and subsequent annealing of Cu–Ni–Al–Co–Cr–Fe–Ti alloys, Mater. Chem. Phys. 118 (2-3) (2009) 354–361.

[49] S. Varalakshmi, M. Kamaraj, B.S. Murty, "Formation and stability of equiatomic and nonequiatomic nanocrystalline CuNiCoZnAlTi high-entropy alloys by mechanical alloying, Metall. Mater. Trans. A 41 (2010) 2703–2709.
[50] C.D. Gómez-Esparza, et al., "Microstructure of NiCoAlFeCuCr multi-component systems synthesized by mechanical alloying, J. Alloy. Compd. 509 (2011) S279–S283.
[51] S. Praveen, B.S. Murty, Ravi S. Kottada, "Alloying behavior in multi-component AlCoCrCuFe and NiCoCrCuFe high entropy alloys, Mater. Sci. Eng.: A 534 (2012) 83–89.
[52] S. Varalakshmi, M. Kamaraj, B.S. Murty, "Synthesis and characterization of nanocrystalline AlFeTiCrZnCu high entropy solid solution by mechanical alloying, J. Alloy. Compd. 460 (1-2) (2008) 253–257.
[53] Yu-Liang Chen, et al., "Structural evolution during mechanical milling and subsequent annealing of Cu–Ni–Al–Co–Cr–Fe–Ti alloys, Mater. Chem. Phys. 118 (2-3) (2009) 354–361.
[54] K.B. Zhang, et al., "Nanocrystalline CoCrFeNiCuAl high-entropy solid solution synthesized by mechanical alloying, J. Alloy. Compd. 485 (1-2) (2009) L31–L34.
[55] Kui Bao Zhang, et al., "Characterization of nanocrystalline CoCrFeNiCuAl high-entropy alloy powder processed by mechanical alloying, in: Materials Science Forum, 620, Trans Tech Publications Ltd, 2009.
[56] S. Varalakshmi, M. Kamaraj, B.S. Murty, "Processing and properties of nanocrystalline CuNiCoZnAlTi high entropy alloys by mechanical alloying, Mater. Sci. Eng.: A 527 (4-5) (2010) 1027–1030.
[57] S. Varalakshmi, M. Kamaraj, B.S. Murty, "Formation and stability of equiatomic and nonequiatomic nanocrystalline CuNiCoZnAlTi high-entropy alloys by mechanical alloying, Metall. Mater. Trans. A 41 (2010) 2703–2709.
[58] Xiu Wei, et al., "Thermal stability of the Al70Ni10Ti10Zr5Ta5 amorphous alloy powder fabricated by mechanical alloying, J. Alloy. Compd. 496 (1-2) (2010) 313–316.
[59] S. Varalakshmi, et al., "Hot consolidation and mechanical properties of nanocrystalline equiatomicAlFeTiCrZnCu high entropy alloy after mechanical alloying, J. Mater. Sci. 45 (2010) 5158–5163.
[60] K.B. Zhang, et al., "Characterization of nanocrystalline CoCrFeNiTiAl high-entropy solid solution processed by mechanical alloying, J. Alloy. Compd. 495 (1) (2010) 33–38.
[61] Vura Sandeep, et al., Synthesis and characterization of AlFeCrNi four component high entropy alloy by mechanical alloying, Int. J. Eng. Sci. Technol. IJEST 3 (5) (2011) 3876–3880.
[62] C.D. Gómez-Esparza, et al., "Microstructure of NiCoAlFeCuCr multi-component systems synthesized by mechanical alloying, J. Alloy. Compd. 509 (2011) S279–S283.
[63] C. Gómez-Esparza, et al., "Sintering Process on Microstructure Evolution of Ni-Co-Al-Fe-Cu-Cr-Ti High-Entropy Alloys, Microsc. Microanal. 17 (S2) (2011) 1880–1881.
[64] S. Praveen, B.S. Murty, Ravi S. Kottada, "Alloying behavior in multi-component AlCoCrCuFe and NiCoCrCuFe high entropy alloys, Mater. Sci. Eng.: A 534 (2012) 83–89.
[65] Esparza, C. Gómez, et al., "NiCoAlFeCrTi High Entropy Alloys Produced In Solid State, Microsc. Microanal. 18 (S2) (2012) 1920–1921.
[66] R. Sriharitha, B.S. Murty, Ravi S. Kottada, "Phase formation in mechanically alloyed AlxCoCrCuFeNi (x= 0.45, 1, 2.5, 5 mol) high entropy alloys, Intermetallics 32 (2013) 119–126.
[67] N.T.B.N. Koundinya, et al., "Phase evolution and thermal analysis of nanocrystalline AlCrCuFeNiZn high entropy alloy produced by mechanical alloying, J. Mater. Eng. Perform. 22 (2013) 3077–3084.
[68] S. Praveen, et al., "Characterization of oxide dispersed AlCoCrFe high entropy alloy synthesized by mechanical alloying and spark plasma sintering, Trans. Indian Inst. Met. 66 (2013) 369–373.
[69] Sanghita Mridha, et al., "Processing and consolidation of nanocrystalline Cu-Zn-Ti-Fe-Cr high-entropy alloys via mechanical alloying, Metall. Mater. Trans. A 44 (2013) 4532–4541.
[70] Weiping Chen, et al., "Alloying behavior, microstructure and mechanical properties in a FeNiCrCo0. 3Al0. 7 high entropy alloy, Mater. Des. 51 (2013) 854–860.
[71] Zhiqiang Fu, et al., "Alloying behavior and deformation twinning in a CoNiFeCrAl0. 6Ti0. 4 high entropy alloy processed by spark plasma sintering, J. Alloy. Compd. 553 (2013) 316–323.
[72] Weiping Chen, et al., "Processing, microstructure and properties of Al0. 6CoNiFeTi0. 4 high entropy alloy with nanoscale twins, Mater. Sci. Eng.: A 565 (2013) 439–444.
[73] Gang Zhu, Ying Liu, Jinwen Ye, "Fabrication and properties of Ti (C, N)-based cermets with multi-component AlCoCrFeNi high-entropy alloys binder, Mater. Lett. 113 (2013) 80–82.
[74] É . Fazakas, B. Varga, L.K. Varga, "Processing and properties of nanocrystalline CoCrFeNiCuAlTiXVMo (X= Zn, Mn) high entropy alloys by mechanical alloying, Int. Sch. Res. Not. 2013 (1) (2013) 167869.
[75] K. Sivaprasad, V. Muthupandi, Jerzy A. Szpunar, "Characterization of nanocrystalline AlCoCrCuNiFeZn high entropy alloy produced by mechanical alloying, Procedia Mater. Sci. 5 (2014) 1020–1026.
[76] Sutanuka Mohanty, N.P. Gurao, Krishanu Biswas, "Sinter ageing of equiatomic Al20Co20Cu20Zn20Ni20 high entropy alloy via mechanical alloying, Mater. Sci. Eng.: A 617 (2014) 211–218.
[77] Chao Wang, Wei Ji, Zhengyi Fu, "Mechanical alloying and spark plasma sintering of CoCrFeNiMnAl high-entropy alloy, Adv. Powder Technol. 25 (4) (2014) 1334–1338.
[78] Sicong Fang, Weiping Chen, Zhiqiang Fu, "Microstructure and mechanical properties of twinned Al0. 5CrFeNiCo0. 3C0. 2 high entropy alloy processed by mechanical alloying and spark plasma sintering, Mater. Des. (1980-2015 54 (2014) 973–979.
[79] K. Sivaprasad, V. Muthupandi, Jerzy A. Szpunar, "Characterization of nanocrystalline AlCoCrCuNiFeZn high entropy alloy produced by mechanical alloying, Procedia Mater. Sci. 5 (2014) 1020–1026.
[80] Wei Ji, et al., "Mechanical alloying synthesis and spark plasma sintering consolidation of CoCrFeNiAl high-entropy alloy, J. Alloy. Compd. 589 (2014) 61–66.
[81] Jian Wang, et al., "Microstructure and magnetic properties of mechanically alloyed FeSiBAlNi (Nb) high entropy alloys, J. Magn. Magn. Mater. 355 (2014) 58–64.
[82] Wei Ji, et al., "Alloying behavior and novel properties of CoCrFeNiMn high-entropy alloy fabricated by mechanical alloying and spark plasma sintering, Intermetallics 56 (2015) 24–27.
[83] Zhen Chen, et al., "Effects of Co and Ti on microstructure and mechanical behavior of Al0. 75FeNiCrCo high entropy alloy prepared by mechanical alloying and spark plasma sintering, Mater. Sci. Eng.: A 648 (2015) 217–224.
[84] Andrew Siao Ming Ang, et al., "Plasma-sprayed high entropy alloys: Microstructure and properties of AlCoCrFeNi and MnCoCrFeNi, Metall. Mater. Trans. A 46 (2015) 791–800.
[85] F.J. Baldenebro-Lopez, et al., "Simultaneous effect of mechanical alloying and arc-melting processes in the microstructure and hardness of an AlCoFeMoNiTi high-entropy alloy, J. Alloy. Compd. 643 (2015) S250–S255.
[86] Jian Chen, et al., "Fabrication and mechanical properties of AlCoNiCrFe high-entropy alloy particle reinforced Cu matrix composites, J. Alloy. Compd. 649 (2015) 630–634.
[87] Murali, Muthamizhdan, et al., "Synthesis and characterization of AlCoCrCuFeZnx high-entropy alloy by mechanical alloying, Prog. Nat. Sci.: Mater. Int. 26 (4) (2016) 380–384.
[88] P.F. Yu, et al., "The high-entropy alloys with high hardness and soft magnetic property prepared by mechanical alloying and high-pressure sintering, Intermetallics 70 (2016) 82–87.
[89] B. Niu, et al., "Alloying and thermal behaviour of CoCrFeNiMn0. 5Ti0. 5 high-entropy alloy synthesised by mechanical alloying, Mater. Sci. Technol. 32 (1) (2016) 94–98.
[90] Cynthia Deisy Gómez-Esparza, et al., "Series of nanocrystalline NiCoAlFe (Cr, Cu, Mo, Ti) high-entropy alloys produced by mechanical alloying, Mater. Res. 19 (1) (2016) 39–46.
[91] F. Salemi, M.H. Abbasi, F. Karimzadeh, "Synthesis and thermodynamic analysis of nanostructured CuNiCoZnAl high entropy alloy produced by mechanical alloying, J. Alloy. Compd. 685 (2016) 278–286.
[92] Xin-Rong Tan, et al., "Effects of milling on the microstructure and hardness of Al2NbTi3V2Zr high-entropy alloy, Mater. Des. 109 (2016) 27–36.
[93] Devesh Kumar, et al., "Microstructure and characterization of mechanically alloyed equiatomicAlCuCrFeMnW high entropy alloy, Mater. Today.: Proc. 3 (9) (2016) 2926–2933.
[94] Jing Xu, et al., "Effects of elemental addition on the microstructure, thermal stability, and magnetic properties of the mechanically alloyed FeSiBAlNi high entropy alloys, Adv. Powder Technol. 27 (4) (2016) 1418–1426.
[95] Shanmugasundaram Thangaraju, Emmanuel Bouzy, Alain Hazotte, "Phase stability of a mechanically alloyed CoCrCuFeNi high entropy alloy, Adv. Eng. Mater. 19 (8) (2017) 1700095.
[96] S. Mohanty, et al., "Powder metallurgical processing of equiatomicAlCoCrFeNi high entropy alloy: Microstructure and mechanical properties, Mater. Sci. Eng.: A 679 (2017) 299–313.
[97] Igor Moravcik, et al., "Microstructure and mechanical properties of Ni1, 5Co1, 5CrFeTi0, 5 high entropy alloy fabricated by mechanical alloying and spark plasma sintering, Mater. Des. 119 (2017) 141–150.
[98] S.-H. Joo, et al., "Structure and properties of ultrafine-grained CoCrFeMnNi high-entropy alloys produced by mechanical alloying and spark plasma sintering, J. Alloy. Compd. 698 (2017) 591–604.
[99] Caiyun Shang, et al., "CoCrFeNi (W1− xMox) high-entropy alloy coatings with excellent mechanical properties and corrosion resistance prepared by mechanical alloying and hot-pressing sintering, Mater. Des. 117 (2017) 193–202.
[100] Wenjuan Ge, et al., "Characterization and properties of CuZrAlTiNi high entropy alloy coating obtained by mechanical alloying and vacuum hot-pressing sintering, Adv. Powder Technol. 28 (10) (2017) 2556–2563.
[101] Ramya Sree Ganji, et al., "Strengthening mechanisms in equiatomic ultrafine grained AlCoCrCuFeNi high-entropy alloy studied by micro-and nanoindentation methods, Acta Mater. 125 (2017) 58–68.
[102] Hari Prasad, Sheela Singh, Bharat B. Panigrahi, "Mechanical activated synthesis of alumina dispersed FeNiCoCrAlMn high entropy alloy, J. Alloy. Compd. 692 (2017) 720–726.
[103] Anil Kumar, et al., "Analysis of Si addition on phase formation in AlCoCrCuFeNiSix high entropy alloys, Mater. Lett. 188 (2017) 73–76.
[104] A.M. Rameshbabu, et al., "Diffraction, microstructure and thermal stability analysis in a double phase nanocrystalline Al20Mg20Ni20Cr20Ti20 high entropy alloy, J. Mech. Behav. Mater. 26 (3-4) (2017) 127–132.
[105] Mayur Vaidya, et al., "Influence of sequence of elemental addition on phase evolution in nanocrystalline AlCoCrFeNi: Novel approach to alloy synthesis using mechanical alloying, Mater. Des. 126 (2017) 37–46.
[106] R. Bureš, et al., "FeSiBAlNiMo high entropy alloy prepared by mechanical alloying, Acta Phys. Pol. A 131 (4) (2017) 771–773.

[107] Praveen Sathiyamoorthi, et al., "Thermal stability and grain boundary strengthening in ultrafine-grained CoCrFeNi high entropy alloy composite, Mater. Des. 134 (2017) 426–433.
[108] Jiayi Pan, et al., "Microstructure and mechanical properties of Nb25Mo25Ta25W25 and Ti8Nb23Mo23Ta23W23 high entropy alloys prepared by mechanical alloying and spark plasma sintering, Mater. Sci. Eng.: A 738 (2018) 362–366.
[109] Jiayi Pan, et al., "Microstructure and mechanical properties of Nb25Mo25Ta25W25 and Ti8Nb23Mo23Ta23W23 high entropy alloys prepared by mechanical alloying and spark plasma sintering, Mater. Sci. Eng.: A 738 (2018) 362–366.
[110] Lihui Tian, Ming Fu, Wei Xiong, "Microstructural evolution of AlCoCrFeNiSi high-entropy alloy powder during mechanical alloying and its coating performance, Materials 11 (2) (2018) 320.
[111] Dariusz Oleszak, Anna Antolak-Dudka, Tadeusz Kulik, "High entropy multicomponent WMoNbZrV alloy processed by mechanical alloying, Mater. Lett. 232 (2018) 160–162.
[112] Sujit Das, P.S. Robi, "Mechanical alloying of W-Mo-V-Cr-Ta high entropy alloys, in: IOP Conference Series: Materials Science and Engineering, 346, IOP Publishing, 2018.
[113] Vikas Shivam, et al., "Mechano-chemical synthesis, thermal stability and phase evolution in AlCoCrFeNiMn high entropy alloy, J. Alloy. Compd. 757 (2018) 87–97.
[114] Yan Long, et al., "Enhanced strength of a mechanical alloyed NbMoTaWVTi refractory high entropy alloy, Materials 11 (5) (2018) 669.
[115] Anil Kumar, Akhilesh Kumar Swarnakar, Manoj Chopkar, "Phase evolution and mechanical properties of AlCoCrFeNiSi x high-entropy alloys synthesized by mechanical alloying and spark plasma sintering, J. Mater. Eng. Perform. 27 (2018) 3304–3314.
[116] Yanchong Xie, et al., "Effects of N addition on microstructure and mechanical properties of CoCrFeNiMn high entropy alloy produced by mechanical alloying and vacuum hot-pressing sintering, Intermetallics 93 (2018) 228–234.
[117] Rizaldy M. Pohan, et al., "Microstructures and mechanical properties of mechanically alloyed and spark plasma sintered Al0. 3CoCrFeMnNi high entropy alloy, Mater. Chem. Phys. 210 (2018) 62–70.
[118] Wen Wang, et al., "Alloying behavior and properties of FeSiBAlNiCo x high entropy alloys fabricated by mechanical alloying and spark plasma sintering, Met. Mater. Int. 24 (2018) 1112–1119.
[119] Vikas Shivam, et al., "Alloying behaviour, thermal stability and phase evolution in quinary AlCoCrFeNi high entropy alloy, Adv. Powder Technol. 29 (9) (2018) 2221–2230.
[120] S. Praveen, et al., "Phase evolution and thermal stability of AlCoCrFe high entropy alloy with carbon as unsolicited addition from milling media, Mater. Chem. Phys. 210 (2018) 57–61.
[121] Anil Kumar, et al., "Phase evolution of CoCrCuFeNiSix high-entropy alloys prepared by mechanical alloying and spark plasma sintering, Mater. Res. Express 6 (2) (2018) 026532.
[122] Qiumin Yang, et al., "Microstructures and properties of CoCrCuFeNiMox high-entropy alloys fabricated by mechanical alloying and spark plasma sintering, Powder Metall. 61 (2) (2018) 115–122.
[123] F. Alijani, M. Reihanian, Kh Gheisari, "Study on phase formation in magnetic FeCoNiMnV high entropy alloy produced by mechanical alloying, J. Alloy. Compd. 773 (2019) 623–630.
[124] Guofeng Wang, et al., "Synthesis and thermal stability of a nanocrystalline MoNbTaTiV refractory high-entropy alloy via mechanical alloying, Int. J. Refract. Met. Hard Mater. 84 (2019) 104988.
[125] Cheng, Hu, et al., "Microstructure and mechanical properties of FeCoCrNiMnAlx high-entropy alloys prepared by mechanical alloying and hot-pressed sintering, J. Alloy. Compd. 775 (2019) 742–751.
[126] Ali Arab, et al., "Fabrication of nanocrystalline AlCoCrFeNi high entropy alloy through shock consolidation and mechanical alloying, Entropy 21 (9) (2019) 880.
[127] Tian, Ye, et al., "Microstructure and corrosion property of CrMnFeCoNi high entropy alloy coating on Q235 substrate via mechanical alloying method, Surf. Interfaces 15 (2019) 135–140.
[128] Xiaoqiang Liu, et al., "Microstructure and mechanical properties of FeCoCrNiMnTi0. 1C0. 1 high-entropy alloy produced by mechanical alloying and vacuum hot-pressing sintering, Vacuum 165 (2019) 297–304.
[129] Vikas Shivam, et al., "Alloying behavior and thermal stability of mechanically alloyed nano AlCoCrFeNiTi high-entropy alloy, J. Mater. Res. 34 (5) (2019) 787–795.
[130] Alexandra Yurkova, Ivanovna, et al., "Structure formation and mechanical properties of the high-entropy AlCuNiFeCr alloy prepared by mechanical alloying and spark plasma sintering, J. Alloy. Compd. 786 (2019) 139–148.
[131] Chun-Liang Chen, "Effects of nano-dispersoids on synthesis and characterization of low Cr-containing CoNiFeMnCr high entropy alloy by mechanical alloying, Intermetallics 113 (2019) 106570.
[132] Yuchen Sun, et al., "Phases, microstructures and mechanical properties of CoCrNiCuZn high-entropy alloy prepared by mechanical alloying and spark plasma sintering, Entropy 21 (2) (2019) 122.
[133] Lavanya Raman, et al., "Phase evolution of refractory high-entropy alloy CrMoNbTiW during mechanical alloying and spark plasma sintering, J. Mater. Res. 34 (5) (2019) 756–766.
[134] M. Ghanbariha, M. Farvizi, T. Ebadzadeh, "Microstructural development in nanostructured AlCoCrFeNi–ZrO2 high-entropy alloy composite prepared with mechanical alloying and spark plasma sintering methods, Mater. Res. Express 6 (12) (2019) 1265b5.
[135] Changqing Shu, et al., "Effect of V and ball milling time on microstructure and thermal properties of CoCrCuFeNiVX by mechanical alloying, Phys. B: Condens. Matter 571 (2019) 235–242.
[136] Qing Liu, et al., "Microstructure and mechanical properties of ultra-fine grained MoNbTaTiV refractory high-entropy alloy fabricated by spark plasma sintering, J. Mater. Sci. Technol. 35 (11) (2019) 2600–2607.
[137] Yan Long, et al., "A fine-grained NbMoTaWVCr refractory high-entropy alloy with ultra-high strength: Microstructural evolution and mechanical properties, J. Alloy. Compd. 780 (2019) 607–617.
[138] Xuyao Ni, et al., "Microstructure and properties of CrMnFeCoNi high-entropy alloy prepared by mechanical alloying and spark plasma sintering, Powder Metall. 62 (1) (2019) 38–43.
[139] Sekhar, R. Anand, et al., "Microstructure and mechanical properties of Ti-Al-Ni-Co-Fe based high entropy alloys prepared by powder metallurgy route, J. Alloy. Compd. 787 (2019) 123–132.
[140] Rajesh K. Mishra, P.P. Sahay, Rohit R. Shahi, "Alloying, magnetic and corrosion behavior of AlCrFeMnNiTi high entropy alloy, J. Mater. Sci. 54 (2019) 4433–4443.
[141] M. Vaidya, et al., "Phase evolution and stability of nanocrystalline CoCrFeNi and CoCrFeMnNi high entropy alloys, J. Alloy. Compd. 770 (2019) 1004–1015.
[142] Liming Sang, Yi Xu, "Amorphous behavior of ZrxFeNiSi0. 4B0. 6 high entropy alloys synthesized by mechanical alloying, J. Non-Cryst. Solids 530 (2020) 119854.
[143] Chun-Liang Chen, "Microstructure and mechanical properties of AlCuNiFeCr high entropy alloy coatings by mechanical alloying, Surf. Coat. Technol. 386 (2020) 125443.
[144] Vikas Shivam, et al., "Evolution of phases, hardness and magnetic properties of AlCoCrFeNi high entropy alloy processed by mechanical alloying, J. Alloy. Compd. 832 (2020) 154826.
[145] K.átia Regina Cardoso, et al., "Mechanical alloying and spark plasma sintering of AlCrCuFeZn high entropy alloy, Mater. Sci. Technol. 36 (17) (2020) 1861–1869.
[146] Rahul John, et al., "Microstructure and mechanical properties of a high entropy alloy with a eutectic composition (AlCoCrFeNi2. 1) synthesized by mechanical alloying and spark plasma sintering, J. Alloy. Compd. 835 (2020) 155424.
[147] Kaouther Zaara, et al., "High-Entropy FeCoNiB0. 5Si0. 5 alloy synthesized by mechanical alloying and spark plasma sintering, Crystals 10 (10) (2020) 929.
[148] Zhang Yingzhe, et al., "Synthesis of FeCoNiCuZn single-phase high-entropy alloy by high-frequency electromagnetic-field assisted ball milling, J. Magn. Magn. Mater. 498 (2020) 166151.
[149] Pranjal Chauhan, et al., "Development of a novel light weight Al35Cr14Mg6Ti35V10 high entropy alloy using mechanical alloying and spark plasma sintering, J. Alloy. Compd. 820 (2020) 153367.
[150] Vivek Kumar Pandey, et al., "Phase evolution and thermal stability of mechanically alloyed CoCrCuFeNi high entropy alloy, Mater. Res. Express 6 (12) (2020) 1265b9.
[151] Nandini Singh, Yagnesh Shadangi, Nilay Krishna Mukhopadhyay, "Phase evolution and thermal stability of low-density MgAlSiCrFe high-entropy alloy processed through mechanical alloying, Trans. Indian Inst. Met. 73 (9) (2020) 2377–2386.
[152] M.A. Avila-Rubio, et al., "Effect of Mo and Ti on the microstructure and microhardness in AlCoFeNiMoTi high entropy alloys prepared by mechanical alloying and conventional sintering, Adv. Powder Technol. 31 (4) (2020) 1693–1701.
[153] Alexander S. Rogachev, et al., "High-energy ball milling and spark plasma sintering of the CoCrFeNiAl high-entropy alloy, Metals 10 (11) (2020) 1489.
[154] Marcelo Orpinelli de Marco, et al., "Mechanical synthesis and hydrogen storage characterization of MgVCr and MgVTiCrFe high-entropy alloy, Adv. Eng. Mater. 22 (2) (2020) 1901079.
[155] Sujata Singh, et al., "Microstructural homogenization and substantial improvement in corrosion resistance of mechanically alloyed FeCoCrNiCu high entropy alloys by incorporation of carbon nanotubes, Materialia 14 (2020) 100917.
[156] Dewangan, Sheetal Kumar, et al., "Synthesis and characterization of hydrogenated novel AlCrFeMnNiW high entropy alloy, Int. J. Hydrog. Energy 45 (34) (2020) 16984–16991.
[157] Vikas Shivam, Vadapalli Sanjana, N.K. Mukhopadhyay, "Phase evolution and thermal stability of mechanically alloyed AlCrFeCoNiZn high-entropy alloy, Trans. Indian Inst. Met. 73 (3) (2020) 821–830.
[158] Filip Průša, et al., "High-strength ultrafine-grained CoCrFeNiNb high-entropy alloy prepared by mechanical alloying: properties and strengthening mechanism, J. Alloy. Compd. 835 (2020) 155308.
[159] Chenglong Zhu, et al., "Microstructure and mechanical properties of the TiZrNbMoTa refractory high-entropy alloy produced by mechanical alloying and spark plasma sintering, Int. J. Refract. Met. Hard Mater. 93 (2020) 105357.
[160] Juliette Normand, et al., "Development of a TiNbTaMoZr-Based High Entropy Alloy with Low Young´s Modulus by Mechanical Alloying Route, Metals 10 (11) (2020) 1463.
[161] Natalia Shkodich, et al., "Refractory high-entropy HfTaTiNbZr-based alloys by combined use of ball milling and spark plasma sintering: Effect of milling intensity, Metals 10 (9) (2020) 1268.
[162] Yaser A. Alshataif, et al., "Synthesis, structure, and mechanical response of Cr0. 26Fe0. 24Al0. 5 and Cr0. 15Fe0. 14Al0. 30Cu0. 13Si0. 28 nanocrystallite entropy alloys, Adv. Powder Technol. 31 (5) (2020) 2161–2177.
[163] Sajid Alvi, et al., "Synthesis and mechanical characterization of a CuMoTaWV high-entropy film by magnetron sputtering, ACS Appl. Mater. Interfaces 12 (18) (2020) 21070–21079.

[164] N.F. Shkodich, et al., "Structural evolution and magnetic properties of high-entropy CuCrFeTiNi alloys prepared by high-energy ball milling and spark plasma sintering, J. Alloy. Compd. 816 (2020) 152611.
[165] M. Vaidya, et al., "Suppression of σ-phase in nanocrystalline CoCrFeMnNiV high entropy alloy by unsolicited contamination during mechanical alloying and spark plasma sintering, Mater. Chem. Phys. 255 (2020) 123558.
[166] A. Fourmont, et al., "Effects of planetary ball milling on AlCoCrFeNi high entropy alloys prepared by Spark Plasma Sintering: Experiments and molecular dynamics study, J. Alloy. Compd. 820 (2020) 153448.
[167] C.W. Wang, et al., "Microwave vacuum sintering of FeCoNi1· 5CuB0· 5Y0. 2 high-entropy alloy: Effect of heat treatment on microstructure and mechanical property, Vacuum 181 (2020) 109738.
[168] Hosein Ziaei, et al., "Phase evolution in mechanical alloying and spark plasma sintering of Al x CoCrCuFeNi HEAs, Mater. Sci. Technol. 36 (5) (2020) 604–614.
[169] Arun Raphel, P. Vivekanandhan, S. Kumaran, "High entropy phenomena induced low thermal conductivity in BiSbTe1. 5Se1. 5 thermoelectric alloy through mechanical alloying and spark plasma sintering, Mater. Lett. 269 (2020) 127672.
[170] K.Raja Rao, Sudip K. Sinha, "Effect of sintering temperature on microstructural and mechanical properties of SPS processed CoCrCuFeNi based ODS high entropy alloy, Mater. Chem. Phys. 256 (2020) 123709.
[171] Rajesh K. Mishra, Rohit R. Shahi, "A novel low-density semi-hard magnetic Al20Fe20Mg20Ni20Ti20 high entropy alloy, J. Magn. Magn. Mater. 516 (2020) 167342.
[172] D.O. Moskovskikh, et al., "High-entropy (HfTaTiNbZr) C and (HfTaTiNbMo) C carbides fabricated through reactive high-energy ball milling and spark plasma sintering, Ceram. Int. 46 (11) (2020) 19008–19014.
[173] Ashutosh Sharma, Min Chul Oh, Byungmin Ahn, "Microstructural evolution and mechanical properties of non-Cantor AlCuSiZnFe lightweight high entropy alloy processed by advanced powder metallurgy, Mater. Sci. Eng.: A 797 (2020) 140066.
[174] Danni Yang, et al., "A novel FeCrNiAlTi-based high entropy alloy strengthened by refined grains, J. Alloy. Compd. 823 (2020) 153729.
[175] Yuping Duan, et al., "Optimizing the electromagnetic properties of the FeCoNiAlCrx high entropy alloy powders by composition adjustment and annealing treatment, J. Magn. Magn. Mater. 497 (2020) 165947.
[176] Rathinavelu Sokkalingam, et al., "Powder metallurgy of Al0. 1CoCrFeNi high-entropy alloy, J. Mater. Res. 35 (21) (2020) 2835–2847.
[177] Aeran Roh, et al., "NbMoTaW refractory high entropy alloy composites strengthened by in-situ metal-non-metal compounds, J. Alloy. Compd. 822 (2020) 153423.
[178] A. Vallimanalan, et al., "Corrosion behaviour of thermally sprayed Mo added AlCoCrNi high entropy alloy coating, Mater. Today.: Proc. 27 (2020) 2398–2400.
[179] D.Yu, N.A. Kovalev, Kochetov, I.I. Chuev, "Fabrication of high-entropy carbide (TiZrHfTaNb) C by high-energy ball milling, Ceram. Int. 47 (23) (2021) 32626–32633.
[180] Chun-Liang Chen, "Study of (Ni, Cr) pre-milling for synthesis of CoFe (NiCr) Mn high entropy alloy by mechanical alloying, Mater. Sci. Eng.: A 807 (2021) 140810.
[181] Jianjian Zhang, et al., "Effect of Co on the microstructure and oxidation behavior of CoxCrCuFeMnNi high entropy alloy powders, Micron 142 (2021) 102995.
[182] M.A. Ruiz-Esparza-Rodríguez, et al., "Influence of process control agent and Al concentration on synthesis and phase stability of a mechanically alloyed AlxCoCrFeMnNi high-entropy alloy, J. Alloy. Compd. 882 (2021) 160770.
[183] Hany R. Ammar, et al., "Synthesis, microstructural investigation and compaction behavior of Al0. 3CrFeNiCo0. 3Si0. 4 nanocrystalline high entropy alloy, Adv. Powder Technol. 32 (2) (2021) 398–412.
[184] A.S. Rogachev, et al., "Evolution of crystal structure in high-entropy AlCoCrFeNi alloy: An in situ high-temperature X-ray diffraction study, J. Alloy. Compd. 861 (2021) 158562.
[185] Chun-Liang Chen, "Study of NiFeCoCr medium entropy alloy as a binder phase on W–Mo heavy tungsten alloy by secondary ball milling, Intermetallics 138 (2021) 107320.
[186] Dewangan, Sheetal Kumar, et al., "Microstructure and mechanical properties of nanocrystalline AlCrFeMnNiWx (x= 0, 0.05, 0.1, 0.5) high-entropy alloys prepared by powder metallurgy route, J. Mater. Eng. Perform. 30 (6) (2021) 4421–4431.
[187] Vivek Kumar Pandey, et al., "Synthesis, characterization and thermal stability of nanocrystalline MgAlMnFeCu low-density high-entropy alloy, Trans. Indian Inst. Met. 74 (2021) 33–44.
[188] K.átia R. Cardoso, et al., "Hydrogen storage in MgAlTiFeNi high entropy alloy, J. Alloy. Compd. 858 (2021) 158357.
[189] Robert Bololoi, Viorel, et al., "AlCrFeNiTi high entropy alloy produced by solid state processing, UPB Sci. Bull. 83 (2021) 265–274.
[190] A.I. Yurkova, D.V. Hushchyk, A.V. Minitsky, "Synthesis of high-entropy AlNiCoFeCrTi coating by cold spraying, Powder Metall. Met. Ceram. 59 (11) (2021) 681–694.
[191] Seungjin Nam, et al., "High-temperature mechanical and thermochemical properties of NbMoTaW refractory high-entropy alloy coatings produced via Nano Particle Deposition System (NPDS), Int. J. Refract. Met. Hard Mater. 99 (2021) 105594.
[192] Abhinav Parakh, et al., "Effect of crystal structure and grain size on corrosion properties of AlCoCrFeNi high entropy alloy, J. Alloy. Compd. 863 (2021) 158056.
[193] Adrien Fourmont, et al., "Effects of mechanical activation on chemical homogeneity and contamination level in dual-phase AlCoCrFeNi high entropy alloy, Mater. Chem. Phys. 272 (2021) 125000.
[194] Parisa Akhlaghi, Mostafa Amirjan, Nader Parvin, "The effect of processing parameters and heat-treatment on the microstructure and mechanical properties of PM CoCrFeMnNiTi0. 1 high-entropy alloy, Mater. Chem. Phys. 257 (2021) 123722.
[195] Minsu Kim, et al., "Microstructural evolution of AlCuFeMnTi-0.75 Si high entropy alloy processed by mechanical alloying and spark plasma sintering, *Arch. Metall. Mater.* 66. 3 (2021) 703–707.
[196] Tao Xiang, et al., "Dual phase equal-atomic NbTaTiZr high-entropy alloy with ultra-fine grain and excellent mechanical properties fabricated by spark plasma sintering, J. Mater. Sci. Technol. 90 (2021) 150–158.
[197] Tao Wang, et al., "Development of a novel (Ni40Fe30Co20Al10) 90Ti10 high-entropy alloy with excellent photocatalytic performance, Mater. Lett. 283 (2021) 128817.
[198] Myoung Jin Chae, et al., "Effect of light (X= Mg, Si) and heavy (X= Zn) metals on the microstructural evolution and densification of AlCuFeMnTi-X high-entropy alloy processed by advanced powder metallurgy, Powder Metall. 64 (3) (2021) 228–234.
[199] Yunzi Liu, et al., "Core-shell structure mediated microstructure and mechanical properties of high entropy alloy CoCrFeNi/Al composites, Vacuum 192 (2021) 110454.
[200] Parisa Moazzen, Mohammad Reza Toroghinejad, Pasquale Cavaliere, "Effect of Iron content on the microstructure evolution, mechanical properties and wear resistance of FeXCoCrNi high-entropy alloy† system produced via MA-SPS, J. Alloy. Compd. 870 (2021) 159410.
[201] Nandini Singh, et al., "MgAlSiCrFeNi low-density high entropy alloy processed by mechanical alloying and spark plasma sintering: Effect on phase evolution and thermal stability, J. Alloy. Compd. 875 (2021) 159923.
[202] Hadi Jahangiri, et al., "Microstructure development and mechanical performance of Al2CrFeMnTi light-weight high entropy alloy, Intermetallics 139 (2021) 107376.
[203] Mustafa Tekin, et al., "Grain size stabilization of oxide dispersion strengthened CoCrFeNi-Y2O3 high entropy alloys synthesized by mechanical alloying, J. Alloy. Compd. 887 (2021) 161363.
[204] Qian Zhi, et al., "Effect of Zr content on microstructure and mechanical properties of lightweight Al2NbTi3V2Zrx high entropy alloy, Micron 144 (2021) 103031.
[205] Wei-Bing Liao, et al., "Microstructures and mechanical properties of CoCrFeNiMn high-entropy alloy coatings by detonation spraying, Intermetallics 132 (2021) 107138.
[206] Azmi Erdogan, et al., "Microstructure, wear and oxidation behavior of AlCrFeNiX (X= Cu, Si, Co) high entropy alloys produced by powder metallurgy, Vacuum 187 (2021) 110143.
[207] Nandini Singh, et al., "Fabrication of MgAlSiCrFe low-density high-entropy alloy by mechanical alloying and spark plasma sintering, Trans. Indian Inst. Met. 74 (9) (2021) 2203–2219.
[208] Rituraj Chandrakar, et al., "Microstructural and mechanical properties of AlCoCrCuFeNiSix (x= 0 and 0.9) high entropy alloys, Vacuum 184 (2021) 109943.
[209] R. Sekhar, A.S. Anand, Shifin, N. Firoz, "Microstructure and mechanical properties of AlCoCrNiTi–C high entropy alloy processed through spark plasma sintering, Mater. Chem. Phys. 270 (2021) 124846.
[210] Byungchul Kang, et al., "Superior mechanical properties and strengthening mechanisms of lightweight AlxCrNbVMo refractory high-entropy alloys (x= 0, 0.5, 1.0) fabricated by the powder metallurgy process, J. Mater. Sci. Technol. 69 (2021) 32–41.
[211] M. Ghanbariha, et al., "Effect of ZrO2 particles on the nanomechanical properties and wear behavior of AlCoCrFeNi–ZrO2 high entropy alloy composites, *Wear* 484 (2021) 204032.
[212] Jun Zhou, et al., "Carbon-alloyed Fe35Mn10Cr20Ni35 high entropy alloy synthesized by mechanical alloying plus spark plasma sintering, J. Alloy. Compd. 859 (2021) 157851.
[213] Gabriela E. Ruiz-Jasso, et al., "Synthesis of CuCrFeNiTiAl x high entropy alloys by means of mechanical alloying and spark plasma sintering, Can. Metall. Q. 60 (2) (2021) 66–74.
[214] Antão, Francisco, et al., "The effects of mechanical alloying on the physical and thermal properties of CuCrFeTiV alloy, Mater. Sci. Eng.: B 263 (2021) 114805.
[215] Yaser A. Alshataif, et al., "Synthesis, microstructures and mechanical behaviour of Cr 0.21 Fe 0.20 Al 0.41 Cu 0.18 and Cr 0.14 Fe 0.13 Al 0.26 Cu 0.11 Si 0.25 Zn 0.11 nanocrystallite entropy alloys prepared by mechanical alloying and hot-pressing, Met. Mater. Int. 27 (2021) 139–155.
[216] Mingming Xue, et al., "Comparison of micro-nano FeCoNiCrAl and FeCoNiCrMn coatings prepared from mechanical alloyed high-entropy alloy powders, J. Therm. Spray. Technol. 30 (6) (2021) 1666–1678.
[217] Myoung Jin Chae, et al., "Lightweight AlCuFeMnMgTi high entropy alloy with high strength-to-density ratio processed by powder metallurgy, Met. Mater. Int. 27 (2021) 629–638.
[218] Subbarayan Sivasankaran, Fahad A. Al-Mufadi, Hany R. Ammar, "Influence of V and Zn in FeCrCuMnTi high-entropy alloys on microstructures and uniaxial compaction behavior prepared by mechanical alloying, Crystals 11 (11) (2021) 1413.
[219] Rajesh K. Mishra, et al., "Design and development of Co35Cr5Fe20− xNi20+ xTi20 High Entropy Alloy with excellent magnetic softness, J. Alloy. Compd. 889 (2021) 161773.
[220] K.Raja Rao, Sudip K. Sinha, "Phase evolution in novel Y2O3 dispersed CrCuFeNiZn nanocrystalline multicomponent alloy prepared by mechanical alloying, Vacuum 184 (2021) 109802.

[221] F. Salemi, F. Karimzadeh, M.H. Abbasi, "Evaluation of Thermal and Mechanical Behavior of CuNiCoZnAl High-Entropy Alloy Fabricated Using Mechanical Alloying and Spark Plasma Sintering, Metall. Mater. Trans. A 52 (2021) 1947–1962.
[222] M.A. Avila-Rubio, et al., "Microstructure and microhardness of high entropy alloys with Zn addition: AlCoFeNiZn and AlCoFeNiMoTiZn, Adv. Powder Technol. 32 (12) (2021) 4687–4696.
[223] Min Chul Oh, et al., "Phase separation and mechanical behavior of AlCoCrFeNi-X (X= Cu, Mn, Ti) high entropy alloys processed via powder metallurgy, Intermetallics 139 (2021) 107369.
[224] Chenliang Chu, et al., "Microstructure and mechanical behavior of FeNiCoCr and FeNiCoCrMn high-entropy alloys fabricated by powder metallurgy, Acta Metall. (Engl. Lett.) 34 (2021) 445–454.
[225] Hosein Ziaei, et al., "Crystal structure evolution in mehcanical alloying and spark plasma sintering of AlxCoCrCuFeNi HEAs, Powder Metall. 64 (1) (2021) 54–63.
[226] Mohammad Reza Toroghinejad, Hossein Pirmoradian, Ali Shabani, "Synthesis of FeCrCoNiCu high entropy alloy through mechanical alloying and spark plasma sintering processes, Mater. Chem. Phys. 289 (2022) 126433.
[227] Minjie Huang, et al., "Effects of milling process parameters and PCAs on the synthesis of Al0. 8Co0. 5Cr1. 5CuFeNi high entropy alloy powder by mechanical alloying, Mater. Des. 217 (2022) 110637.
[228] N.F. Shkodich, et al., "Fast mechanical synthesis, structure evolution, and thermal stability of nanostructured CoCrFeNiCu high entropy alloy, J. Alloy. Compd. 893 (2022) 161839.
[229] Syam Narayana Addepalli, et al., "Effect of mechanical alloying on the microstructure of CoCrNiTiMo x high entropy alloy, J. Therm. Spray. Technol. 31 (4) (2022) 1045–1055.
[230] Zhen Zhang, et al., "Microstructure evolution and mechanical properties of CoCrFeNiAl0. 3 high entropy alloy produced by ball milling in combination with thermomechanical consolidation, Mater. Charact. 187 (2022) 111833.
[231] Armita Shahbazkhan, Hamed Sabet, Mehrdad Abbasi, "Microstructural and mechanical properties of NiCoCrAlSi high entropy alloy fabricated by mechanical alloying and spark plasma sintering, J. Alloy. Compd. 896 (2022) 163041.
[232] Sara Daryoush, Hamed Mirzadeh, Abolghasem Ataie, "Amorphization, mechano-crystallization, and crystallization kinetics of mechanically alloyed AlFeCuZnTi high-entropy alloys, Mater. Lett. 307 (2022) 131098.
[233] Fei Gao, et al., "Microstructural evolution and thermal stability in a nanocrystalline lightweight TiAlV0. 5CrMo refractory high-entropy alloy synthesized by mechanical alloying, Mater. Lett. 329 (2022) 133179.
[234] G.D. Avila-Rubio, et al., "Influence of Milling Time on Microstructure of AlCoCrMnMo High-entropy Alloy Produced by Mechanical Alloying, Microsc. Microanal. 28 (S1) (2022) 2840–2842.
[235] Mohammad Reza Toroghinejad, Fatemeh Ebrahimi, Ali Shabani, "Synthesis of the AlCrCuMnNi high entropy alloy through mechanical alloying and spark plasma sintering and investigation of its wear behavior, J. Mater. Res. Technol. 21 (2022) 3262–3273.
[236] Helia Kalantari, et al., "The production of nanocrystalline AlCoCrFeNiTiZn high entropy alloy via mechanical alloying: study of the formation mechanism, microstructural evolution, and magnetic properties of the alloy, Intermetallics 150 (2022) 107694.
[237] Ashok Kumar, et al., "Fabrication, microstructure, mechanical, and electrochemical properties of NiMnFeCu high entropy alloy from elemental powders, Metals 12 (1) (2022) 167.
[238] Xin Hu, et al., "A high-density non-equiatomicWTaMoNbV high-entropy alloy: Alloying behavior, microstructure and mechanical properties, J. Alloy. Compd. 894 (2022) 162505.
[239] Yang Zhang, et al., "Preparation and microstructure and properties of AlCuFeMnTiV lightweight high entropy alloy, J. Alloy. Compd. 900 (2022) 163352.
[240] A.I. Yurkova, et al., "Nanostructured AlCoFeCrVNi and AlCoFeCrVTi high-entropy alloys resulted from mechanical alloying and sintering, Appl. Nanosci. 12 (4) (2022) 849–860.
[241] Haoran Zhou, et al., "Ultrawide-frequency electromagnetic-wave absorption based on FeCoNiCu x Mn high entropy alloys synthesized through swing ball-milling, J. Mater. Chem. C. 10 (44) (2022) 16696–16705.
[242] Alican Yakın, et al., "The effect of Cr and Nb addition on the structural, morphological, and magnetic properties of the mechanically alloyed high entropy FeCoNi alloys, Appl. Phys. A 128 (8) (2022) 686.
[243] Rahul Bhattacharya, et al., "Evolution of phase constitution with mechanical alloying and spark plasma sintering of nanocrystalline Al x CoCrFeNi (x= 0, 0.3, 0.6, 1 mol) high-entropy alloys, J. Mater. Res. 37 (4) (2022) 959–975.
[244] Mariana de Brito Ferraz, Walter José Botta, Guilherme Zepon, "Synthesis, characterization and first hydrogen absorption/desorption of the Mg35Al15Ti25V10Zn15 high entropy alloy, Int. J. Hydrog. Energy 47 (54) (2022) 22881–22892.
[245] Farhad Abdi, Hossein Aghajani, Shahin Khameneh Asl, Mechanical Alloying and Spark Plasma Sintering of EquiatomicAlCoCrFeMnNi High Entropy Alloy. *J. Adv. Mater. Process.* 10. 1 (2022) 27–38.
[246] Cheenepalli Nagarjuna, et al., "Strengthening the mechanical properties and wear resistance of CoCrFeMnNi high entropy alloy fabricated by powder metallurgy, Adv. Powder Technol. 33 (4) (2022) 103519.
[247] Prakash, Om, et al., "Phase evolution of novel MoNbSiTiW refractory high-entropy alloy prepared by mechanical alloying, JOM 74 (9) (2022) 3329–3333.
[248] Makhmutov Tagir, Razumov Nikolay, Popovich Anatoliy, "Synthesis of single-phase high-entropy carbides from a mixture of pre-mechanically alloyed CrNbMoWV HEA powders and carbon, Mater. Lett. 309 (2022) 131363.
[249] Nai-ran Wang, et al., "Alloying behavior and characterization of (CoCrFeNiMn) 90M10 (M= Al, Hf) high-entropy materials fabricated by mechanical alloying, Trans. Nonferrous Met. Soc. China 32 (7) (2022) 2253–2265.
[250] Sina Kavak, et al., "Synthesis and characterization of (HfMoTiWZr) C high entropy carbide ceramics, Ceram. Int. 48 (6) (2022) 7695–7705.
[251] Hamed Naser-Zoshki, Ali-Reza Kiani-Rashid, Jalil Vahdati-Khaki, "Non-equiatomic W10Mo27Cr21Ti22Al20 high-entropy alloy produced by mechanical alloying and spark plasma sintering: Phase evolution and mechanical properties, Proc. Inst. Mech. Eng., Part L: J. Mater.: Des. Appl. 236 (4) (2022) 695–703.
[252] K.Raja Rao, Sudip K. Sinha, "Strengthening of AlCoCrFeNi based high entropy alloy with nano-Y2O3 dispersion, Mater. Sci. Eng.: B 281 (2022) 115720.
[253] Alexander Yurievich Ivannikov, et al., "Fabrication, microstructure, and physico-mechanical properties of Fe–Cr–Ni–Mo–W high-entropy alloys from elemental powders, Metals 12 (10) (2022) 1764.
[254] Jagadeesh Sure, D. Sri Maha Vishnu, Carsten Schwandt, "Single-step electrochemical synthesis of nano-crystalline CoCrFeNi high-entropy alloy powder, Electrochem. Commun. 143 (2022) 107392.
[255] A.S. Rogachev, et al., "Mechanical alloying in the Co-Fe-Ni powder mixture: Experimental study and molecular dynamics simulation, Powder Technol. 399 (2022) 117187.
[256] Stasiak, Tomasz, et al., "Preparation and characterisation of the Al-Cr-Fe-Mn-Mo high-entropy alloy reinforced by in-situ formed carbides, Philos. Mag. Lett. 102 (11-12) (2022) 368–377.
[257] Changbao Huan, et al., "Properties of AlFeNiCrCoTi0. 5 high-entropy alloy particle-reinforced 6061Al composites prepared by extrusion, Metals 12 (8) (2022) 1325.
[258] Lav Kush, Sanjay Srivastava, "Effect of mechanical milling and sintering on magnetic entropy of Ni-based Ni2CuCrFeAl x (x= 0.5, 1.0, 1.5 and 2.5) high entropy alloys, Phase Transit. 95 (5) (2022) 406–421.
[259] Tri Dinh Vo, et al., "Fabrication and characterization of a low-cost Co-free Al0. 8CrFeNi2. 2 eutectic high entropy alloy based solid self-lubricating composite: Microstructure, mechanical and wear properties, J. Alloy. Compd. 928 (2022) 167087.
[260] Helia Kalantari, Gholam Reza Khayati, Mandana Adeli, "A high entropy alloy of AlCrFeNiTiZn synthesized through mechanical alloying and sintering, Intermetallics 161 (2023) 107981.
[261] Sudhansu Maharana, et al., "Effect of sintering parameters on phase evolution, microstructural development and mechanical behavior of Ni46Al12Co18Cr8Fe12Mo4 high entropy alloy synthesized via mechanical alloying and spark plasma sintering, Mater. Sci. Eng.: A 886 (2023) 145695.
[262] Qianqian Cheng, et al., "Comparative study of the microstructure and phase evolution of FeCoCrNiAl high-entropy alloy-matrix WC nanocomposite powders prepared by mechanical alloying, J. Alloy. Compd. 938 (2023) 168518.
[263] Baofeng Zhang, et al., "Mechanical alloying behavior and thermal stability of CoCrCuFeMnNix high-entropy alloy powders prepared via MA, Materials 16 (8) (2023) 3179.
[264] Hirotada Hashimoto, et al., "Synthesis of Li-Mg-Al-Ti based lightweight high entropy alloys by mechanical alloying and investigation of conditions for solid solution formation, J. Alloy. Metall. Syst. 4 (2023) 100037.
[265] A.S. Rogachev, et al., "Long term stability of a high-entropy CoCrFeNiTi alloy fabricated by mechanical alloying, J. Alloy. Compd. 931 (2023) 167470.
[266] Y.Y. Kambarov, et al., "Mechanochemical synthesis of AlCoCrFeNi powders via high-energy ball milling, Bull. Karaganda Univ." Phys. Ser. 112 (4) (2023) 76–81.
[267] Sushil Yebaji, et al., "Phase stability of AlCoTiZn high-entropy alloy prepared by mechanical alloying, J. Mater. Eng. Perform. 32 (8) (2023) 3668–3677.
[268] Li, Li, et al., "Influences of Milling Time and NbC on Microstructure of AlCoCrFeNi2. 1 High Entropy Alloy by Mechanical Alloying, J. Wuhan. Univ. Technol. -Mater. Sci. Ed. 38 (2) (2023) 423–429.
[269] Priyatosh Pradhan, et al., "Powder metallurgical processing of CrMnFeCoMo high entropy alloy: phase evolution, microstructure, thermal stability and mechanical properties, J. Alloy. Compd. 935 (2023) 168002.
[270] Le Liu, et al., Microstructure and mechanical properties of CoCrCuFeNi high-entropy alloys synthesized by powder metallurgy and spark plasma sintering. J. Mater. Eng. Perform. (2023) 1–11.
[271] Liqiang Zhan, et al., "Study on mechanical alloying behavior and thermal stability of HfMoNbTaTi refractory high-entropy alloy, Mater. Charact. 203 (2023) 113122.
[272] Helia Kalantari, Gholam Reza Khayati, Mandana Adeli, "Structure investigation of AlFeNiTiZn nanocrystalline high entropy alloy, Vacuum 210 (2023) 111878.
[273] Malihe Zeraati, Mohammad Hossein Khazaei Feizabad, Gholam Reza Khayati, "An investigation of the magnetic, mechanical, and kinetic characteristics of CuCrFeTiNi high entropy alloy by mechanical alloying and spark plasma sintering, J. Alloy. Compd. 958 (2023) 170347.
[274] Ammar, Chérif Ben, *et al.* "Properties of High-Entropy Fe [sub. 30] Co [sub. 20] Ni [sub. 20] Mn [sub. 20] Al [sub. 10] Alloy Produced by High-Energy Ball Milling." Materials 17.1 (2023): NA-NA.
[275] M. Javdan, Kh Gheisari, M. Reihanian, "Mechanically alloyed (FeCoNi) 75Cu25−xSix high entropy alloys: phase evaluation and magnetic properties, J. Alloy. Compd. 952 (2023) 170030.
[276] Chérif Ben Ammar, et al., "Properties of High-Entropy Fe30Co20Ni20Mn20Al10 Alloy Produced by High-Energy Ball Milling, Materials 17 (1) (2023) 234.
[277] Sedat Özbilen, et al., "Mechanical milling/alloying, characterization and phase formation prediction of Al0. 1–0.5 (Mn) CoCrCuFeNi-HEA powder feedstocks for cold spray deposition processing, J. Alloy. Compd. 961 (2023) 170854.
[278] Fei Gao, et al., "Microstructure and strengthening mechanisms of novel lightweight TiAlV0. 5CrMo refractory high-entropy alloy fabricated by

mechanical alloying and spark plasma sintering, J. Alloy. Compd. 932 (2023) 167659.
[279] Harsh Jain, et al., "Low-density Fe40Mn19Ni15Al15Si10C1 high entropy steel processed by mechanical alloying and spark plasma sintering: phase evolution, microstructure and mechanical properties, Mater. Sci. Eng.: A 869 (2023) 144776.
[280] Pourmohammadi, Sahar, et al., "Phase stability, microstructure, and mechanical properties of spark plasma sintered nanocrystalline boron-doped AlCoFeMnNi high-entropy alloy, Metals 13 (6) (2023) 1025.
[281] A. Kumar, et al., "Facile synthesis of a NiMnFeCrCu high entropy alloy for electrocatalytic oxygen evolution reactions, Mater. Today Sustain. 22 (2023) 100360.
[282] Hakan Yaykaşlı, et al., "CoCrFeNiSi high entropy alloy: Synthesis, structural and radiation shielding properties, Prog. Nucl. Energy 165 (2023) 104930.
[283] Pan Dai, et al., "Insight of novel CoCrFeMnNi–Al2O3p high entropy alloy matrix composites by mechanical alloying and spark plasma sintering, J. Mater. Res. Technol. 26 (2023) 4871–4886.
[284] Amritava Sarkar, A. Srinivasan, P.S. Robi, "Processing and characterization of TiNbMoTaW refractory high entropy alloy by mechanical alloying, Adv. Powder Technol. 34 (12) (2023) 104276.
[285] Safia Alleg, et al., "Effect of Aluminum Addition on the Microstructure, Magnetic, and Mechanical Properties of FeCrCoNiMn High-Entropy Alloy, Crystals 13 (10) (2023) 1483.
[286] ZhiPei Chen, et al., "Design and experimental investigation of the high-entropy alloys AlCrFeNiCu and AlCrFeNbMo, J. Mater. Res. Technol. 26 (2023) 3118–3135.
[287] Ciprian Alexandru Manea, et al., "CoxCrFeNiTi High-Entropy Alloys Prepared via Mechanical Alloying and Spark Plasma Sintering for Magnetron Sputtering Coatings, Materials 16 (19) (2023) 6386.
[288] Nazaretyan, Kh, et al., "AlCo-rich AlCoNiFe and AlCoNiFeCr high entropy alloys: Synthesis and interaction pathway at high heating rates, J. Alloy. Compd. 931 (2023) 167589.
[289] Elahe Mansouri, Hamid Khorsand, "Synthesis of dual-phase face-centered cubic crystal structure in nanocrystalline AlCoCuFeNi high-entropy alloy, J. Ultra Graine Nanostruct. Mater. 56 (2) (2023) 233–246.
[290] Helia Kalantari, et al., "Nanocrystalline AlCoFeNiTiZn high entropy Alloy: Microstructural, Magnetic, and thermodynamic properties, Adv. Powder Technol. 34 (5) (2023) 104009.
[291] Wenqi Luo, et al., "Effects of milling time on the microstructure and properties of FeCoNiMnAl magnetic high-entropy alloys, Mater. Today Commun. 34 (2023) 104777.
[292] Y. Xing, et al., "Strengthening and deformation mechanism of high-strength CrMnFeCoNi high entropy alloy prepared by powder metallurgy, J. Mater. Sci. Technol. 132 (2023) 119–131.
[293] Hansung Lee, Ashutosh Sharma, Byungmin Ahn, "Exploring strengthening mechanism of FeCoNiAl high-entropy alloy by non-metallic silicon addition produced via powder metallurgy, J. Alloy. Compd. 947 (2023) 169545.
[294] Anay del Ángel-González, et al., "Microstructure, Phase Evolution, and Chemical Behavior of CrCuFeNiTiAlx High Entropy Alloys Processed by Mechanical Alloying, Entropy 25 (2) (2023) 256.
[295] Yagnesh Shadangi, Kausik Chattopadhyay, Nilay Krishna Mukhopadhyay, "Powder metallurgical processing of Al matrix composite reinforced with AlSiCrMnFeNiCu high-entropy alloys: Microstructure, thermal stability, and microhardness, J. Mater. Res. 38 (1) (2023) 248–264.
[296] Chun-Liang Chen, Jyun-Hong Lin, "Effects of Alloying Elements and Mechanical Alloying on Characteristics of WVTaTiCr Refractory High-Entropy Alloys, Materials 16 (18) (2023) 6194.
[297] Burçak Boztemur, et al., "Mechanically alloyed and spark plasma sintered WNbMoVTa refractory high entropy alloys: Effects of Cr and Al on the microstructural and mechanical properties, J. Alloy. Compd. 965 (2023) 171415.
[298] N. Jahani, M. Reihanian, Kh Gheisari, "Alloying, phases and magnetic behaviour of mechanically alloyed FeNiMnCu-based high entropy alloys, Mater. Sci. Technol. 39 (14) (2023) 1745–1759.
[299] Nozari Nezhad, Masoume, *et al.* "Synthesis, Characterization and Study on Phase Formation of Novel Alxcocrfeninb1-X-Si0. 1 High Entropy Alloy by Mechanical Alloying." Available at SSRN 4421765.
[300] Haoran Zhou, et al., "Structure evolution and electromagnetic-wave absorption performances of multifunctional FeCoNiMnVx high entropy alloys with harsh-environment resistance, J. Alloy. Compd. 946 (2023) 169402.
[301] Pradip Verma, Alok Singh Kumar, Akshay Kumar, "Microstructure characterization and phase evolution of equiatomicAlCoMoFeNi high entropy alloy synthesized by mechanical alloying, Mater. Chem. Phys. 318 (2024) 129325.
[302] Vivek Sharma, et al., "Nanostructured Al–Ti–Fe–Mn–Ni High-Entropy Alloy by Mechanical Alloying: Synthesis and Characterization, Arab. J. Sci. Eng. (2024) 1–12.
[303] Caner Bulut, et al., "The Effect of Milling Time and Hot-Pressing on the Structural Properties and Wear Behavior of CoCrFeMnNi High-Entropy Alloys Fabricated by Mechanical Alloying, High. Temp. Corros. Mater. 101 (2) (2024) 225–249.
[304] Samaneh Mamnooni, Ehsan Borhani, Mehdi Shahedi Asl, "Nanocrystalline Ni25Co20Cu10Fe25Mn20 High-Entropy Alloys Prepared by Mechanical Alloying, JOM (2024) 1–12.
[305] Artur Olejarz, et al., "Cr-rich structure evolution and enhanced mechanical properties of CoCrFeNi high entropy alloys by mechanical alloying, J. Mater. Res. Technol. 30 (2024) 1490–1504.
[306] Aisa Grace D. Custodio, Gobinda C. Saha, Clodualdo Aranas Jr, "Mechanical alloying of AlCoCrFe and AlCoCrFeNi: Design and experimental evaluation of medium-and high-entropy alloy particles for cold spraying, Powder Technol. 437 (2024) 119556.
[307] Mustafa Okumuş, Feyzullah Kaya, "Effect of Ti content and ball-milling time on the microstructural, thermal, and microhardness properties of AlCoCuNiTi high entropy alloys, Mater. Chem. Phys. 311 (2024) 128591.
[308] K.Raja Rao, et al., "Microstructure and mechanical characteristics of AlCoCrFeNi-based ODS high-entropy alloys consolidated by vacuum hot pressing, Met. Mater. Int. 30 (3) (2024) 726–734.
[309] Xingchang Tang, et al., "Microstructure and mechanical properties of CoCrFeNiTa high entropy alloy prepared by mechanical alloying and spark plasma sintering, Mater. Charact. 210 (2024) 113826.
[310] Sushma, U. Devi, et al., "Effect of pre-milling (Ni and Al) on the sintering behavior of NiAlFeCoCr high entropy alloy, Adv. Powder Technol. 35 (3) (2024) 104378.
[311] Marwa A. Abbas, Wesam M. Sadek, Samir A. Ibrahim, "Effect of Milling Time on the Structure Stability of FeMnNiCrAl Non-equiatomic High-Entropy Alloy, Trans. Indian Inst. Met. (2024) 1–9.
[312] Turin Datta, Indranil Manna, Jyotsna Dutta Majumdar, "Synthesis of Multi-component Alloys (Co20Cr20Fe20Mn20Ti20 and Co20Cr20Fe20Mn20Ti20Ni20) by Mechanical Alloying Route, High. Entropy Alloy. Mater. 2 (1) (2024) 1–15.
[313] Petr Kratochvíl, et al., "The role of the preparation route on microstructure and mechanical properties of AlCoCrFeNi high entropy alloy, J. Mater. Res. Technol. 30 (2024) 4248–4260.
[314] Yujun Han, et al., "Microstructural study on in-situ high-entropy (NbMoTaWV) C reinforced nanocrystalline NbMoTaWVC refractory high entropy alloys prepared by mechanically alloying, Mater. Charact. 212 (2024) 113953.
[315] Soroosh Mohammadi, Farshad Akhlaghi, "Effect of Al content on the microstructure and mechanical alloying behavior of AlCoCuMnNi and Al0. 25CoCuMnNi high entropy powders, Mater. Chem. Phys. 313 (2024) 128768.
[316] Turin Datta, Indranil Manna, Jyotsna Dutta Majumdar, "Synthesis of EquiatomicCoCrFeMnTiNi Multicomponent Alloy by Sequential Alloying Using Mechanical Alloying and Vacuum Arc Melting, J. Mater. Eng. Perform. (2024) 1–9.
[317] Ali Basem, et al., "Characterization of FeCoNiCr high-entropy alloys manufactured by powder metallurgy technique, J. Mater. Res. Technol. 30 (2024) 88–100.
[318] Narjess Hajilou, et al., "Investigation of the electrochemical behavior of AlCoCrFeNi–ZrO2 high entropy alloy composites prepared with mechanical alloying and spark plasma sintering, J. Appl. Electrochem. 54 (2) (2024) 457–466.
[319] Tao Sun, et al., "Investigation of Cu-diamond/Cu-diamond-high-entropy alloys bi-layer coating via mechanical alloying, Surf. Eng. 40 (2) (2024) 246–257.
[320] Tuncay Simsek, et al., "Effects of Cr and W in TiMoNb Refractory High Entropy Alloys, Trans. Indian Inst. Met. (2024) 1–14.
[321] Shengqing Gao, et al., "Effect of Ti content on microstructure and mechanical properties of TaMoNbCrTix refractory high-entropy alloy, Mater. Sci. Eng.: A 898 (2024) 146394.
[322] Vivek Sharma, M.R. Rahul, Ashis Mallick, "Microstructural, mechanical, and tribological behaviors of Cu40Fe30Mn20Cr5Ti5 high entropy alloy via powder metallurgy route, Mater. Today Commun. 38 (2024) 108313.
[323] E. Sakar, et al., "Effect of oxidation on radiation shielding capacity of ZrNbTaMoW Refractory High Entropy Alloys (RHEA) for nuclear reactor applications: Experimental and theoretical assessment, J. Alloy. Compd. 997 (2024) 174917.
[324] Shashi Kant Mohapatra, Priyanka Kumari, Rohit R. Shahi, "Combinatorial approach to enhance the magnetic properties of nanocrystalline Co35 Fe10Ni30Ti20M5 (M= Mn, Cu, and Al) high entropy alloys, Appl. Phys. A 130 (6) (2024) 1–16.
[325] Tolentino, Marvin S., *et al.* "Microstructural Analysis of MoNbZrTiV Refractory High-Entropy Alloy Developed via High-Energy Mechanical Alloying." TMS Annual Meeting & Exhibition. Cham: Springer Nature Switzerland, 2024.
[326] M. Javdan, Kh Gheisari, M. Reihanian, "(FeCoNi) 75Cu25-xSix high entropy alloys prepared by mechanical alloying and spark plasma sintering: Microstructure, deformation behavior and dynamic recrystallization kinetics, Mater. Charact. 211 (2024) 113861.
[327] Yongchul Yoo, et al., "Spark plasma sintering of tungsten-based WTaVCr refractory high entropy alloys for nuclear fusion applications, Int. J. Miner., Metall. Mater. 31 (1) (2024) 146–154.
[328] Kovalev, Dmitry Yu, Sergey G. Vadchenko, and Alexander S. Rogachev. "In Situ High-Temperature X-ray Diffraction Study of the Thermal Stability of the Co0. 22Cr0. 23Fe0. 29Ni0. 20Ti0. 06 High-Entropy Alloy Produced by High-Energy Ball Milling." Advanced Engineering Materials: 2401107.
[329] Praveen J. Mane, Venkatesh Murthy R, M. Shantharaja, "Influence of FeCoNiMnCr high-entropy alloy particulate fillers on morphology and mechanical behaviour of epoxy composites, J. Reinf. Plast. Compos. (2024) 07316844241238506.
[330] Zirui Chen, et al., "Microstructure and Mechanical Properties of the Ti62Nb12Mo12Ta12W2 Refractory High Entropy Alloy Prepared through Spark Plasma Sintering, Acta Metall. (Engl. Lett.) (2024) 1–12.
[331] Haichao Wang, et al., "Effect of Ti and C addition on oxidation resistance of FeCoCrNiMn high entropy alloys prepared by powder metallurgy, Anti-Corros. Methods Mater. 71 (3) (2024) 307–314.
[332] Yeqing Wang, et al., Effects of milling time and sintering temperature on the mechanical properties of 8 wt% WC/AlCoCrFeNiTi0. 5 high entropy alloy matrix composites. J. Alloy. Compd. 976 (2024) 173203.

[333] N. Jahani, M. Reihanian, Kh Gheisari, "Alloying and corrosion characteristics of FeNiMnCu-based high entropy alloys, Mater. Chem. Phys. 315 (2024) 128990.
[334] O. Zakir, O. Guler, R. Idouhli, A. Nayad, M.E. Khadiri, S.H. Guler, B. Dikici, Enhanced photocatalytic abilities of innovative high-entropy alloys (HEAs): a comparative analysis with its high entropy oxide (HEO) counterpart, J. Mater. Sci. 59 (26) (2024) 12050–12064.
[335] Singh, A., Kumari, P., Sahoo, S.K., & Shahi, R.R. (2024). Studies on hydrogen storage properties of TiVFeNi, (TiVFeNi) 95Zr5 and (TiVFeNi) 90Zr10 high entropy alloys. International Journal of Hydrogen Energy.
[336] P. Sharma, S. Rohila, U. Hasan, P.H. Krishna, C. Ugwuegbu, A. Tiwari, M. Joshi, Multiscale modeling-driven synthesis of Cu40Zn24Ni24Ag8Hg4 high entropy alloy with antibacterial properties, Nano-Struct. Nano-Objects 40 (2024) 101391.
[337] H. Jain, Y. Shadangi, D. Chakravarty, A.K. Dubey, N.K. Mukhopadhyay, Structure and properties of Fe40Mn20Cr20Ti10Al10 high-entropy alloy fabricated by mechanical alloying and spark plasma sintering, J. Mater. Sci. (2024) 1–21.
[338] Y. Han, Z. Li, H. Li, Y. Jia, Y. Zhu, Y. Chu, B. Zhang, Microstructural study on in-situ high-entropy (NbMoTaWV) C reinforced nanocrystalline NbMoTaWVC refractory high entropy alloys prepared by mechanically alloying, Mater. Charact. 212 (2024) 113953.
[339] Jimenez-Arevalo, V.M., Martin, P., Pio, E., Pavez, J., Aguilar, C.C., Suryanarayana, C., & Páez, M. Energy Transfer by Mechanical Alloying and Electrocatalytic Performance of the As-Sintered Self-Supported High-Entropy Alloy FeNiCoCuMo. Advanced Engineering Materials, 2400807.
[340] M. Zhao, J. Xu, W. Ye, Y. Gui, J. Zhao, Y. Qiao, Y. Yan, Microstructure and tensile properties of Y2O3-dispersion strengthened CoCrFeNi high entropy alloys prepared via mechanical alloying using pre-alloyed powder, J. Mater. Res. Technol. 33 (2024) 349–360.
[341] K.R. Rao, V.K. Soni, A.H. Seikh, A. Ghosh, S.K. Sinha, Microstructural evolution of CrCuFeNiZn nanocrystalline high entropy alloy prepared by mechanical alloying, Proc. Inst. Mech. Eng., Part C: J. Mech. Eng. Sci. 238 (21) (2024) 10404–10408.
[342] N. Jahani, M. Reihanian, K. Gheisari, Microstructure, deformation behavior, and dynamic recrystallization kinetics of FeNiMnCu-based high entropy alloys prepared by mechanical alloying and spark plasma sintering, J. Alloy. Compd. 977 (2024) 173408.
[343] D. Jeyasimman, V. Vijayaraghavan, S. Venkateshwara, Synthesis and Characterization Study of Al10Cr25Co20Ni25Fe20 High-Entropy Alloy Powders through Mechanical Alloying, J. Mater. Eng. Perform. (2024) 1–11.
[344] C.L. Chen, P.H. Lin, Influences of Ta content and mechanical alloying on synthesis and characteristics of CoCrNiFeTa$_x$ high entropy alloys, Intermetallics 172 (2024) 108362.
[345] Yong Zhang, High entropy materials, 1498, IntechOpen, Rijeka, 2023.
[346] Easo P. George, Dierk Raabe, Robert O. Ritchie, "High-entropy alloys, Nat. Rev. Mater. 4 (8) (2019) 515–534.
[347] Sheng Guo, et al., "Effect of valence electron concentration on stability of fcc or bcc phase in high entropy alloys, J. Appl. Phys. 109 (10) (2011).
[348] Ruirun Chen, et al., "Composition design of high entropy alloys using the valence electron concentration to balance strength and ductility, Acta Mater. 144 (2018) 129–137.
[349] G.U.O. Sheng, and Chain Tsuan Liu. "Phase stability in high entropy alloys: Formation of solid-solution phase or amorphous phase, Prog. Nat. Sci.: Mater. Int. 21. 6 (2011) 433–446.
[350] Xiao Yang, Yong Zhang, "Prediction of high-entropy stabilized solid-solution in multi-component alloys, Mater. Chem. Phys. 132 (2-3) (2012) 233–238.
[351] Robert Carroll, et al., "Experiments and model for serration statistics in low-entropy, medium-entropy and high-entropy alloys, Sci. Rep. 5 (1) (2015) 16997.
[352] Sheng Guo, "Phase selection rules for cast high entropy alloys: an overview, Mater. Sci. Technol. 31 (10) (2015) 1223–1230.
[353] Xuejiao Chang, et al., "Phase engineering of high-entropy alloys, Adv. Mater. 32 (14) (2020) 1907226.
[354] Weiran Zhang, Peter K. Liaw, Yong Zhang, "Science and technology in high-entropy alloys, Sci. China Mater. 61 (1) (2018) 2–22.
[355] Daniel B. Miracle, Oleg N. Senkov, "A critical review of high entropy alloys and related concepts, Acta Mater. 122 (2017) 448–511.
[356] Abhishek Kumar, et al., "Hydrogen storage performance of C14 type Ti0. 24V0. 17Zr0. 17Mn0. 17Co0. 17Fe0. 08 high entropy intermetallics, Trans. Indian Natl. Acad. Eng. 9 (2023) 1.
[357] Abhishek Kumar, Thakur Prasad Yadav, Nilay Krishna Mukhopadhyay, "Notable hydrogen storage in Ti–Zr–V–Cr–Ni high entropy alloy, Int. J. Hydrog. Energy 47 (54) (2022) 22893–22900.
[358] S.S. Mishra, et al., "Formation and stability of C14 type Laves phase in multi component high-entropy alloys, J. Alloy. Compd. 832 (2020) 153764.
[359] Jien-Wei Yeh, "Physical metallurgy of high-entropy alloys, Jom 67 (10) (2015) 2254–2261.
[360] Y.K. Yadav, M.A. Shaz, N.K. Mukhopadhyay, T.P. Yadav, Formation of B2 phase and its stability in equiatomic Al-Cu-Fe-Ni-Ti high entropy alloy, J. Alloy. Metall. Syst. 8 (2024) 100137.
[361] A.K. Niessen, et al., "Enthalpies of formation of liquid and solid binary alloys based on 3d metals: IV. Alloys of cobalt, Phys. B+ C. 151 (3) (1988) 401–432.
[362] Reza Kamachali, Darvishi, Lei Wang, "Elastic energy of multi-component solid solutions and strain origins of phase stability in high-entropy alloys, Scr. Mater. 206 (2022) 114226.
[363] T.P. Yadav, S. Mukhopadhyay, S.S. Mishra, N.K. Mukhopadhyay, O.N. Srivastava, Synthesis of a single phase of high-entropy Laves intermetallics in the Ti–Zr–V–Cr–Ni equiatomic alloy, Philos. Mag. Lett. 97 (12) (2017) 494–503.
[364] Hao Wu, et al., "A cost-effective eutectic high entropy alloy with an excellent strength–ductility combination designed by VEC criterion, J. Mater. Res. Technol. 19 (2022) 1759–1765.
[365] Andrew Cunliffe, Diss. University of Sheffield, Orig. Prop. High. Entropy Alloy. (2018).
[366] Harsh Jain, et al., "High entropy steel processed through mechanical alloying and spark plasma sintering: alloying behaviour, thermal stability and mechanical properties, Mater. Sci. Eng.: A 856 (2022) 144029.
[367] David R. Gaskell, E.Laughlin David, Introduction to the Thermodynamics of Materials, CRC press, 2017.
[368] Chung-Jin Tong, et al., "Microstructure characterization of Al x CoCrCuFeNi high-entropy alloy system with multiprincipal elements, Metall. Mater. Trans. A 36 (2005) 881–893.
[369] Soo-Hyun Joo, et al., "Beating thermal coarsening in nanoporous materials via high-entropy design, Adv. Mater. 32 (6) (2020) 1906160.
[370] Ming-Hung Tsai, "Physical properties of high entropy alloys, Entropy 15 (12) (2013) 5338–5345.
[371] Keng-Hao Cheng, et al., "Recent progress in multi-element alloy and nitride coatings sputtered from high-entropy alloy targets, Ann. De. Chim. (Paris. 1914). 31 (6) (2006).
[372] K.-Y. Tsai, M.-H. Tsai, J.-W. Yeh, "Sluggish diffusion in co–cr–fe–mn–ni high-entropy alloys, Acta Mater. 61 (13) (2013) 4887–4897.
[373] Yiqiong Zhang, Dongdong Wang, Shuangyin Wang, "High-entropy alloys for electrocatalysis: design, characterization, and applications, Small 18 (7) (2022) 2104339.
[374] Juliusz Dąbrowa, Marek Danielewski, "State-of-the-art diffusion studies in the high entropy alloys, Metals 10 (3) (2020) 347.
[375] Yong Zhang, Qiuwei Xing, "High entropy alloys: Manufacturing routes. Reference Module in Materials Science and Materials Engineering, Elsevier, Amsterdam, The Netherlands, 2020.
[376] Yaser A. Alshataif, et al., "Manufacturing methods, microstructural and mechanical properties evolutions of high-entropy alloys: a review, Met. Mater. Int. 26 (2020) 1099–1133.
[377] Ahmad Moghaddam, Ostovari, et al., "Additive manufacturing of high entropy alloys: A practical review, J. Mater. Sci. Technol. 77 (2021) 131–162.
[378] Yiping Lu, et al., "Directly cast bulk eutectic and near-eutectic high entropy alloys with balanced strength and ductility in a wide temperature range, Acta Mater. 124 (2017) 143–150.
[379] Changjun Han, et al., "Recent advances on high-entropy alloys for 3D printing, Adv. Mater. 32 (26) (2020) 1903855.
[380] Jithin Joseph, et al., "Comparative study of the microstructures and mechanical properties of direct laser fabricated and arc-melted AlxCoCrFeNi high entropy alloys, Mater. Sci. Eng.: A 633 (2015) 184–193.
[381] Priyatosh Pradhan, et al., "Powder metallurgical processing of CrMnFeCoMo high entropy alloy: phase evolution, microstructure, thermal stability and mechanical properties, J. Alloy. Compd. 935 (2023) 168002.
[382] Nadine Eißmann, et al., "High-entropy alloy CoCrFeMnNi produced by powder metallurgy, Powder Metall. 60 (3) (2017) 184–197.
[383] Lawrence E. Murr, "A metallographic review of 3D printing/additive manufacturing of metal and alloy products and components, Metallogr., Microstruct., Anal. 7 (2018) 103–132.
[384] Amit Bandyopadhyay, Bryan Heer, "Additive manufacturing of multi-material structures, Mater. Sci. Eng.: R: Rep. 129 (2018) 1–16.
[385] Shuying Chen, Yang Tong, Peter K. Liaw, "Additive manufacturing of high-entropy alloys: a review, Entropy 20 (12) (2018) 937.
[386] Amit S. Sharma, et al., "High-entropy alloys and metallic nanocomposites: Processing challenges, microstructure development and property enhancement, Mater. Sci. Eng.: R: Rep. 131 (2018) 1–42.
[387] Shao, Yiru. "Structure and mechanical properties of multicomponent AlNiCoFeCrTiMo alloy obtained by mechanical alloying and sintering." (2021).
[388] A. Fourmont, et al., "Effects of planetary ball milling on AlCoCrFeNi high entropy alloys prepared by Spark Plasma Sintering: Experiments and molecular dynamics study, J. Alloy. Compd. 820 (2020) 153448.
[389] Arunachalam Ramanathan, Pradeep Kumar Krishnan, Rajaraman Muraliraja, "A review on the production of metal matrix composites through stir casting–Furnace design, properties, challenges, and research opportunities, J. Manuf. Process. 42 (2019) 213–245.
[390] Hongxu Cheng, et al., "Corrosion-resistant high-entropy alloy coatings: a review, J. Electrochem. Soc. 168 (11) (2021) 111502.
[391] Ahmed Aliyu, Chandan Srivastava, "Microstructure-corrosion property correlation in electrodeposited AlCrFeCoNiCu high entropy alloys-graphene oxide composite coatings, Thin Solid Films 686 (2019) 137434.
[392] Smith Salifu, Peter Apata Olubambi, "Effects of fabrication techniques on the mechanical properties of high entropy alloys: a review, Int. J. Lightweight Mater. Manuf. 7 (1) (2024) 97–121.
[393] Yaser A. Alshataif, et al., "Synthesis, structure, and mechanical response of Cr0. 26Fe0. 24Al0. 5 and Cr0. 15Fe0. 14Al0. 30Cu0. 13Si0. 28 nanocrystallite entropy alloys, Adv. Powder Technol. 31 (5) (2020) 2161–2177.
[394] Challapalli Suryanarayana, "Mechanical alloying: a novel technique to synthesize advanced materials, Research (2019).
[395] Xiuyun Sun, Yugang Sun, "Synthesis of metallic high-entropy alloy nanoparticles, Chem. Soc. Rev. (2024).
[396] N.K. Mukhopadhyay, T.P. Yadav, O.N. Srivastava, Effects of ball milling and annealing in Al-Fe-Cu system: Implications for phase equilibria, Philos. Mag. Lett. 83 (2003) 423–432.

[397] T.P. Yadav, N.K. Mukhopadhyay, O.N. Srivastava, Synthesis of nano-quasicrystalline decagonal phase, Indian J. Phys. A 78 (2004) 189–191.
[398] T.P. Yadav, N.K. Mukhopadhyay, O.N. Srivastava, Synthesis of nano-quasicrystalline $Al_{70}Ni_{15}Co_{15}$ decagonal phase through high energy ball milling, J. Non-Cryst. Solids 334-335 (2004) 57–61.
[399] T.P. Yadav, N.K. Mukhopadhyay, M.A. Shaz, R.S. Tiwari, O.N. Srivastava, Studies on Al–Ni–Fe decagonal quasicrystalline alloy prepared by mechanical alloying, Philos. Mag. 87 (18-21) (2007) 3117–3125.
[400] D. Maurice, T.H. Courtney, "Modeling of mechanical alloying: Part I. deformation, coalescence, bdand fragmentation mechanisms, Metall. Mater. Trans. A 25 (1994) 147–158.
[401] T.P. Yadav, N.K. Mukhopadhyay, R.S. Tiwari, O.N. Srivastava, Synthesis of nanocrystalline (Co, Ni) Al2O4 spinel powder by mechanical milling of quasicrystalline material, J. Nanosci. Nanotechnol. 7 (2) (2007) 575–579.
[402] Rajeev Kumar Gupta, B.S. Murty, Nick Birbilis, An overview of high-energy ball milled nanocrystalline aluminum alloys, Springer International Publishing, Cham, 2017.
[403] T.P. Yadav, N.K. Mukhopadhyay, R.S. Tiwari, O.N. Srivastava, Low-temperature synthesis of nanocrystalline spinel powder by mechanical milling and annealing of Al-Ni-Fe decagonal quasicrystals, Philos. Mag. 88 (13-15) (2008) 2227–2236.
[404] Omoyemi Temitope Onawale, et al., "Synthesis route, microstructural evolution, and mechanical property relationship of high-entropy alloys (HEAs): A review, Materials 14 (11) (2021) 3065.
[405] T.P. Yadav, N.K. Mukhopadhayay, R.S. Tiwari, O.N. Srivastava, Evolution of a nanocrystalline (Co, Ni) Al2O4 spinel phase from quasicrystalline precursor, Int. *J. Appl. Ceram. Technol.* 5 (5) (2008) 449–457.
[406] C. Suryanarayana, Eugene Ivanov, V.V. Boldyrev, "The science and technology of mechanical alloying, Mater. Sci. Eng.: A 304 (2001) 151–158.
[407] Akshay Kumar, Alok Singh, Amit Suhane, "A critical review on mechanically alloyed high entropy alloys: processing challenges and properties, Mater. Res. Express 9 (5) (2022) 052001.
[408] N.K. Mukhopadhyay, T.P. Yadav, R.S. Tiwari, M.A. Shaz, O.N. Srivastava, Synthesis of nanocrystalline spinel phase by mechanical milling of Al—Cu—Fe and Al—Cu—Cr—Fe quasicrystalline alloys, Z. *fur Krist.* 223 (11-12) (2008) 716–720.
[409] R.S. Tiwari, T.P. Yadav, N.K. Mukhopadhyay, O.N. Srivastava, Nanocrystallization and structural correlation in quasicrystalline and crystalline phases during mechanical milling, Z. fur Krist. 224 (1-2) (2009) 26–30.
[410] Olejarz, Artur, et al., "Microstructure and mechanical properties of mechanically-alloyed CoCrFeNi high-entropy alloys using low ball-to-powder ratio, J. Alloy. Compd. 938 (2023) 168196.
[411] N.K. Mukhopadhyay, F. Ali, V.C. Srivastava, T.P. Yadav, M. Sakaliyska, K. B. Surreddi, S. Scudino, V. Uhlenwinkel, J. Eckert, Strain-induced structural transformation of single-phase Al–Cu–Fe icosahedral quasicrystal during mechanical milling, Philos. Mag. 91 (2011) 2482–2490.
[412] Pengfei Wang, et al., "Effects of annealing process parameters on microstructural evolution and strength-ductility combination of CoCrFeMnNi high-entropy alloy, Mater. Sci. Eng.: A 840 (2022) 142880.
[413] S.W. Wu, et al., "Enhancement of strength-ductility trade-off in a high-entropy alloy through a heterogeneous structure, Acta Mater. 165 (2019) 444–458.
[414] Yan-Xin Zhuang, Xiu-Lan Zhang, Xian-Yu Gu, "Effect of annealing on microstructure and mechanical properties of Al0. 5CoCrFeMoxNi high-entropy alloys, Entropy 20 (11) (2018) 812.
[415] M.H. Bocanegra-Bernal, "Hot isostatic pressing (HIP) technology and its applications to metals and ceramics, J. Mater. Sci. 39 (21) (2004) 6399–6420.
[416] Zhi Tang, et al., "Tensile ductility of an AlCoCrFeNi multi-phase high-entropy alloy through hot isostatic pressing (HIP) and homogenization, Mater. Sci. Eng.: A 647 (2015) 229–240.
[417] Jithin Joseph, et al., "Effect of hot isostatic pressing on the microstructure and mechanical properties of additive manufactured AlxCoCrFeNi high entropy alloys, Mater. Sci. Eng.: A 733 (2018) 59–70.
[418] S. Varalakshmi, et al., "Hot consolidation and mechanical properties of nanocrystalline equiatomicAlFeTiCrZnCu high entropy alloy after mechanical alloying, J. Mater. Sci. 45 (2010) 5158–5163.
[419] Wei Ji, et al., "Alloying behavior and novel properties of CoCrFeNiMn high-entropy alloy fabricated by mechanical alloying and spark plasma sintering, Intermetallics 56 (2015) 24–27.
[420] Wei Ji, et al., "Mechanical alloying synthesis and spark plasma sintering consolidation of CoCrFeNiAl high-entropy alloy, J. Alloy. Compd. 589 (2014) 61–66.
[421] Zhiqiang Fu, et al., "Alloying behavior and deformation twinning in a CoNiFeCrAl0. 6Ti0. 4 high entropy alloy processed by spark plasma sintering, J. Alloy. Compd. 553 (2013) 316–323.
[422] Robert Howard, Neils Bogh, D. Scott MacKenzie, "Heat treating processes and equipment, *Handb. Alum.* 1 (2003) 881–916.
[423] Tao-Tsung Shun, et al., "Age heat treatment of the CoCrFeNiTi0. 3 high-entropy alloy, Mater. Trans. 59 (5) (2018) 730–733.
[424] D.G. Shaysultanov, et al., "Effect of heat treatment on the structure and hardness of high-entropy alloys CoCrFeNiMnV x (x= 0.25, 0.5, 0.75, 1), Phys. Met. Metallogr. 118 (2017) 579–590.
[425] Harihar Rakshit Sistla, W.Newkirk Joseph, F. Frank Liou, Effect of Al/Ni ratio, heat treatment on phase transformations and microstructure of AlxFeCoCrNi2− x (x= 0.3, 1) high entropy alloys. Mater. Des. 81 (2015) 113–121.
[426] A. Munitz, et al., "Heat treatment influence on the microstructure and mechanical properties of AlCrFeNiTi0. 5 high entropy alloys, Mater. Sci. Eng.: A 742 (2019) 1–14.
[427] Majid Abdellahi, Maryam Bahmanpour, "A novel technology for minimizing the synthesis time of nanostructured powders in planetary mills, Mater. Res. 17 (2014) 781–791.
[428] B.S. Murty, S.J.M.R. Ranganathan, "Novel materials synthesis by mechanical alloying/milling, Int. Mater. Rev. 43 (3) (1998) 101–141.
[429] Huynh Xuan Kho, et al., "Planetary ball mill process in aspect of milling energy, J. Powder Mater. 21 (2) (2014) 155–164.
[430] S. Rosenkranz, S. Breitung-Faes, A. Kwade, "Experimental investigations and modelling of the ball motion in planetary ball mills, Powder Technol. 212 (1) (2011) 224–230.
[431] Lynch, Alban J., and Chester A.Rowland. The history of grinding. SME, 2005.
[432] Sheng-Yong Lu, et al., "Simulation of ball motion and energy transfer in a planetary ball mill, Chin. Phys. B 21 (7) (2012) 078201.
[433] Marica Broseghini, et al., "Effect of jar shape on high-energy planetary ball milling efficiency: Simulations and experiments, Mater. Des. 110 (2016) 365–374.
[434] Szegvari, A., M. Yang, and Arno Szegvari. "Attritor grinding and dispersing equipment." Akron, Ohio (1999).
[435] G.ábor Mucsi, "A review on mechanical activation and mechanical alloying in stirred media mill, Chem. Eng. Res. Des. 148 (2019) 460–474.
[436] Xuzhe Zhao, Leon Shaw, "Modeling and analysis of high-energy ball milling through attritors, Metall. Mater. Trans. A 48 (2017) 4324–4333.
[437] George Saravacos, et al., "Mechanical processing equipment, Handb. Food Process. Equip. (2016) 149–232.
[438] Ian Krycer, John A. Hersey, "Fine powder mixing in a vibratory ball mill, Int. J. Pharm. 6 (2) (1980) 119–129.
[439] Nirmal Kumar, Sekhar Tiwary Chandra, Krishanu Biswas, "Preparation of nanocrystalline high-entropy alloys via cryomilling of cast ingots, J. Mater. Sci. 53 (2018) 13411–13423.
[440] Sina Kavak, et al., "Synthesis and characterization of (HfMoTiWZr) C high entropy carbide ceramics, Ceram. Int. 48 (6) (2022) 7695–7705.
[441] Peter Baláž, Peter Baláž, "High-energy milling, Mechanochemistry Nanosci. Miner. Eng. (2008) 103–132.
[442] Neikov, Oleg D., *et al*. "Mechanical alloying." Handbook of Non-Ferrous Metal Powders; Neikov, OD, Naboychenko, SS, Murashova, IV, Gopienko, VG, Frishberg, IV, Lotsko, DVS, Eds (2019): 63-79.
[443] Sopicka-Lizer, Ma.łgorzata, ed. High-energy ball milling: mechanochemical processing of nanopowders. Elsevier, 2010.
[444] Peter Baláž, Peter Baláž, "High-energy milling, Mechanochemistry Nanosci. Miner. Eng. (2008) 103–132.
[445] Francioli, Daniel Mendonça. "Effect of operational variables on ball milling." UFRJ/Escola Politécnica (2015).
[446] Vladimir Šepelák, Sylvie Bégin-Colin, Gerard Le Caer, "Transformations in oxides induced by high-energy ball-milling, Dalton Trans. 41 (39) (2012) 11927–11948.
[447] Jinzhi Liao, Ming-Jen Tan, "Mixing of carbon nanotubes (CNTs) and aluminum powder for powder metallurgy use, Powder Technol. 208 (1) (2011) 42–48.
[448] Trish Partyka, Denis Yan, "Fine grinding in a horizontal ball mill, Miner. Eng. 20 (4) (2007) 320–326.
[449] Boschetto, Alberto, et al., "Particle tracking in horizontal ball milling, Eng. Syst. Des. Anal. 42517 (2006).
[450] Andrzej Marczuk, et al., "Modeling and simulation of particle motion in the operation area of a centrifugal rotary chopper machine, Sustainability 11 (18) (2019) 4873.
[451] D.B. Witkin, Enrique J. Lavernia, "Synthesis and mechanical behavior of nanostructured materials via cryomilling, Prog. Mater. Sci. 51 (1) (2006) 1–60.
[452] M. Laurent-Brocq, et al., "Microstructure and mechanical properties of a CoCrFeMnNi high entropy alloy processed by milling and spark plasma sintering, J. Alloy. Compd. 780 (2019) 856–865.
[453] Nirmal Kumar, Sekhar Chandra, Tiwary, Krishanu Biswas, "Preparation of nanocrystalline high-entropy alloys via cryomilling of cast ingots, J. Mater. Sci. 53 (2018) 13411–13423.
[454] D.J.M. King, et al., "Predicting the formation and stability of single phase high-entropy alloys, Acta Mater. 104 (2016) 172–179.
[455] Akshay Kumar, Alok Singh, Amit Suhane, "Mechanically alloyed high entropy alloys: existing challenges and opportunities, J. Mater. Res. Technol. 17 (2022) 2431–2456.
[456] M. Vaidya, A. Karati, A. Marshal, K.G. Pradeep, B.S. Murty, Phase evolution and stability of nanocrystalline CoCrFeNi and CoCrFeMnNi high entropy alloys, J. Alloy. Compd. 770 (2019) 1004–1015.
[457] RuoKang Song, et al., "Phase formation and strengthening mechanisms in a dual-phase nanocrystalline CrMnFeVTi high-entropy alloy with ultrahigh hardness, J. Alloy. Compd. 744 (2018) 552–560.
[458] Kang Yang, et al., "Microstructure Evolution and Formation of Dual-Phase AlCoCrFeNiSi0. 5 High-Entropy Alloy Powders by Mechanical Alloying, J. Therm. Spray. Technol. (2024) 1–18.
[459] N. Jahani, M. Reihanian, K. Gheisari, Alloying, phases and magnetic behaviour of mechanically alloyed FeNiMnCu-based high entropy alloys, Mater. Sci. Technol. 39 (14) (2023) 1745–1759.
[460] R. Sriharitha, B.S. Murty, R.S. Kottada, Phase formation in mechanically alloyed AlxCoCrCuFeNi (x= 0.45, 1, 2.5, 5 mol) high entropy alloys, Intermetallics 32 (2013) 119–126.
[461] K.B. Zhang, Z.Y. Fu, J.Y. Zhang, W.M. Wang, S.W. Lee, K. Niihara, Characterization of nanocrystalline CoCrFeNiTiAl high-entropy solid solution processed by mechanical alloying, J. Alloy. Compd. 495 (1) (2010) 33–38.
[462] S. Praveen, B.S. Murty, R.S. Kottada, Alloying behavior in multi-component AlCoCrCuFe and NiCoCrCuFe high entropy alloys, Mater. Sci. Eng.: A 534 (2012) 83–89.

[463] G.ökhan Polat, Mustafa Tekîn, Hasan Kotan, "Role of yttrium addition and annealing temperature on thermal stability and hardness of nanocrystalline CoCrFeNi high entropy alloy, Intermetallics 146 (2022) 107589.
[464] Zou, Yu, et al., "Nanocrystalline high-entropy alloys: a new paradigm in high-temperature strength and stability, Nano Lett. 17 (3) (2017) 1569–1574.
[465] Junchen Li, et al., "A review on high entropy alloys coatings: fabrication processes and property assessment, Adv. Eng. Mater. 21 (8) (2019) 1900343.
[466] B.S. Murty, "Mechanical alloying—a novel synthesis route for amorphous phases, Bull. Mater. Sci. 16 (1993) 1–17.
[467] T.P. Yadav, S.S. Mishra, O.N. Srivastava, "Copper nanocubes on Al65Cu20Fe15 quasicrystalline surface, J. Alloy. Compd. 712 (2017) 134–138.
[468] F.C. Li, et al., "Amorphous–nanocrystalline alloys: fabrication, properties, and applications, Mater. Today Adv. 4 (2019) 100027.
[469] Lili Xiao, et al., "Superior anticorrosion performance of crystal-amorphous FeMnCoCrNi high-entropy alloy, Scr. Mater. 210 (2022) 114454.
[470] Aijun Zhang, et al., "A novel CoCrFeNi high entropy alloy matrix self-lubricating composite, J. Alloy. Compd. 725 (2017) 700–710.
[471] Deekshith G. Kalali, et al., "On the origins of ultra-high hardness and strain gradient plasticity in multi-phase nanocrystalline MoNbTaTiW based refractory high-entropy alloy, Mater. Sci. Eng.: A 812 (2021) 141098.
[472] Liangbin Chen, et al., "Gradient structure design to strengthen carbon interstitial Fe40Mn40Co10Cr10 high entropy alloys, *Mater. Sci. Eng.*: A 772 (2020) 138661.
[473] Zi-Yu Liu, et al., "Novel high-entropy oxides for energy storage and conversion: From fundamentals to practical applications, Green. Energy Environ. 8 (5) (2023) 1341–1357.
[474] Weizhai Bao, et al., "High-entropy oxides for energy storage and conversion, J. Mater. Chem. A (2024).
[475] Mustafa Tekin, et al., "Grain size stabilization of oxide dispersion strengthened CoCrFeNi-Y2O3 high entropy alloys synthesized by mechanical alloying, J. Alloy. Compd. 887 (2021) 161363.
[476] Mateusz Balcerzak, et al., "Mechanochemical synthesis of (Co, Cu, Mg, Ni, Zn) O high-entropy oxide and its physicochemical properties, J. Electron. Mater. 48 (2019) 7105–7113.
[477] M. Vaidya, G.M. Muralikrishna, B.S. Murty, High-entropy alloys by mechanical alloying: A review, J. Mater. Res. 34 (5) (2019) 664–686.
[478] W. Zhai, L. Bai, R. Zhou, X. Fan, G. Kang, Y. Liu, K. Zhou, Recent progress on wear-resistant materials: designs, properties, and applications, Adv. Sci. 8 (11) (2021) 2003739.
[479] O.T. Onawale, P.V. Cobbinah, R.A. Nzeukou, W.R. Matizamhuka, Synthesis route, microstructural evolution, and mechanical property relationship of high-entropy alloys (HEAs): A review, Materials 14 (11) (2021) 3065.
[480] J. Liu, Z. Lv, Z. Wu, J. Zhang, C. Zheng, C. Chen, L. Che, Research progress on the influence of alloying elements on the corrosion resistance of high-entropy alloys, J. Alloy. Compd. (2024) 175394.
[481] Y.K. Yadav, M.A. Shaz, T.P. Yadav, Solid-state hydrogen storage properties of Al–Cu–Fe–Ni–Ti high entropy alloy, Int. J. Hydrog. Energy 99 (2025) 985–995.
[482] A. Kumar, T.P. Yadav, M.A. Shaz, N.K. Mukhopadhyay, Hydrogen storage performance of C14 type Ti0. 24V0. 17Zr0. 17Mn0. 17Co0. 17Fe0. 08 high entropy intermetallics, Trans. Indian Natl. Acad. Eng. 9 (3) (2024) 585–593.
[483] Y.K. Yadav, M.A. Shaz, T.P. Yadav, Storage of hydrogen in solid-state materials. In *Hydrogen Energy*, CRC Press, 2024, pp. 181–208.
[484] A. Kumar, N.K. Mukhopadhyay, T.P. Yadav, Hydrogen storage in high entropy alloys. In *Towards Hydrogen Infrastructure*, Elsevier, 2024, pp. 133–164.
[485] Y.K. Yadav, M.A. Shaz, T.P. Yadav, Al–Cu–Fe–Ni–Ti high entropy alloy nanoparticles as new catalyst for hydrogen sorption in MgH2, Int. J. Hydrog. Energy (2024), https://doi.org/10.1016/j.ijhydene.2024.08.095.
[486] S.K. Verma, S.S. Mishra, N.K. Mukhopadhyay, T.P. Yadav, Superior catalytic action of high-entropy alloy on hydrogen sorption properties of MgH2, Int. J. Hydrog. Energy 50 (2024) 749–762.